

THESIS

INTEGRATED WATER AND POWER MODELING FRAMEWORK FOR RENEWABLE
ENERGY INTEGRATION

Submitted by

André Dozier

Department of Civil and Environmental Engineering

In partial fulfillment of the requirements

For the Degree of Master of Science

Colorado State University

Fort Collins, Colorado

Fall 2012

Master's Committee:

Advisor: John W. Labadie

Dan Zimmerle
Jose Salas

Copyright by André Quinton Dozier 2012

All Rights Reserved

ABSTRACT

INTEGRATED WATER AND POWER MODELING FRAMEWORK FOR RENEWABLE ENERGY INTEGRATION

Increasing penetration of intermittent renewable energy sources into the bulk electricity system has caused new operational challenges requiring large ramping rate and reserve capacity as well as increased transmission congestion due to unscheduled flow. Contemporary literature and recent renewable energy integration studies indicate that more realism needs to be incorporated into renewable energy studies. Many detailed water and power models have been developed in their respective fields, but no free-of-charge integrated water and power system model that considers constraints and objectives in both systems jointly has been constructed. Therefore, an integrated water and power model structure that addresses some contemporary challenges is formulated as a long-term goal, but only a small portion of the model structure is actually implemented as software.

A water network model called MODSIM is adapted using a conditional gradient method to be able to connect to an overarching optimization routine that decomposes the water and power problems. The water network model is connected to a simple power dispatch model that uses a linear programming approach to dispatch hydropower resources to mitigate power flows across a transmission line. The power dispatch model first decides optimal power injections from each of the hydropower reservoirs, which are then used as hydropower targets for the water network model to achieve. Any unsatisfied power demand or congested transmission line is assumed to be met by imported power.

A case study was performed on the Mid-Columbia River in the U.S. to test the capabilities of the integrated water and power model. Results indicate that hydropower resources can accommodate transmission congestion and energy capacity on wind production up until a particular threshold on the penetration level, after which hydropower resources provide no added benefit to the system. Effects of operational decisions to mitigate wind power penetration level and transmission capacity on simulated total dissolved gases were negligible. Finally, future work on the integrated water and power model is discussed along with expected results from the fully implemented model and its potential applications.

ACKNOWLEDGEMENTS

I would like to thank my advisor, Dr. John Labadie, for his advice throughout my time as a Masters candidate. I would also like to thank Dr. Jose Salas, Dan Zimmerle, Dr. Timothy Gates, Dr. Darrell Fontane, Dr. Jeffrey Niemann, Dr. Neil Grigg, and Dr. Siddharth Suryanarayanan for their help and wealth of knowledge about water resources and interconnected power systems. I also thank my lab mates, Dr. Ryan Bailey, Eric Morway, Joy Labadie, Keith Morse, Greg Steed, Mike Weber, Corey Wallace, Justin Kattnig, and Cale Mages, for keeping me company and making my learning experience fun. I thank Steve Barton for sharing his knowledge of the Columbia River. I thank my former co-workers Jordan Lanini, Chad Hall, Tony Spencer, and Adam Jokerst for their contribution to my desire to develop my skills by pursuing a more advanced degree and build my computer programming skills. I give my thanks to Andrew Meyer as well for all of our talks about life, math, and computer programming. I thank my family and “family” from Summitview Community Church for their support, for sanity checks, and for pointing me to the One who matters more than life itself. More than all these, I thank my lovely bride, Rachel, for her support, care, and all the homemade lunches. Most of all, I thank you, God, creator of such a complex and fascinating world filled with challenging engineering problems. I look forward to learning more and more from you, the ultimate engineer, holy and loving Father.

TABLE OF CONTENTS

I	Introduction.....	ix
1	Operational Considerations within a Water System	3
2	Operational Considerations within a Power System.....	5
3	Potential for Hydropower Operations to Alleviate Challenges	9
4	Research Objective	13
5	Summary of Chapters	13
II	Literature Review.....	16
1	Integrated Water and Power Systems Operations Models.....	19
2	Areas Lacking in Research	20
3	Requirements for an integrated water and power system model	25
III	Model Structure – The Long-Term Goal	28
1	Water Network Formulation.....	31
2	Power Systems Operations Model Formulations.....	38
3	Multiple Objectives: Environment and Economic Efficiency	42
4	Lagrangian Relaxation to Connect Water and Power Models.....	45
5	Artificial intelligence	53
6	Dynamic Optimal Policies	56
IV	Implementation of Water Network Model.....	62
1	New Hydropower Objects	64

2	Hydropower Output	77
3	Successive Approximations	81
4	Conditional Gradient Method Implementation	84
4.1	Customizing the objective function	94
4.2	Built-in capabilities	102
5	Discussion	115
V	Implementation of Simplified Integrated Model	121
1	The Power Model in Code	125
VI	Case Study of Grand Coulee, Banks Lake, and Chief Joseph	128
1	Model Calibration	131
1.1	Linear Model of Total Dissolved Gas (TDG)	135
2	Scenario Setup	139
3	Results	143
VII	Future Work on IWPM	161
1	Expected Results	163
2	Potential Applications	165
VIII	References	169

LIST OF TABLES

Table 1: Timescales of power system management. Reproduced from Sharp et al. (1998), DeMeo et al. (2005), and Xie et al. (2011).	18
Table 2: Economic factors in water and power systems operations	44
Table 3: Social and environmental concerns due to water and power systems operations	44
Table 4: Literature describing the application of Lagrangian relaxation to unit commitment problems.....	47
Table 5: Lagged routing factors between Chief Joseph and Grand Coulee.....	133
Table 6: Transmission capacity and wind penetration scenarios.....	142

LIST OF FIGURES

Figure 1: Simple diagram of energy storage in conventional hydropower.....	11
Figure 2: Simple diagram of energy storage in a pumped storage plant	11
Figure 3: Three-level simulation and optimization model structure diagram.....	29
Figure 4: Flow diagram of the conditional gradient algorithm applied to a network flow problem	37
Figure 5: Modeling timescale coordination between water and power operations where M steady- state power system solutions are solved within one water system solution	42
Figure 6: A simplified diagram of the Lagrangian Relaxation procedure applied to the integrated water and power systems problem.....	48
Figure 7: Flow diagram of the Lagrangian relaxation solution procedure	50
Figure 8: Solution flow of the optimality condition decomposition procedure as applied to the IWPM problem	52
Figure 9: Flow diagram for implementation of the reinforcement learning algorithm with other two levels of the IWPM structure	57
Figure 10: Conceptual diagram of the reinforcement learning procedure applied to the IWPM and optimizing dynamic policies	59
Figure 11: Reinforcement learning in parallel to determine optimal policies for stochastically generated sample input sets	60
Figure 12: An example MODSIM network to display the use and application of the new hydropower unit structure.....	65
Figure 13: Context menu shown when right-clicking on link with hydropower unit defined.....	65
Figure 14: A form used for building the conventional hydropower unit below Grand Coulee....	67

Figure 15: Stage-storage relationship for the reservoir behind Grand Coulee (GCL).....	68
Figure 16: Tailwater elevation curve defined at power plant elevation.....	69
Figure 17: The hydropower unit form after creating a new efficiency table	70
Figure 18: The form displaying multiple hydropower units defined within the network.....	72
Figure 19: Spreadsheet containing data for copying 7 new identical pumping units into the hydropower controller.....	73
Figure 20: Context menu that allows users to copy and paste the table of hydropower units to and from the form	73
Figure 21: Multi-hydropower unit table after pasting new units into the table	74
Figure 22: Default generating hours associated with any new hydropower unit pasted into the multi-hydropower unit table	75
Figure 23: Single hydropower target dialog that defines a hydropower target.....	76
Figure 24: Multi-hydropower target dialog that defines multiple targets.....	77
Figure 25: Extension manager to turn hydropower controller on.....	78
Figure 26: Hydropower unit and target output structure within output database	79
Figure 27: A sample hydropower unit output showing energy and hydropower unit discharge ..	80
Figure 28: Hydropower targets displayed in the graphical output.....	81
Figure 29: Simulation options presented to the user at runtime when hydropower targets are present in the system.....	82
Figure 30: Hydropower target link structure of routing link before (a) and after (b) initialization of the model at runtime	83
Figure 31: Mapping of event occurrences from a MODSIM <i>Model</i> object to a <i>OptiModel</i> object	85

Figure 32: Link structure for simple example.....	88
Figure 33: Flow diagram of interaction that the conditional gradient solver has with a class implementing the <i>IConditionalGradientSolvableModel</i> interface using event subscribers	93
Figure 34: Simple network to illustrate customizability.....	96
Figure 35: Inflows to the reservoir in the simple network.....	97
Figure 36: Release schedule for simple example network.....	98
Figure 37: Graphical outputs of simple example network.....	102
Figure 38: Class diagram of built-in objective functions.....	103
Figure 39: Class diagram of the <i>OptiFunctionBase</i> class.....	105
Figure 40: Network setup with routing link prior to simulation. Figure adapted from Labadie (2010).....	106
Figure 41: Network setup with routing link after simulation starts. Figure adapted from Labadie (2010).....	106
Figure 42: Flow through the zero-flow link with (bottom) and without (top) routing terms in the objective function.....	108
Figure 43: Diagram of attributes within the <i>HydroTargetSeeker</i> class	110
Figure 44: Fitted polynomials for Stage-Storage relationships of Banks Lake, Grand Coulee, and Chief Joseph.....	113
Figure 45: Tailwater elevation curves from Grand Coulee and Chief Joseph.....	114
Figure 46: Convergence limitations.....	117

Figure 47: Simulated and observed hydropower production from Banks Lake (top), Grand Coulee (middle), and Chief Joseph (bottom) using the successive approximations approach.....	119
Figure 48: Simulated and observed hydropower production from Banks Lake (top), Grand Coulee (middle), and Chief Joseph (bottom) using the conditional gradient method	120
Figure 49: One-line diagram of the generic two-bus system.....	126
Figure 50: Total dissolved gas (TDG), inflow and outflow at Grand Coulee	130
Figure 51: Schematic of MODSIM calibration model used to calculate local inflows	132
Figure 52: Schematic of MODSIM simulation model.....	132
Figure 53: Simulated energy production, energy targets, and production minus targets at Grand Coulee	134
Figure 54: Simulated energy production, energy targets, and production minus targets at Chief Joseph.....	135
Figure 55: Total dissolved gas (TDG) at Grand Coulee as a function of Spill.....	136
Figure 56: Simulated tailwater TDG versus measured tailwater TDG at Grand Coulee.....	137
Figure 57: Weights associated with each variable in the linear TDG model.....	138
Figure 58: Simulated total dissolved gas using historical reservoir information along with a “perturbed” simulation where spills were set to zero	139
Figure 59: Schematic of two-bus system used to test systems model of mid-Columbia dams ..	140
Figure 60: Power flows across 2-bus system for year 2011 when $L1$ load on the left bus is represented using 31% of total load at each timestep	141
Figure 61: Increasing wind data penetration modeled using a scalar multiplier	142

Figure 62: Effect of transmission capacity with increasing wind penetration on dispatched hydropower energy targets at Chief Joseph	145
Figure 63: Effect of transmission capacity with increasing wind penetration on dispatched hydropower energy targets at Grand Coulee	146
Figure 64: Power flows as a result of dispatched hydropower resources resulting from various scenarios of transmission capacity and wind penetration	147
Figure 65: Power flows as a result of dispatched hydropower resources resulting from increased wind penetration and a transmission capacity of 1500 MW	148
Figure 66: Power flows as a result of dispatch hydropower resources resulting from increased wind penetration and a transmission capacity of 750 MW	148
Figure 67: Power flows compared between two transmission scenarios for the entire modeled time period	149
Figure 68: Storage levels at Grand Coulee (top), Banks Lake (middle), and Chief Joseph (bottom) as a result of restricted transmission capacity with no additional wind capacity	150
Figure 69: Storage levels at Grand Coulee (top), Banks Lake (middle), and Chief Joseph (bottom) as a result of restricted transmission capacity with extreme wind capacity penetration (<i>Scalar</i> = 30x)	152
Figure 70: Power flow targets for high wind penetration scenario	153
Figure 71: Simulated power flows for high wind penetration scenario	154
Figure 72: Simulated power imports into the right bus to mitigate high wind power penetration scenario without inclusion of water or non-power constraints, and are therefore called “targets”	155

Figure 73: Simulated power imports into the right bus to mitigate high wind power penetration scenario with inclusion of water constraints	156
Figure 74: Simulated power imports into the right bus to mitigate power flows across the transmission line with no wind power penetration	156
Figure 75: Average power import at right bus compared to average wind power penetration level in MW	157
Figure 76: Simulated total dissolved gases for various wind penetration scenarios.....	158
Figure 77: Simulated total dissolved gases for various transmission capacity scenarios	159

I Introduction

Increasingly stringent environmental standards within the U.S. may prove beneficial for long-term sustainability of natural resources, but they inherently impose significant challenges and tradeoffs with other societal criteria. Many environmental regulations have been imposed on man-made structures such as dams, power generation facilities, and transmission of both water and electric power. Such regulations generally require builders and operators to spend more money to satisfy the stricter environmental codes. Operations of such facilities often require reevaluation and approval to account for environmental conditions, particularly in the water and air, but changing operations means other operational objectives may be suffering as a result. Analyzing tradeoffs between competing objectives of multiple sectors of government and society may provide benefits to society and environment as a whole by offering decision makers the ability to choose between various scenarios.

Increasing renewable energy integration is a particular environmental goal for many entities throughout the U.S. that rendering operations of interconnected power systems more challenging. Renewable energy sources (RESs) are energy sources that can be considered “renewable” because of the lack of reliance on limited resources such as fossil fuels. Many RESs that provide electric power to the grid, known as the bulk electricity system (BES), are currently in operation such as wind power, solar power, hydrokinetic power, conventional hydropower, biomass fuels, and geothermal energy. Some RESs are highly variable and uncertain when attached to the grid such as wind, solar, and many times hydrokinetics. Traditional power system operations have been used with dispatchable power resources, which simplifies operation because generation must match load exactly at all times, and load was the only uncertain factor, which could generally be predicted with reasonable accuracy. However, with elements of

uncertainty on the power generation side, operations become much more challenging. Small portions of variable and uncertain power generation are relatively easy to integrate into power grid operations with current balancing resources, but with increasingly ambitious renewable energy goals throughout the world, RES integration is beginning to significantly impact grid operations, balancing resources, and grid reliability and security. Section 2 discusses operational considerations within interconnected power systems.

Electrical energy storage, when operated in conjunction with RES power production may potentially provide a renewable, dispatchable resource that provides scheduled power to the grid and decreases overhead balancing costs. In fact, without energy storage, it may not be possible to integrate enough RESs to achieve some entities' goals, unless grid reliability become much less of a priority to power system operators and power consumers, which is highly unlikely. Energy storage devices and associated literature are discussed in detail in Section 3.

Systems of rivers and reservoirs ("water systems") provide unique capabilities to store both water and energy in the form of elevation head. Electric power can be generated from the potential energy stored in water behind a dam, termed hydropower. Hydropower facilities can provide rapid responses and significant amounts of energy storage that could potentially help to mitigate variability in power generation from RESs. However, operations between rivers and reservoirs are not solely focused on hydropower production, but also a variety of other concerns compromise the flexibility of hydropower facilities to provide grid services. Tradeoffs and conflicting priorities in hydropower systems are discussed in more detail in Section 1.

Operational and modeling challenges for both water and power systems motivate the use of computers as decision support systems because of the scale of such problems, potentially containing hundreds of thousands of decision variables and intermediate engineering

calculations. Sections 1 and 2 describe in detail significant challenges to be overcome by operators in order to safely, effectively, and efficiently operate both water and power system. As a result of such challenges, generalized decision support systems (DSSs) have been built for water systems and other DSSs have been built for power systems. Some water system models may even house some power related criteria, such as hydropower targets or maximizing profit based on preset or randomly generated energy prices, but these only represent a small subset of power system considerations. Some power system models also house some water related criteria, but these also tend to be highly simplified. No generalized, integrated framework that incorporates a reasonable amount of realism from both water and power systems has been developed free-of-charge to be used for research purposes, which would be particularly useful on the topic of RES integration.

Challenges in water and power systems operations along with the potential for integrated operations to benefit electric power reliability with significant amounts of RES penetration have motivated the development of an integrated water and power model (IWPM) that aids research in integrated system operations as well as potentially multiobjective analyses between water and power sectors and associated economic, social, and environmental criteria.

1 Operational Considerations within a Water System

Conflicting objectives within a water system are unavoidable. Eight main categories of water use seem to govern most water system operations: water supply, irrigation, flood control, navigation, water quality, fish and wildlife, recreation, and hydropower. Water system operators need to meet water demands including irrigation and municipal demands which may conflict with instream flow requirements for sustainable aquatic life habitats. Many dams have flood control as a primary operational objective. A few dams operate to meet electric power needs in

the electricity system by generating hydroelectric power, but are still required by law to meet water supply demands and comply with environmental policy. Along large rivers, systems of locks and dams provide navigable river segments for transportation of goods. Of course, boaters, swimmers, and fisherman enjoy water resources for its recreational benefits. Economics also affect operations during purchasing and trading of water rights, recreational and navigational fees, and delivering treated water to consumers at metered ends of a distribution system. Opposing public interest groups will oppose water projects due to concerns about environmental sustainability, economics, and cultural considerations.

Water managers cannot control the amount of the incoming water resource, which is a function of weather, topography, hypsography, and operations of dams by other water managers within the same system of reservoirs. Often, inflow from streams is not gaged fully. Groundwater flow cannot be measured on a widespread basis with current measuring techniques, and groundwater flow models cannot work perfectly because underground geologic structures cannot be measured. In other words, spatially and temporally complete datasets of aquifer systems cannot be totally and non-intrusively measured. Such immeasurable factors affecting groundwater flow include soil bulk density, particle size, chemical makeup, various geological formations that interrupt or speed up groundwater flow, aquifer depth, etc. Additionally, evaporation from reservoirs cannot be directly measured. Therefore, for modeling purposes, stochastically-varying inputs are required to evaluate uncertainties in incoming and outgoing fluxes across river reaches and reservoirs. Routines for estimating and forecasting uncertain variables are critical to effective water resource management.

The multiple objectives of water system management and operation and the numerous constraints, regulations, and administrative rules governing these operations, are highly complex

and often ill-defined. For example, many factors affect stream water quality, including the distribution and extent of irrigated farm lands, efficiency of and type of irrigation practice, amount and timing of irrigation, municipal usage, flow regime and geometry of the stream itself, seepage from mining, and industrial usage. In order to meet a particular water quality standard, a model of such poorly understood processes would need to be constructed with a limited input dataset. Models tend to be conceptual or empirical in nature due to the large uncertainty, but many physically-based models have been constructed as well. However, with limited data, every model has uncertainty in predicting features of the simulated processes. The job of operators is to control these challenging systems in a way that satisfies multiple uses and objectives of the water resources. Such challenges practically require the use of computer-aided modeling tools. An equivalent level of complexity exists in power system operation.

2 Operational Considerations within a Power System

Power systems offer another challenging systems operations problem, similar to water systems. Interconnected power systems in the bulk electricity system (BES) require many services in order to operate reliably. Such services include power for base load, power for peak load, energy imbalance, load following, regulation, reactive power control, transient and voltage stability and control, loss compensation, system protection, generator angle, black start, time correction, operating reserves, standby reserves, planning reserves, scheduling and dispatch, redispatch, transmission, power quality, planning, engineering, and accounting services (Hirst and Kirby 1996). Power engineers and system operators attempt to optimally select various services for every moment of every day, since electricity is used at all times. Many system challenges arise due to the complexity of nonlinear system interactions, operational constraints

arising from government policies, uncertainty of production and consumption of electricity, and response plans during brownouts and blackouts.

Operators protect power generation, transmission, and distribution systems as well as other electrical and electronics devices by using standards. The natural law of conservation of energy holds that power must be consumed at almost the exact same time that it is generated. Rotating machines within the U.S. produce alternating current (AC) power, and in order to ensure compatibility, standards on electrical frequency and voltage delivered from power systems within the U.S. are imposed. A maximum deviation of ± 0.2 Hz from the standard 60 Hz frequency is allowable within most U.S. balancing areas (BAs), and a deviation of $\pm 5\%$ from nominal voltage on a line. In addition, transmission lines have a power rating or capacity due to heating of the elements within the line, which restricts amount of power flow that can traverse the line. Individual power generating units have limits to power generating capacity, ramp rate, reserve capacity, and fuel in many cases. These restrictions complicate the safe and secure operation of interconnected power systems within the BES.

Environmental policy affects many operational decisions in a power system as well. Thermal plants with coal as a fuel have emissions constraints, as do natural gas plants. Nuclear power plants need to properly dispose of nuclear waste, and hydropower reservoirs can only be operated while complying with environmental policies regarding water quality as well as maintaining fish and wildlife habitat.

Uncertainty is inevitable in power system operations and planning due to the lack of foreknowledge regarding unpredictable factors and the uneconomical capability to perfectly measure all power system states. No one can predict when a lightning bolt will strike or another type of fault will occur in the system. Weather impacts power system demand as well as RES

power production. Since weather is highly uncertain due to the incapability of current sensors and measuring devices to capture complete spatial and temporal datasets, RES power production and power demand from load centers are also uncertain. During dry years, hydropower may produce less power, and on hot or cold days, electric consumption may significantly increase because of electric heaters and air conditioners. Since renewable energy such as wind and solar are highly uncertain and intermittent, they are not dispatchable (Kamath 2010; Bitar et al. 2011a; Makarov et al. 2011). With low levels of penetration, highly variable generation sources may not exceed regulating and load following capabilities of current systems. However, as renewable penetration increases, a nontrivial need for other solutions will arise including large and rapid load following and regulation, better forecasting methods, distributed generation and demand response, curtailment, aggregation of geographically diverse variable generation, and improved energy storage technologies (Holtinen 2009; GE Energy 2010; Bitar et al. 2011a; Bitar et al. 2011b; Jonas 2011).

Flexible AC Transmission Systems (FACTS) are receiving much more attention as smart grids evolve into the state-of-the-art for operating energy grids worldwide. Such devices have complicated operating rules, rendering them difficult to model (Pandya and Joshi 2008). Smart grid technology may add a lot of flexibility and efficiency into power systems, but it also adds substantial operational complexity.

Economics significantly impact operations of power systems both on a real-time and long-term basis. Before discussing the intricacies involved with power system economics, two different operating paradigms or environments must first be introduced: regulated and deregulated electricity markets. A regulated electricity market has a top-down structure, where the electric utility generates, transmits, and distributes the power to individual load centers. A

regulated system operates within a monopoly where all the customers must obtain their electricity from a single provider, and pay the price that the provider decides. However, a fully deregulated electricity market introduces competition by dividing power generation, transmission, and distribution into separate entities so that distributors have a choice from whom to buy wholesale electric power, and energy users have a choice to purchase from separate distribution companies (Kirschen and Strbac 2004). The motivation behind a deregulated market is to promote economic efficiency by creating an incentive to make technology innovations and by preventing deadweight loss incurred by regulatory type intervention within a market. A handful of electricity markets have deregulated and others are in the process of deregulating. Singh and Chauhan (2011) describe experiences of various countries in deregulation and introduce the complexity of individual problems for each country. Some countries have had success with deregulation of electricity markets including the United Kingdom, Australia, New Zealand, Argentina, Chile, and 16 states in the U.S. [U.S. Energy Information Administration (EIA) 2010; Huneault 2001].

Electricity within a regulated market is managed by a vertically integrated entity that owns all generation, transmission, and distribution assets for its customers. For the most part, entities attempt to schedule generators in a way that meets system load reliably while reducing costs which are passed down to the consumers. Such a problem is inherently challenging since it requires the system operator to forecast both short-term and long-term electric power demands, as well as to estimate generation, transmission, and operating costs. However, the economic dispatch, unit commitment, short-term planning, and long-term planning problems are even more challenging when operating within a deregulated electricity market.

Within a deregulated market, electricity is treated as a commodity, and profit seeking entities attempt to make a profit by selling electric power to potential customers by supplying efficiently-generated, cheap electricity. Simulation of a deregulated, or reformed, power market must incorporate a private firm's market strategy in addition to complexities previously discussed for a regulated electricity market. To complicate a deregulated system even more, several different electricity markets exist, where electricity and bilateral contracts can be sold or traded in forwards, futures, and spot markets. Entities can also exercise Options such as "Put" or "Call," or enter into a Contract for Differences (CFD) with another company, and additionally provide ancillary services. However, supply must always equal demand within a power system. A system operator must schedule resources accordingly by attempting to find market clearing price at market equilibrium (Kirschen and Strbac 2004). Therefore, electric generation from a particular entity is determined not only on how it bid within different markets, but also on how other competitors bid in any market. For a firm to maximize its profit, it is beneficial to estimate the bid of all the other entities within the market.

3 Potential for Hydropower Operations to Alleviate Challenges

Hydropower connects a system of rivers, reservoirs, water utilities, irrigation canals, and other water infrastructure with a regional-scale system of electric power generators, load centers, transmission lines, and substations. As discussed above, both water and power systems have operational challenges requiring estimation and simulation of immeasurable, nonlinear, non-continuous, discrete, stochastically-varying, and interdependent variables. Informed decisions cannot be made without the use of Decision Support Systems (DSSs), or modeling frameworks with user interfacing capabilities (Labadie 2004). Computer-aided water and power management has aided to improved efficiency of water and power systems operations since the widespread

onset of computers. However, with a large dichotomy between water system management and power system management, a segregated modeling framework of the two systems has prevailed.

Recent reports and literature seem to show that the current modeling framework insufficiently addresses operational challenges within either system because of the interdependence of the systems. Bitar et al. (2011b) showed that energy storage located near wind farms improved expected profit and risk of shorting on power delivery contracts. Heussen et al. (2010) and Jonas (2011) indicated similar results. Small types of energy storage can be located geographically close to RESs, but have not yet sufficiently demonstrated viability, reliability and economic feasibility with pilot projects (USDOE 2011). Such storage technologies include batteries, thermal heat storage, flywheels, superconducting magnetic energy storage (SMES), and ultra-capacitors (USDOE 2011). Other larger energy storage can also be used such as compressed air energy storage (CAES).

Some studies indicate that hydropower may potentially be instrumental in mitigating the uncertainty of wind power generation because of its range of operation, rapid response, energy storage capabilities, and proven technologies (Holtinen et al. 2009; GE Energy 2010; Hodge et al. 2011; Loose 2011). Hydropower is a dispatchable RES, unlike wind and solar, and is cheap, clean (non-polluting) energy. Renewable energy storage in hydropower systems provides some flexibility to power system operators to mitigate uncertain renewable energy production in the form of additional water head resulting from either decreased water releases as in the case of conventional hydropower resources (see Figure 1) or water pumped to a reservoir at higher elevation as in the case of pumped storage hydropower (see Figure 2). The major disadvantages of hydropower and pumped storage hydropower, however, include high capital costs, environmental and social damages due to flooding of land, long project completion time, and the

incapability to rapidly transition from pump-mode to turbine-mode specifically in pumped storage systems. The latter disadvantage can be mitigated by operating a pumping unit simultaneously with a turbine unit in order to provide better ramping rates and peak-shaving support (Beaudin et al. 2010). Also, conventional and pumped storage hydropower facilities can only be located in certain geographic locations because of watershed hydrology, land ownership rights, political factors, and economic feasibility.

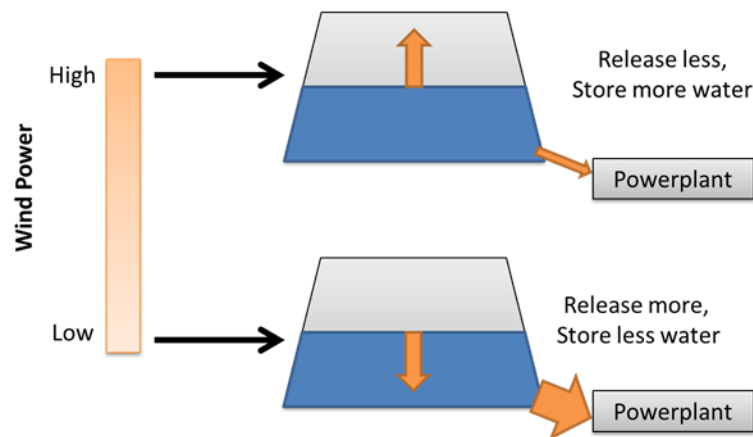


Figure 1: Simple diagram of energy storage in conventional hydropower

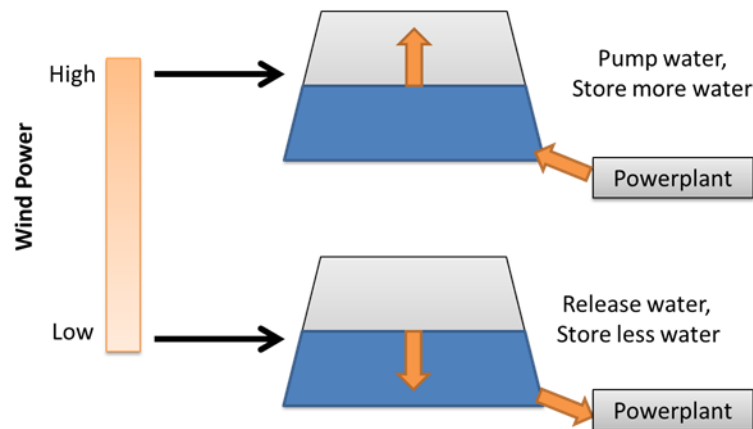


Figure 2: Simple diagram of energy storage in a pumped storage plant

Hydropower reservoirs store large amounts of energy in the form of water behind dams. Not only do reservoirs provide flood protection as well as irrigation water and instream flows, but can often provide black start services, which is a case when generators do not require exciters

or other external electricity sources to continue operation. Hydropower can practically participate in every form of electric power ancillary service as well as offering power system security. However, there is the need to analyze the capacity to which it can provide such services while meeting all water system demands and constraints. Incorporation of uncertainty in hydroelectric unit commitment and trading within a deregulated electricity market is an extremely difficult problem to solve (Jacobs and Schultz 2002).

Due to the complexity of both water and power systems operations problems, software modeling tools have become indispensable in order to ensure that all decisions reflect management priorities. Many scheduling intricacies and conflicts often arise that cannot be optimally overcome without integrated systems simulation and optimization. Many simulation and optimization models have been developed for both water and power systems. Some are tailored towards researchers and others for industrial use. A motivation behind an integrated water and power model is to unite two traditionally separate engineering and management fields (the electrical and water industries) to provide better understanding for both industries within academia as well as in practical management applications. Additionally, due to larger and larger penetrations of renewable energy in particular, more utilities are interested in firming wind power generation. Due to the large set of services that contemporary hydropower facilities can offer, hydropower may have a large role in integrating other renewables. A more tightly coupled simulation and optimization between water and power models is necessary in order to fully realize the potential of hydropower to match the swelling challenges introduced by renewable energy and smart grid technology.

4 Research Objective

In light of operational challenges within both water and power systems, the main objective of this research is to establish a framework both in formulation and as computer software that would aid operations research in both water and power systems using a tightly integrated approach. Several tasks are required to accomplish this goal as follows:

- a) Show the need for integrated water and power systems modeling in literature,
- b) Select an integrated water and power model structure,
- c) Adapt a free-of-charge generalized water system operations model to be compatible with the integrated water and power model structure,
- d) Build a static, overarching optimization routine to connect water and power models,
- e) Test the framework on the pump-generation plant at Grand Coulee and Banks Lake, and downstream plant Chief Joseph as proof of concept, and
- f) Provide recommendations for future research that will refine, generalize, improve and complete the integrated modeling system.

Each task has been performed and is discussed in detail within the chapters of this thesis, which are summarized in the next section.

5 Summary of Chapters

This chapter has introduced the operational challenges of water and power systems as well as the importance and potential for hydropower facilities to mitigate and improve operations within both water and power systems. Computer-aided modeling of the systems has been presented, and other chapters build on this notion by defining the problem in literature, selecting a modeling structure and framework, describing work on a generalized water network model to bring it to compatibility within an integrated modeling framework, discussing development of a

simple power network model, applying the framework to a case study, and recommending future work.

Chapter II describes a literature review that was performed on the topic of integrated water and power systems. Generalized water network models are discussed in detail and power systems modeling infrastructure is introduced. Advantages and disadvantages of other integrated water and power systems models are discussed. Literature indicates a lack of realism in hydropower modeling for most RES integration studies, which is a main motivation behind developing an integrated modeling framework to account for both water and power system criteria and objectives. Criteria for features within an integrated water and power modeling framework are then discussed.

A formulation of a model structure that meets criteria for an integrated water and power model defined in Chapter II are discussed in Chapter III for the water network model, the power network model, and overarching optimization routines. Multiple objectives between the two systems are discussed and optimization routines that are implicitly able to perform multiobjective analysis are contrasted with traditional mathematical optimization routines. Two methods are proposed for adapting the water network model to match specified hydropower targets via a successive approximations approach and the conditional gradient algorithm. Methods of optimization for power systems are analyzed. Static optimization routines (optimization over a single timestep) and dynamic optimization routines (optimization over multiple timesteps) are compared and contrasted, and a static-level optimization routine using Lagrangian Relaxation is formulated. Dynamic optimization and the Lagrangian Relaxation method have not been fully formulated, developed or implemented, which is an area for future research and development discussed in Chapter VII.

Chapter IV describes the enhancement of a water network model called MODSIM to make it compatible with the integrated modeling framework formulated in Chapter III. Hydropower objects were built within the model and hydropower output is generated and displayed within the MODSIM interface. A successive approximations approach in addition to a conditional gradient algorithm was implemented to match a specified hydropower target. The conditional gradient method was implemented so as to have a customizable objective function, which is described in detail with coding examples. Several in-built features within the conditional gradient optimization routines are described.

Chapter V describes an application of the integrated water and power model to Grand Coulee, Banks Lake, and Chief Joseph. The calibration process that was used to find incremental inflows and losses is explained along with the model setup and associated objective functions for both water and power models. Scenarios were run in order to examine the flexibility of hydropower with regard to wind integration and the effect of transmission capacity on integrated wind-hydro operations.

Recommended future work, expected results, and potential applications of the integrated water and power modeling framework are discussed in Chapter VII. A free-of-charge generalized optimal power flow model should still be fully integrated into the framework using the full formulation of the overarching static optimization via Lagrangian Relaxation found in Chapter III. In addition, a dynamic optimization routine still needs to be formulated and developed that determines optimal operating policies while considering uncertain inputs including future RES power production, load, and streamflows.

II Literature Review

Many software tools have been developed to simulate and optimize water systems and associated operations. Simulating portions of a water system exist in the form of physically-based models, empirical models, and stochastic process relationships. A few examples include models for determining irrigation requirements, minimum instream flows for optimal fish habitat, or selective withdrawal for reservoir water quality models. Output from these field-scale or watershed-scale models are generally inputs for higher-level generalized river basin management models (RBMs), which attempt to operate the water system at the river-basin scale in an optimal way, considering operational constraints and objectives previously (or simultaneously) determined by finer scale models. A few widely-used, generalized RBMs are CALSIM [California Department of Water Resources (CDWR) 2002], RIBASIM (Deltares 2009), RiverWare [Center for Advanced Decision Support for Water and Environmental Systems (CADSWES) 2007], HEC-ResSim [U.S. Army Corps of Engineers (USACE) 2011], Mike Basin [Danish Hydraulic Institute (DHI) 2011], MODSIM (Labadie 2011), and WRAP (Wurbs 2011).

All of the RBMs employ static optimization of operations by allocating water based on priority within the current timestep. In addition, RiverWare provides an option for dynamic optimization via piece-wise linear programming that aids in defining optimal reservoir guide curves (CADSWES 2012). With regard to hydropower, both RiverWare and HEC-ResSim allow the user to specify electric power demand to control operations at a reservoir in addition to the normal guide curves or reservoir zones that are common to reservoir operations. Other RBMs simply calculate the power that could be generated from the water system given its operation without consideration of operations based on power demand.

Due to the complexity and individuality of every river basin, customization of an RBM is vital for generalization purposes. Several existing RBMs include some level of customization capability without reprogramming. RiverWare and CALSIM use interpreted languages (scripts) called Riverware Policy Language (RPL) and Water Resources Engineering Simulation Language (WRESL) respectively (CADSWES 2010; CDWR 2002). HEC-ResSim allows the user to define custom code using Jython scripting language, a Java-based implementation of Python. MODSIM utilizes events within its solution structure that allow a user to develop custom compiled code in any .Net language (C++, VB, or C#) and change any basin parameter during the iterative solution process (Labadie 2010).

Numerous power system models exist and serve electric grid management purposes globally. As in a water system, there are layers of complexity and detail within each model. Power grid operations are performed at many different timescales, with traditional power system management timescales described as shown in Table 1. However, variability in RES power production has caused a paradigm shift in contemporary operating practices, particularly with respect to formerly separable operating timescales (Xie et al. 2011). Boundaries between unit commitment and power dispatch problems are becoming increasingly blurred as extremes in wind power variability and uncertainty play a larger role within hourly and sub-hourly operations of interconnected power systems (GE Energy 2010; Xie et al. 2011).

Table 1: Timescales of power system management. Reproduced from Sharp et al. (1998), DeMeo et al. (2005), and Xie et al. (2011).

Function	Timescale
Automatic protection	Instantaneous
Disturbance response	Instantaneous to hours
Regulation and voltage control	Seconds to minutes
Load following	Minutes to hours
Economic dispatch	Minutes to hours
Transmission loading relief	Minutes to hours
Unit commitment	Hours to days
Transmission scheduling	Hour ahead to week ahead
Maintenance schedule	1 to 3 years
Transmission cost planning	2 to 10 years
Generation planning	2 to 10 years

A system of reservoirs can help mitigate the uncertainty of intermittent and highly variable wind and solar electric power sources by providing load following services, used interchangeably here as “firming.” This reduces uncertainty by providing a schedulable amount of power for a specific amount of time with limited variability within the time period, which aids operators of a system to provide a more reliable service. Several factors affect the modeling approach for load following with a group of reservoirs. Congestion and other transmission constraints should not be ignored since committing one hydropower unit instead of another unit should have a value associated with it if it relieves congestion, regulates frequency or voltage, or reactive power flow (Xie et al. 2011). Additionally, operational decisions of a system of large hydroelectric plants can impact the price of electric energy, which renders such plants as price-makers instead of price-takers within the electricity market. Such impacts on energy price can only be realistically determined when transmission constraints are considered within the model due to the economic cost of regulating transmission of power (Kirschen and Strbac 2004). Security constraints such as contingency failures can cause brown out and black outs in the system, and therefore the model should account for such failures. Traditional security-constrained economic dispatch and optimal power flow models minimize total cost of power

production, while satisfying some of the aforementioned security criteria. These models can be adapted to include look-ahead capability, or can be used as pure simulation models at operational timescales of interest for renewable integration. Other critical issues include quantifying and mitigating the loss of load expectation in the most economically viable fashion with high penetrations of intermittent RESs.

Many freeware, open-source, and proprietary economic dispatch and optimal power flow models exist for a wide range of applications. For research purposes, free software that allows customization via programming or scripting is essential (Milano 2005). For model development purposes, compatibility with other software via application programming interfaces (APIs) is also important. Writing input files, running an executable file, and reading output files from the hard drive is an undesirable task since these tasks might need to be performed multiple times during the simulation of a single timestep, and would therefore be computationally time consuming. Ideally, the model would have programmatic interaction capabilities within main memory, which is more computationally efficient process than reading and writing to disk assuming that enough main memory exists to house all the data being transferred.

1 Integrated Water and Power Systems Operations Models

Connolly et al. (2010) list computer models that simulate and optimize operations of power systems with renewable energy sources, generally for microgrids and distribution systems. ProdRisk is a hydro scheduling model that allows simulation of thermal, wind, convention hydropower, and pumped storage hydropower, but is not free and does not incorporate transmission constraints. EnergyPLAN is free and accounts for hydro power among many other power systems at the short-term scheduling timescale, but includes no transmission constraints and is limited by an over-simplified water system representation (Lund 2011). Other renewable

energy models are capable of accounting for other types of energy storage, but do not consider hydropower specifically. These models are primarily design for medium- to long-term planning, are expensive or otherwise unavailable, or cannot be used with high-voltage transmission systems (Connolly et al. 2010).

Vista is a proprietary model that optimizes scheduling and dispatch of water and power systems via successive linear optimization, and for some portions of the problem, dynamic programming (Bridgeman et al. n.d.). Vista utilizes a direct optimization approach (as opposed to a simulation-based optimization approach), wherein constraints of the water and power systems are satisfied within the optimization process, but require linearization assumptions, which are not appropriate for AC power flow models or hydropower optimization, which are nonlinear in nature.

Another program, HydroSCOPE (Laird 2011), is currently being developed by four different national laboratories: Argonne, Pacific Northwest, Oakridge, and Sandia, but is not presently available for public use. Work on HydroSCOPE contains five different major separable “pieces” as follows: 1) hydrologic forecasting, 2) seasonal hydro-systems analysis, 3) environmental performance, 4) unit and plant efficiency, and 5) day-ahead scheduling and real-time operations. HydroSCOPE generalizes the “commodity” in the network and allows users to define multi-commodity interaction such as water and power, but also suffers from the disadvantage of requiring linearization of the entire problem.

2 Areas Lacking in Research

The U.S. Department of Homeland Security Science and Technology Directorate (USDHS 2008) indicated a “serious unmet need” for integrated simulation models between various infrastructures (e.g., water supply and interconnected power systems), to help improve

recovery measures from regional or national-scale incidents within the national power grid. Both water and power system operators need to have the necessary tools to be able to analyze the effect of, for example, renewable energy integration on water system operations and to quantify the flexibility of hydropower facilities to mitigate challenges within power systems (GE Energy 2010; Loose 2011). Short-term hydropower planning models need to incorporate more realistic constraints as well as more reliable results (Vardanyan and Amelin 2011). Shortfalls in previous research areas seem to identify the need for a freely-available, integrated water and power systems operations model (IWPM).

With regard to water resources planning and management, water system research has simplified optimization of power production and associated sales of electricity while complying with environmental and legal constraints. Labadie (2004) describes state-of-the-art techniques used to optimize operations of multireservoir water systems that attempt to meet water supply, flood control, navigation, irrigation, recreation, fish and wildlife, water quality, and hydropower objectives. Most of the studies included hydropower scheduling with a highly simplified analysis of electric power systems or, in some cases, within regulated electricity markets and coarse timescales, which may be sufficient within hydro-thermal systems, but is not within hydro-thermal-renewable systems.

Many water researchers have simply maximized hydropower production while satisfying other water system constraints (Paudyal et al. 1990; Arnold et al. 1994; Tilmant et al. 2002; Yoo 2009; Moeini et al. 2011; Lee et al. 2007). McLaughlin and Velasco (1990) attempted to meet specified power output targets. Yi et al. (2003) maximized operating efficiency of a water and power system in order to meet power load demands, water demands, and reliability and security

requirements for the power system. However, power production and operation is often determined by power system economics.

Several water resources researchers have included power system economics in some form. Grygier and Stedinger (1995) analyzed a combined linear programming and dynamic programming technique while optimizing hydropower revenue with a temporally fixed on-peak and off-peak energy price. Hayes et al. (1998) developed a routine to maximize hydropower revenue while improving water quality downstream of reservoirs with fixed nodal electric energy price values using optimal control theory. Barros et al. (2003) used a single, previously-specified electrical energy price for all hydropower sales in the model. Others used an estimated unit value of hydropower at each reservoir to maximize revenue (Tejada-Guibert 1990; Trezos 1991). Zahraie and Karamouz (2004) utilized estimated total costs for reservoirs and energy price on an hourly basis in order to determine optimal economic dispatch of two reservoirs in parallel using demand-driven stochastic dynamic programming (DDSP). Alemu et al. (2011) incorporated uncertainty of streamflow and energy prices within the hydropower revenue problem by considering an empirically derived energy price error distribution.

In optimizing water system operations for hydropower revenue, current research in the water resources field has not yet realistically considered power system constraints and operational challenges, particularly for integration of renewable energy generation in either a regulated or deregulated electricity market. More sophisticated power system modeling is required for water managers to fully realize hydropower revenues while satisfying the plethora of environmental and legal requirements.

Power system models regarding hydro scheduling and unit commitment will often include representations of a hydropower system. Loose (2011) indicated that most renewable

energy integration studies have not dealt “effectively with the types of operating constraints that pertain to hydro.” GE Energy (2010), Holttinen et al. (2011), and Acker and Pete (2011) also reveal a lack of water system realism within renewable energy modeling studies.

In evaluating the potential integration of wind and solar into the energy grid, GE Energy (2010) and Bucher (2011) simulated and optimized hydropower revenue and production while constraining powerplant outflow between minimum and maximum turbine capacities. Others minimized operational costs in hydro scheduling with fixed bounds on discharge, storage levels, or energy production (Happ et al. 1971; Pereira and Pinto 1982; Le et al. 1983; Shaw et al. 1985; Habibollahzadeh and Bubenko 1986; Tong and Shahidehpour 1990; Yan et al. 1993; Rakic and Markovic 1994; Wong and Wong 1994; Saad et al. 1996; Luh et al. 1998; Rudolf and Bayrleithner 1999; Hindsberger and Ravn 2001; Padhy 2001; Zoumas et al. 2004; Mariano et al. 2009; Flach et al. 2010; Baslis and Bakirtzis 2011; Moussa et al. 2011; Rebennack et al. 2011). Over one hundred similar unit commitment problems that include fixed bounds on unit energy production, minimum up and down time, ramp rates, power balance, “Must run units,” “Must out units,” spinning reserve, and crew constraints (Padhy 2004; Yamin 2004). Madani and Lund (2009) represent and model reservoir storage in energy units for simplicity and ease at the cost of realism. Although hydro specific constraints can be imposed on some of the more sophisticated unit commitment problems, many water management operational decisions are affected by previous operational decisions, which need to be integrated into unit commitment problems for practicality of use at any time-scale.

Many hydrothermal coordination studies have incorporated realistic water system operational constraints. Several researchers have developed hydrothermal coordination models that utilize state-of-the-art hydro system models while minimizing total production cost of

thermal and hydro power resources at hourly and daily timescales (e.g., Turgeon 1980; Sherkat et al. 1985; Duncan et al. 1985; Divi and Ruiu 1989; Li et al. 1997; Li et al. 1998; Orero and Irving 1998; Redondo and Conejo 1999; Gröwe-Kuska et al. 2002; Finardi et al. 2005; Rakic and Markovic 2007; Catalão et al. 2010). Many hydrothermal scheduling models decompose the thermal and hydro problems into subproblems using successive approximations, heuristics, Benders decomposition, Lagrangian relaxation, and Genetic Algorithms (Yamin 2004). One such Lagrangian relaxation algorithm utilizes the advantages of network flow programming for satisfying water mass balance and dynamic programming for thermal unit commitment (Guan et al. 1999). Literature on algorithms using Lagrangian relaxation is discussed in detail in Section 4. Pereira and Pinto (1985) developed a decomposed, stochastic programming approach to minimize operation costs of multireservoir systems in a hydrothermal coordination context that allows for any streamflow simulation model to be represented stochastically. Stochastic dynamic programming approaches involve building multidimensional transition probability matrices for a problem with multiple state variables, which may be difficult and impractical for application in industry or other research efforts. Hydrothermal studies also do not consider highly variable and uncertain generation from deep penetration of renewable energy sources, which requires subhourly timescales and consideration of additional reserve requirements as well as ramping rates to counteract compromised security of electricity supply and delivery.

Models for integrating RESs have been developed, where studies have attempted to quantify the potential for energy storage. There include some common representations of pumped hydropower systems as a means of mitigating the uncertainties involved in sizable penetration of renewable energy sources using a DC power flow algorithm or co-located assumptions (Matevosyan 2008; Heussen et al. 2010; Jonas 2011; Bitar et al. 2011b). Price-taker

assumptions, where production and operational decisions of power generators do not impact the price of energy, are also common in renewable energy studies (Connolly et al. 2010; Bitar et al. 2011b; Vardanyan and Ameline 2011). Holttinen et al. (2009) discuss multiple wind integration studies that ranged from 15 minute timestep resolution to weekly with a variety of hydro and transmission system constraints, only a few of which are realistic. However, a sophisticated representation of the hydro system is required for practical application of renewable energy integration studies. Perhaps, the solution lies in adapting some of the older hydrothermal coordination techniques that incorporated many sophisticated water system operational considerations (as mentioned previously) to incorporate hydro-renewable coordination with consideration of finer timescales, ramping rates, and larger reserve requirements.

3 Requirements for an integrated water and power system model

Operating challenges posed by new environmental legislation, integration of RESs and smart grid technologies, and electricity market deregulation require improved modeling tools that can account for multiple critical resources including water and power systems. Renewable energy systems are extremely variable and unpredictable, unlike thermal plants and combustion type plants, and therefore present significant operational challenges. GE Energy (2010) indicated that for renewable energy integration to be feasible within the western interconnection (i.e., the large synchronous bulk electricity system in the western U.S.), transmission operators will need to make market decisions and generation forecasts at a sub-hourly timescale and that hydropower resources need the capability for more flexible operations. However, the feasibility of hydropower and other energy storage techniques to alleviate challenges introduced to the electric grid by renewable energy sources is location specific (Enernex Corporation 2011; Hessami and Bowly 2011; Hodge et al. 2011; Loose 2011). Therefore, an integrated model that simulates and

optimizes large, regional scale water and power system scheduling within both a deregulated and regulated electricity market structure at the hourly and sub-hourly level must exist for detailed analysis of both water and power system operations, provide security and reliability within each system, and help to establish economically viable solutions as RESs and smart grid technologies become more prevalent.

For research purposes, the integrated system model should be free, have flexible operating rules and elements that can be programmatically updated by users, and allow for fast simulation of many different types of situations. For management and commercialization purposes, an integrated water and power systems model must be robust and be supported by peer-reviewed research. The model must be highly efficient computationally for real-time use, and a user-friendly interface for inputting data. It must provide viable solutions that system operators could execute with confidence. Also, as justified by Xie et al. (2011), accurate simulation of both power systems and water systems must exist within the integrated model for purposes of practicality (i.e., helping to bridge the gap between science and industry), and to facilitate multiobjective optimization studies between unit commitment or economic dispatch problems and environmental considerations. Linear optimization techniques require simplifications that render solutions impractical and highly sensitive to input parameters. Therefore, nonlinear or adaptive learning optimization techniques should be used to incorporate more realism.

An integrated water and power systems operations model (IWPM) should allow the user to specify separate timescales for the water system than that of the power system. Efficiencies, limits on power and storage capacities, ramp rates, head-discharge curves, storage-elevation curves, and fixed and variable costs of each generator should be specified by the user. Large

water and power systems operations should be algorithmically treated differently than micro water and power systems in spatial scale, timescale, and associated assumptions (e.g., reactance-resistance ratio, X/R , for transmission of electricity affects appropriate simplifying assumptions). Due to the uncertainty in wind and solar power production, operating reserves should be treated nontraditionally (Chen et al. 2006). That is, up spinning reserves should be increased above the largest contingency requirement and load uncertainty since RES power production can rapidly decrease. Down spinning reserves also need to be heightened because RES power production can rapidly increase. For the same reasons, ramping rate constraints also need to be included in the generalized IWPM. Users should be able to evaluate the technical potential for hydropower to mitigate renewable energy sources without consideration of economic operation. However, economic dispatch and development of economically optimal dynamic operating policies (unit commitment) should be included in the model toolkit. The selected model structure for this study seems to provide most of the desirable characteristics of an IWPM.

III Model Structure – The Long-Term Goal

The previous two chapters discussed the operational challenges within water and power systems operations, and areas lacking in research, development, and demonstration with regard to inter-operational considerations between the two systems. Lack of realistic reservoir system operations within renewable energy modeling studies and optimization routines may perhaps have led to misleading results. Integrating two separate generalized models, one of water networks and one of power networks, should provide extensive insight into modeling studies such as those used to determine feasible amounts of renewable energy sources (RESs) to meet renewable energy integration goals. An integrated water and power model (IWPM) structure is discussed in this chapter, and has been designed in a way that many of the requirements discussed in Chapter II for an IWPM are reasonably satisfied. A three-level model structure was selected for development of an IWPM, of which only portions of the first level have been implemented. A description of the implemented portions of the IWPM can be found in Chapters IV and V, and its application to a case study in Chapter VI.

The first level consists of a static simulation procedure to satisfy water system priorities and minimize power production while satisfying system constraints for individual timesteps. The second level consists of a static (timestep-by-timestep) optimization procedure that optimally connects operation of both systems given weights or specified criteria to analyze tradeoffs between the two systems. The tradeoff space may include economic, security, and potentially, environmental criteria constrained by physical laws simulated within the first level of the model structure. The third level consists of a dynamic optimization that can account for time-varying and uncertainty factors such as ramp rates, cost of lost generation, startup costs, and lagged water routing. Figure 3 illustrates the selected model structure.

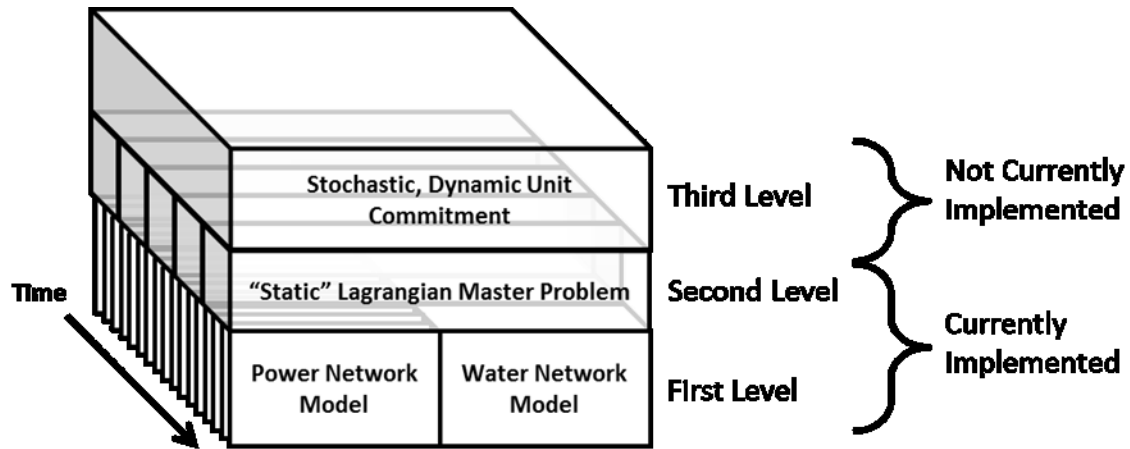


Figure 3: Three-level simulation and optimization model structure diagram

The first level of the model structure is the static optimization portion of the proposed integrated water and power systems operations model. In this model, two subproblems must be solved: water system priorities are optimized and power is scheduled in a cost-effective way that maintains system security constraints. Power dispatch can be done as optimal power flow, direct current power flow, economic dispatch, or other minimization formulations. Power model timestep sizes are user-defined and can be smaller than water network timesteps.

The second level of the model structure is a static optimization that connects the two water and power system models by decomposing them into subproblems. Lagrangian relaxation is a powerful method that can be used to decompose the water and power minimization problems so that they can be solved in parallel, that is, they do not have to be solved as a single integrated optimization problem (Conejo et al. 2006). As part of the method, Lagrangian relaxation places “coupling” constraints into the objective function. In this case, coupling, or complicating, constraints ensure that power produced in the water system model is the same as the power injected in the power system model. Within the objective function, these coupling constraints are multiplied by Lagrange multipliers that are dynamically updated during iterations in order to

ensure that the constraints are satisfied. Lagrange multiplier updating is generally done using a subgradient technique, but other techniques are available.

The third level of the model structure optimizes over the entire time period of the model. There are many optimization-based techniques for doing this, but the first two levels of this model structure restrict the use of such techniques because they are simulation models. Additionally, optimization-based methods might theoretically be used for this problem; however, the constraints would not be as well accounted for and many simplifications would be required for solving both the water and power system equations over the entire time horizon while considering uncertainty. Such simplifications may have been more appropriate before water and power systems were as over-committed and vulnerable as they are today with high demands, high uncertainty, and rapidly changing economic, social, and environmental conditions. Therefore, a simulation-based optimization approach called reinforcement learning (RL) was selected for the third level dynamic optimization. This RL procedure is not implemented yet, but a short description is found here and in Chapter VII for reference in future work.

Simulation-based optimization allows well-calibrated simulation models to be used to model the system while optimizing decisions while accounting for uncertainty and doing so without implicit assumptions about the process. For RL, the simulation model can be nonlinear, nonconvex, nonsmooth, discontinuous, and have other ugly attributes that other optimization routines cannot solve. RL lends itself really well to significant multi-processing and distributed computing. RL optimizes operations in a way similar to that of an operator by utilizing previous knowledge of the system to make a decision at the current timestep. A penalty is associated with making wrong decisions and a reward is associated with making the right decisions. RL “learns” how to achieve rewards and makes decisions based on a tradeoff of achieving the reward and

exploring unknown territory. In this regard, an operator is more likely to understand how this particular machine learning approach works, and can then utilize it to its full potential. Also, during simulation, optimal policies are updated from timestep to timestep, and therefore a fairly good approximation of optimal policies can be made before a simulation has completed, which could be extremely useful in real-time applications such as model-predictive control.

1 Water Network Formulation

Water management varies from system to system, and includes many different stakeholders and operational considerations including water supply, irrigation, flood control, navigation, water quality, fish and wildlife, recreation, and hydropower. Therefore, a generalized model with fast, customizable solving capabilities to optimize water system operations is essential for real-world application.

MODSIM (Labadie 2010) seems to fit the desirable characteristics of a water systems model due to its fast solver, free availability, user interface, easily customizable modeling capabilities, and compiled custom code rather than an interpreted language. Interpreted languages are not only slower than compiled languages when being called upon repeatedly, but they also do not offer system modelers as much flexibility. MODSIM is built on the Microsoft .Net framework, and allows code to be written in C#.Net or VB.Net. MODSIM provides a graphical user interface (GUI) that allows construction of the network topology using drag-and-drop icons of network features such as reservoirs and demand nodes. Users can directly draw desired links connecting to any features. MODSIM also allows the user to create their own custom code using objects within MODSIM compiled libraries, compile their code, create an executable file, and run the executable as optimized, compiled code.

Another reason MODSIM was selected over other packages is the fact that it uses a legitimate linear programming technique for minimization, which renders the conditional gradient method a feasible option. Heuristic techniques for solving water systems, as found in many other water modeling software packages, would not be suitable for the selected overarching optimization routines.

A specialized Lagrangian relaxation algorithm is implemented in MODSIM to solve a network flow problem described by Labadie (2010) which is copied below as Eq. (1) for convenience.

$$\min_{\vec{x}} \sum_{(i,j) \in A} c_{ij} q_{ij} \quad (1)$$

subject to:

$$l_{ij} \leq q_{ij} \leq u_{ij} \quad (2)$$

$$\sum_{\{j|(i,j) \in A\}} q_{ij} - \sum_{\{j|(j,i) \in A\}} q_{ji} = 0; i = 1, \dots, N \quad (3)$$

where arc (i, j) is the link between node i and node j with flow rate q_{ij} , lower bound l_{ij} , upper bound u_{ij} , and cost per unit flow c_{ij} ; N is the total number of nodes, and A is the set of all links in the network. To simplify the formulation, the vectors of costs and flows in will be represented by \mathbf{c} and \mathbf{q} respectively, and the associated objective function will be represented by $\mathbf{c}^T \mathbf{q}$. Link costs do not necessarily represent monetary costs, but provide a way to model system priorities. For example, a link delivering water to a senior water right holder would have a large negative cost associated with it, and a link delivering water to a junior water right holder would have a smaller negative cost. Since the algorithm solves a minimization problem, larger negative costs can be thought of as “benefits” that give a priority to deliver water for certain purposes such as senior water right holders. Labadie (2010) describes the full formulation of the

Lagrangian relaxation method used to iteratively solve the network flow problem and account for nonlinearities using successive approximations, which performs well in water networks since they do not tend to exhibit chaotic behavior.

New functionality in MODSIM was required prior to implementation within the model structure described in above, including sub-daily timesteps. MODSIM required upgrading of its hydropower modeling capabilities, such as allowing multiple hydropower units per reservoir, pumped storage considerations, and the capability to match user-specified hydropower targets or other nonlinear objective functions are defined by the user.

In order to match a particular hydropower target, two algorithms have been formulated: a simple successive approximations technique and a mathematical optimization routine called the conditional gradient method, or Frank-Wolfe algorithm (Bertsekas 1995; Brännlund et al. 1988; Habibollahzadeh et al. 1990; Sheble and Fahd 1994; Dai and Labadie 2001). The successive approximations algorithm sets discharge through hydropower links in a fashion that iteratively brings calculated power closer to a specified power target. The conditional gradient method can utilize the efficient network flow structure in the model and solve a nonlinear objective function.

Successive approximations, which iteratively updates decision variables until a particular objective is met, in this case the objective is to minimize the distance between the calculated hydropower production and a specified hydropower target. At each iteration, the upper bound u_i on a link i representing discharge through a hydropower unit is set using an approximation as shown in Eq. (4). Cost of link i needs to be negative, which draws flow through the link up to its upper bound u_i . Magnitude of the cost is set with respect to the system priority for meeting a hydropower target. This approximation iteratively changes flow through the link until an energy target $E_{targ,k}$ is met or outside the bounds of what can be attained.

$$u_i = \frac{E_{targ,k}}{\sum_{j \in HT_k} \left(k \hat{\eta}_j \hat{h}_j \left[\sum_{i' \in HU_j} \hat{q}_{i'} \right] \Delta t \right)} \hat{q}_i \quad \forall k \in HT \quad (4)$$

Eq. (4) displays the iterative equation used to set the upper bound of a link, when there are multiple links that define discharge through a hydropower unit j and multiple hydropower units used to meet a particular hydropower target k , where HU_j is the set of all links within hydropower unit j , HT_k is the set of all hydropower units used to meet hydropower target k , and HT is the set of all hydropower targets. Variables with the circumflex ($\hat{}$) represent values that were calculated in the previous iteration. This successive approximations approach can be used to match hydropower targets for problems where the head does not decrease faster than increases in outflow relative to their effect on hydropower. In mathematical terms, the derivative of the hydropower production equation with respect to flow through the turbine must be greater than zero in order for discharge increases to result in hydropower production increases as follows in Eq. (5):

$$\frac{\delta P}{\delta q} = k \left(\eta h + q \eta \frac{\delta h}{\delta q} + h \frac{\delta \eta}{\delta q} \right) > 0 \quad (5)$$

If change in efficiency with respect to change in flow $\delta \eta / \delta q$ is relatively small in magnitude, then the condition can be simplified to be:

$$\frac{h}{q} > - \frac{\delta h}{\delta q}$$

If these conditions are not met, then the successive approximations approach may not be able to find the specified target.

To meet a hydropower target, using the conditional gradient method, the objective function can be the squared difference between the simulated hydropower production and the hydropower target. The minimum of this function is the point where outflow, head, and turbine

efficiency produce enough electric power to satisfy the target. Every feasible direction leading away from the optimum is up-sloping because of the squared term. This objective function aids the water network in matching hydropower targets produced by a power system routine. In mathematical terms, the hydropower target problem could be formulated in general as in Eq. (6) for turbines and Eq. (7) for pumps.

$$\min_{q_j} (kq_j h_j \eta_j - P_{gen,j})^2 \quad \forall j \in R_{turbines} \quad (6)$$

$$\min_{q_j} \left(\frac{kq_j h_j}{\eta_j} - P_{use,j} \right)^2 \quad \forall j \in R_{pumps} \quad (7)$$

subject to water system constraints (2) and (3) where $R_{turbines}$ is the set of all hydropower generating units with a power target defined and R_{pumps} is the set of all pumping units. Production and consumption targets $P_{gen,j}$ and $P_{use,j}$ would be generated from a power system model. Other terms q_j , h_j , and η_j are release decisions, elevation head, and efficiency, respectively, for hydroelectric unit or plant j . The constant k contains the specific weight of water, and units conversion terms. For pumps, $P_{use,j}$ is negative and head h_j is defined as the lower elevation minus the higher so that power consumption is considered as power extracted from the power system.

The conditional gradient algorithm has previously been integrated with MODSIM (Dai and Labadie 2001), and can perform optimization without linearization of the objective function. Additionally, the algorithm maintains the original network structure constructed within MODSIM. Therefore, no changes to the MODSIM solver are required to implement the conditional gradient method. The technique rapidly converges to the neighborhood of the optimal solution, but attains highly precise optimal solutions more slowly. However, highly precise solutions are rarely required in real-world applications due to lack of precision in

measurements of model inputs. Nonetheless, the conditional gradient method will provide a method for evaluating tradeoffs between water system objectives and power system objectives with potentially good results (Brännlund et al. 1988; Habibollahzadeh et al. 1990; Sheble and Fahd 1994).

In mathematical terms, the condition gradient method can be described as follows. Given the following objective function:

$$\min_{\mathbf{x}} f(\mathbf{x})$$

subject to:

$$A\mathbf{x} \geq \mathbf{b}$$

$$\mathbf{x} \geq 0$$

During the solution procedure, the conditional gradient method finds a feasible direction by solving a linear programming subproblem of the following form using common linear programming techniques:

$$\min_{\mathbf{x}} \nabla f_{\mathbf{x}}(\mathbf{y}^{(k)}) \cdot \mathbf{x}$$

subject to:

$$A\mathbf{x} \geq \mathbf{b}$$

$$\mathbf{x} \geq 0$$

After solution of the linear programming problem, a linear search to find α is performed over the full nonlinear objective function:

$$\min_{\alpha} f(\alpha \mathbf{y}^{(k)} + (1 - \alpha) \mathbf{y}^{(k-1)})$$

subject to:

$$0 \leq \alpha \leq 1$$

where k is the current iteration and $k - 1$ refers to the previous iteration. Initialization of $\mathbf{y}^{(0)}$ must be a feasible solution and is generally just the optimal answer to the linear programming problem with an arbitrary cost vector. The linear programming solutions only provide a feasible direction, and since the constraint set is linear, all values between solutions $\mathbf{y}^{(k)}$ and $\mathbf{y}^{(k-1)}$ are also feasible. Figure 4 provides a flow chart of the conditional gradient method as applied to a network flow problem such as the solver in MODSIM.

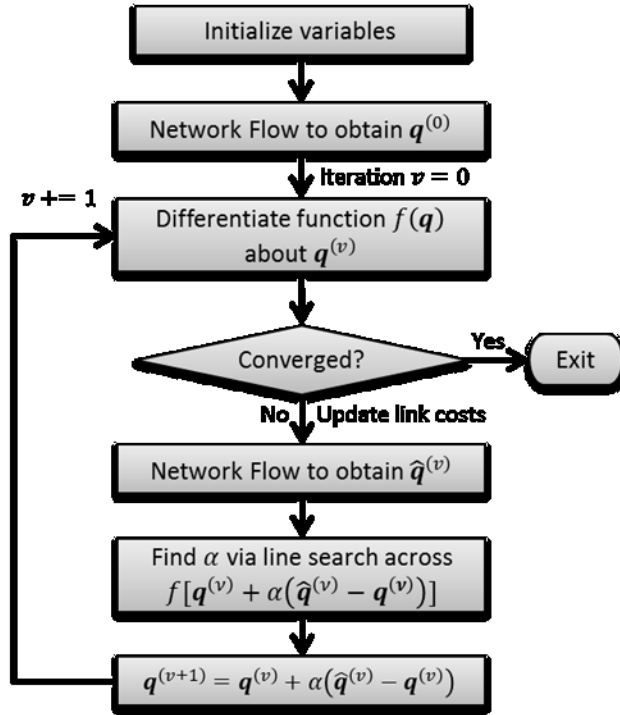


Figure 4: Flow diagram of the conditional gradient algorithm applied to a network flow problem

MODSIM uses successive approximations in order to estimate dampened processes such as reservoir evaporation, groundwater infiltration and time-lagged streamflows. Thus, “network flow” in Figure 4, when applied to MODSIM, refers to the iterative procedure to solve a MODSIM river and reservoir network described by Labadie (2010). Routing is a special linear constraint that violates the network flow structure of the problem, or more precisely, the mass balance within a current timestep. Special considerations needed to be included in the

implementation of the conditional gradient method in order to effectively deal with inter-temporal constraints such as routing, which is discussed in further detail in Chapter IV.

2 Power Systems Operations Model Formulations

Optimal power flow algorithms aim to minimize the total cost of production while satisfying physical laws of electric power flow across transmission lines between interconnected power systems. Basically, it is optimizing over the same production cost equation as in economic dispatch problems with additional constraints: the power flow equations. A simple formulation of the economic dispatch problem is given in Eqs. (8)-(10).

$$\min_{\mathbf{P}} \sum_{i=1}^n f(P_i) \quad (8)$$

subject to:

$$\sum P_i = P_{load} + P_{losses} \quad (9)$$

$$P_{min,i} \leq P_i \leq P_{max,i} \quad (10)$$

where P_i is the scheduled power production at dispatchable units, P_{load} and P_{losses} are the load on the power system and power losses, and $P_{min,i}$ and $P_{max,i}$ are minimum and maximum generating capacities for a particular hydropower unit i .

Happ (1977) provides a more comprehensive formulation of security-constrained economic dispatch problems. Optimal power flow (OPF) goes beyond economic dispatch in the capability to adjust many more parameters that often map to actual control devices such as generator voltage, transformer tap positions, switch capacitor settings, load shedding, etc (Petrovic and Kralj 1993). OPF algorithms use the same objective function as the economic dispatch algorithms, but add power flow constraints to the problem, thereby rendering the

optimal policies more usable and practical for realistic operations. The constraints added to the optimal power flow problem are shown subsequently in Eq. (11).

Power flow problems are configured with structures called buses and branches, representing essentially nodes and links in a network of interconnected power systems. Each branch connects two different buses, and has a resistance and reactance R and X . Resistance is opposition to electrical current, and reactance is opposition to change in the electrical current. A purely reactive line only shifts oscillations of current as it flows through a line, but a resistive line actually extracts power from the system. Impedance is defined as a complex number $Z = R + jX$. According to ohm's law, the voltage drop across a line within a circuit $V = IZ$, where I is the current flowing through the line. Admittance Y is simply the reciprocal of impedance (i.e., $Y = 1/Z$). It therefore follows that the voltage drop across a line is $V = I/Y$ and the current $I = YV$. If the voltage difference between any bus i and ground is denoted as E_i , then the current passing from bus i to bus k is $I_{ik} = Y_{ik}(E_i - E_k)$. In matrix form, this equation is represented as follows:

$$\mathbf{I} = \mathbf{Y}\mathbf{E} \quad (11)$$

Using this equation, a matrix of admittances can be constructed that solves this equation for n buses. The $n \times n$ matrix of admittance values is denoted as \mathbf{Y} for an entire interconnected power system with n buses, with \mathbf{I} defined as a vector of currents injected into the network (i.e., each element I_i is the current injected at bus i), and \mathbf{E} denotes an n -sized vector of voltages at each bus.

Eq. (11) must hold according to the physical laws of electric power flow. Equations can be formulated that incorporate both active power P_i and reactive power Q_i at each bus i , calculated as in Eq. (12).

$$P_i + jQ_i = E_i I_i^* \quad (12)$$

As a note, the conjugate of a complex number is denoted by an asterisk, where the conjugate of $I_i = a + jb$ is $I_i^* = a - jb$. Additional bounding constraints are given in Eqs. (13) and (14), where $|E|$ represents the magnitude of the complex voltage value.

$$Q_{min,i} \leq Q_i \leq Q_{max,i} \quad (13)$$

$$|E_{min,i}| \leq |E_i| \leq |E_{max,i}| \quad (14)$$

A major assumption in application of these equations for transmission systems is that interconnected power systems can be represented as a circuit with a single line connecting two different buses. In reality, there are either three or four transmission lines that connect alternating current (AC) power systems. However, this can be a reasonable approximation as long as generator speeds remain stable and the power system has reached a “steady state.” For more information, Wood and Wollenberg (1984) provide a classic description of power flow and optimal power flow formulations and solution algorithms.

Additional constraints and requirements can be added to the formulation using various techniques. Such additional constraints can be transmission line capacity constraints, system up and down spinning reserve requirements, wind power production curve constraints, etc. OPF can be formulated as multi-area and also solve a decentralized scenario where production cost functions of generators are step functions rather than smooth curves, which are of particular interest in modern deregulated power systems. Conejo et al. (2006) and Lu et al. (2008) describe these other formulations and associated solution algorithms.

For the selected model structure, either static or dynamic power system dispatch could potentially be performed (Xia and Elaiw 2010). Optimal dynamic dispatch (ODD) considers system state at multiple timesteps, unlike static dispatch. ODD therefore provides optimal

dispatch with ramp rate constraints, associated additional costs, and load and generation forecasts. Uncertainties could also be incorporated into ODD problems, but would make the problem much more complicated for systems such as interconnected hydropower units where decisions of one hydropower unit will affect the possible decisions of another hydropower unit in the same river system. ODD also requires more computer time to solve. If an overarching dynamic unit commitment is performed for the entire modeling time period, optimal power flow will need to be solved over each of many every timesteps. If ODD is used as the OPF algorithm at each timestep, computation time for the dynamic unit commitment problem may become lengthy.

A likely way that reservoir units can serve in intermittent RES integration is “load following.” Although load following traditionally refers to following power consumption patterns of load centers, recently the term has also come to mean following variable and uncertain RES production. Load following is on the order of several minutes to a few hours (DeMeo et al. 2005), and has been trending toward the finer part of that timescale due to increasing penetration of uncertain power generators. Water infrastructure is typically operated on the order of hours to days. Steady-state modeling timesteps of each system should more or less be represented according to their corresponding operating timescales. Water network solutions will generally have a coarser timestep than power flow solutions, and an IWPM should allow the user to specify a different timestep for the water system than for the power system. Figure 5 displays the timescale comparison between simulations of the two systems during the static optimization step. Currently, there is a one-to-one ratio of timescales, that is, the timestep size within the water model is the same as that in the power system model. Thus, descriptions

given here are suggestions for and formulations of a generalized IWPM that could be implemented in the future.

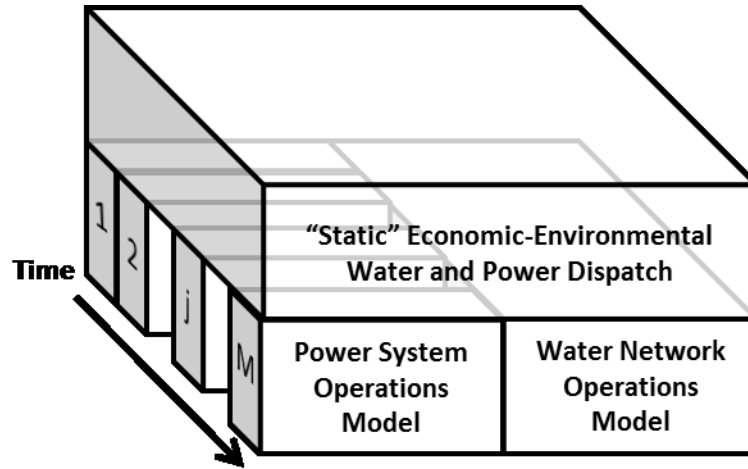


Figure 5: Modeling timescale coordination between water and power operations where M steady-state power system solutions are solved within one water system solution

In reality, regional variations exist for RES load following because of varying degrees of RES penetration. Some load following procedures may be an hour or two, but others may be a quarter of an hour. Typically, load following is not accomplished with automatic generation control, and therefore could not be performed at short time increments such as one-minute.

Ramping rates vary widely between hydropower facilities, where Beaudin et al. (2010) describe a plant with a ramping rate near 100 MW/min, and another at almost 7,000 MW/min. Ramping rates for pumped hydro storage can either be governed by a reversible pump-turbine, or simultaneous operation of a pump and a turbine. A reversible pump may require about 5 minutes to switch directions. Each of these considerations should be included in a generalized IWPM, but have not been fully implemented within this study.

3 Multiple Objectives: Environment and Economic Efficiency

As policy imposes more operational restrictions in support of a sustainable environmental, operators of both water and power systems are increasingly attempting to

dispatch resources in both an economic and environmentally efficient manner. Water system operators often do not even dispatch according to economics, because other priorities such as flood control, water rights, or instream flows take precedence. Economic dispatch aims to economically schedule power resources to meet system load (Petrovic and Kralj 1993). Environmental dispatch is exactly the same except it is aimed at minimizing adverse impacts to the environment or at bringing impacts down to an acceptable level (Petrovic and Kralj 1993). For an IWPM, economic and environmental considerations exist in both water and power systems, as summarized in Table 2 and Table 3. Water systems clearly consider more extensive environmental and social criteria than power systems, and therefore require more stringent social and environmental constraints and objectives.

Table 2: Economic factors in water and power systems operations

Fixed Costs	
Water	Non-Hydro Power
<ul style="list-style-type: none"> • Equipment and construction costs, replacement costs (dams, turbines, conduits, canals, etc.) • Water rights (irrigation, navigation, etc.) • Land, rights of way (backwater for dams, dams) • Preliminary studies and environmental impact statements 	<ul style="list-style-type: none"> • Equipment and construction costs, replacement costs (generators, substations, transmission, etc.) • Water rights (cooling water) • Land, rights of way (transmission lines, substations, generators) • Preliminary studies and environmental impact statements
Operating Costs	
Water	Non-Hydro Power
<ul style="list-style-type: none"> • Labor cost • Efficiency improvements • Environmental compliance (fines and equipment or operating modifications) • Water losses • Flooding • Drought induced expenses (food production, water treatment) • Legal compliance (water rights and interstate agreements) • Cap-and-trade emissions 	<ul style="list-style-type: none"> • Fuel, transmission, labor cost • Efficiency improvements • Environmental compliance (fines and equipment or operating modifications) • Energy losses and equipment usage • Cap-and-trade emissions
Operating Revenue	
Water	Non-Hydro Power
<ul style="list-style-type: none"> • Energy sales • Water rights sales or trades • Agricultural production and sales • Taxes • Recreation (fishing, boating, camping, etc.) • Navigation • Cap-and-trade emissions 	<ul style="list-style-type: none"> • Energy sales • Water rights sales or trades • Taxes • Transmission usage and wheeling sales • Cap-and-trade emissions

Table 3: Social and environmental concerns due to water and power systems operations

Water	Non-Hydro Power
<ul style="list-style-type: none"> • Pollution from temperature, pathogenic organisms, organic waste, chemicals, acid mine drainage, and carcinogens (contribute to diseases, infections, human safety concerns, eutrophication, hypoxia, and algal and other biomass blooms) • Sediments and turbidity (decrease photosynthesis, dissolved oxygen, and fish populations) • Pesticides, nitrate, phosphate, and salt from farming or sewage (contribute to saline surface water and groundwater, and infertile soil) • Water supply, water and wastewater treatment, wastewater return flows • River ecology and ecosystems, endangered species, fisheries, parks, fish & wildlife, and natural flooding • Deforestation • Scenery 	<ul style="list-style-type: none"> • Pollutant, particulates, and greenhouse gas emissions / imission (contribute to smog and acid rain, lower air quality, and climate change) • Water usage: consumption and heat transfer • Nuclear waste • Scenery

Conflicting objectives and tradeoffs need to be explored in order to make informed decisions on operations of such systems. A mathematical technique called Lagrangian Relaxation (LR) could be used to decompose the IWPM problem into water and power subproblems using a scheme that easily allows for parallel computation of both water and power system models.

4 Lagrangian Relaxation to Connect Water and Power Models

Since Petrovic and Kralj (1993) and others have concluded that mathematical programming techniques have clear advantages over heuristic or intuitive methods with regard to economic or environmental dispatch, the latter techniques are not considered herein. Mathematical programming approaches can efficiently solve problems and provide proven optimal answers given smooth, convex objective functions (Xia and Elaiw 2010). Such approaches include linear programming, successive linear programming, successive approximation, the lambda iterative method, Lagrangian relaxation, interior point, generalized reduced gradient, quadratic programming, quasi-Newton methods, and other nonlinear optimization methods. Petrovic and Kralj (1993) described various amounts of detail in objectives, constraints, and problem setup within different mathematical dispatch algorithms under a regulated electricity environment. Wang et al. (2007) discussed and formulated three algorithms to handle the discrete cost functions of deregulated electricity markets. Simplifications of power system and qualitative constraint representations are unavoidable to accommodate mathematical programming structures (Pandya and Joshi 2008; Xia and Elaiw 2010). Additionally, they will likely converge to local optima for multimodal objective functions. Still, mathematical programming techniques are used for their high speed in finding solutions as compared with artificial intelligence techniques described in the next section.

Mathematical decomposition techniques such as Benders decomposition (BD), Lagrangian relaxation (LR), and Cross decomposition (CD) can be used to reduce the large size of unit commitment problems into smaller manageable ones (Padhy 2004; Conejo et al. 2006; Marmolejo et al. 2011). For a realistic coupling between the hydro system and the power system, a nonlinear coupling constraint is to be used. Therefore, BD, and consequently CD, cannot be used because of linear coupling constraint requirements (Li and McCalley 2008).

LR is a popular technique for hydrothermal coordination problems because of its speed and capability to separate water network constraints from power network constraints. Advantages of LR include optimization over the smaller dual problem and subproblems (decomposed over time or space), relative ease of adding new constraints, and generally rapid solution time. Bundle methods, trust region, or evolutionary methods used to traverse the dual surface seem to improve convergence speed and reliability (Luh et al. 1998; Redondo and Conejo 1999; Borghetti et al. 2001; Ongsakul and Petcharaks 2004; Conejo et al. 2006). However, the structure for LR leads to convergence problems and inherently suboptimal answers for nonconvex problems due to a duality gap, which approaches zero for larger systems (Cohen and Sherkat 1987; Xie et al. 2011). Also, since LR is a deterministic optimization method, implicit stochastic optimization is likely required to be able to generate optimal policies based on optimal unit commitment or economic dispatch, although some have introduced stochastic formulations of the LR problem (Carpentier et al. 1996; Dentcheve and Römisch 1998; Takriti and Birge 2000; Gröwe-Kuska et al. 2002; Nowak 2000; Nürnberg and Römisch 2002). Table 4 displays the extensive literature on the application of LR to unit commitment and hydrothermal coordination.

Although all literature on the application of LR in Table 4 applies to unit commitment in general or to hydrothermal coordination, it may be possible to connect hydro scheduling with wind (or other renewable energy source) scheduling in much the same way. A conceptual diagram of the LR procedure as applied within an IWPM setting is shown in Figure 6.

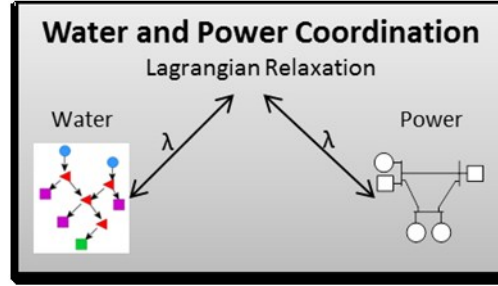


Figure 6: A simplified diagram of the Lagrangian Relaxation procedure applied to the integrated water and power systems problem

Eq. (15) is a formulation of an LR objective function that effectively connects water and power models at each water system timestep. LR decomposes the water and power problems into two subproblems which are connected together through a master problem that solves the dual of the problem to ensure that the coupling constraints are satisfied. In the case of an IWPM, coupling constraints ensure that power produced from the water system model matches the power injected into the power system model. However, there is a slight distinction between non-dispatchable reservoirs and dispatchable reservoirs in the formulation such that non-dispatchable reservoirs are basically considered a negative load in the power system model and are iteratively updated throughout the solution of the master problem.

$$\begin{aligned}
L(\mathbf{q}, \mathbf{P}, \boldsymbol{\lambda}, \boldsymbol{\mu}) = & \mathbf{c}^T \mathbf{q} + \sum_{j \in G} C_j(P_j) \\
& + \sum_{\tau=1}^{N_P} \lambda_{\tau} \left(\frac{\sum_{i \in R_N} k q_i h_i \eta_i}{N_P} + \sum_{j \in G - R_N} P_{j\tau} - D_{\tau} - L_{\tau} \right) \\
& + \sum_{j \in R_D} \mu_j \left(k q_j h_j \eta_j - \frac{\sum_{\tau=1}^{N_P} P_{j\tau}}{N_P} \right)
\end{aligned} \tag{15}$$

subject to (2), (3), and (9)-(14). Constraints (2) and (3) associated with the water network model are not solved within the power network subproblem or the master problem. Similarly, power system constraints (9)-(14) are not solved by the water network subproblem or master problem.

The vectors of costs \mathbf{c} and flows \mathbf{q} refer to costs and flows associated with links within the water network. Active power \mathbf{P} refers to active power injections into the power system model, and h_i , η_i , and k are the same as in (6) as used for calculated active power produced from the water network. The number of power system timesteps within one water network timestep is N_P . D_{τ} and L_{τ} are active power demands and losses; and G , R_N , and R_D are sets of all generation units, non-dispatchable reservoirs, and dispatchable reservoirs, respectively.

Lagrange multipliers $\boldsymbol{\lambda}$ and $\boldsymbol{\mu}$ are multiplied by the coupling constraints between the water and power system. The first coupling constraint multiplied by $\boldsymbol{\lambda}$ ensures that hydro production of non-dispatchable reservoirs (denoted by the set R_N) is included in the power balance equation. The second coupling constraint multiplied by $\boldsymbol{\mu}$ ensures that each dispatchable reservoir produces the same amount of power within the water system model as in the power system model. Lagrange multipliers can be solved using any of the aforementioned techniques, such as subgradient, bundle, trust region, or evolutionary methods. A solution procedure is illustrated in Figure 7.

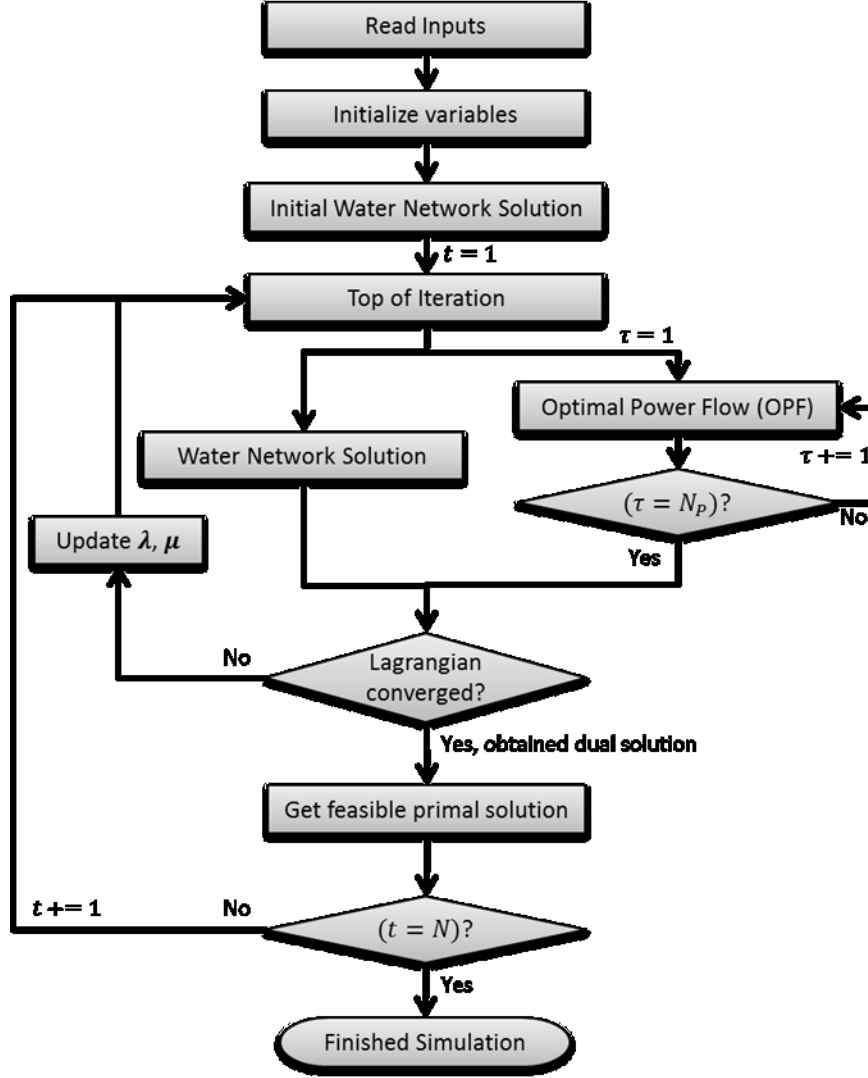


Figure 7: Flow diagram of the Lagrangian relaxation solution procedure

There are N fixed-size water network timesteps within the simulated time period. “Water Network Solution” in Figure 7 refers to a MODSIM solution with the overarching conditional gradient method configuration shown in Figure 4. The power network solution labeled “Optimal Power Flow (OPF)” could also be an economic dispatch or some other type of power dispatch algorithm that is performed N_p times per water network timestep. Updates to Lagrange multipliers are done using equations shown in Figure 8, or could be updated according to Conejo et al. (2006) or Bertsekas (1995). Both water and power simulation models must converge at

each iteration of the Lagrangian relaxation procedure. When the Lagrangian relaxation procedure has converged to a desirable tolerance, a feasible primal solution must be found.

Conejo et al. (2006, pp. 210-223) describes a particular implementation of the LR technique known as the optimality condition decomposition (OCD) procedure for decomposing problems where successive approximations of coupling constraints can be placed as constraints into each individual subproblem. OCD effectively helps to guide the update of Lagrange multipliers by including knowledge of the system from prior iterations, and therefore convergence of Lagrange multipliers occurs in fewer iterations with less oscillating behavior than both LR and Augmented LR. Such characteristics may make OCD a good choice for an IWPM. Figure 8 displays a conceptual design for the OCD procedure as applied to the IWPM problem. Only a simple subgradient technique has been implemented within code to update Lagrange multipliers.

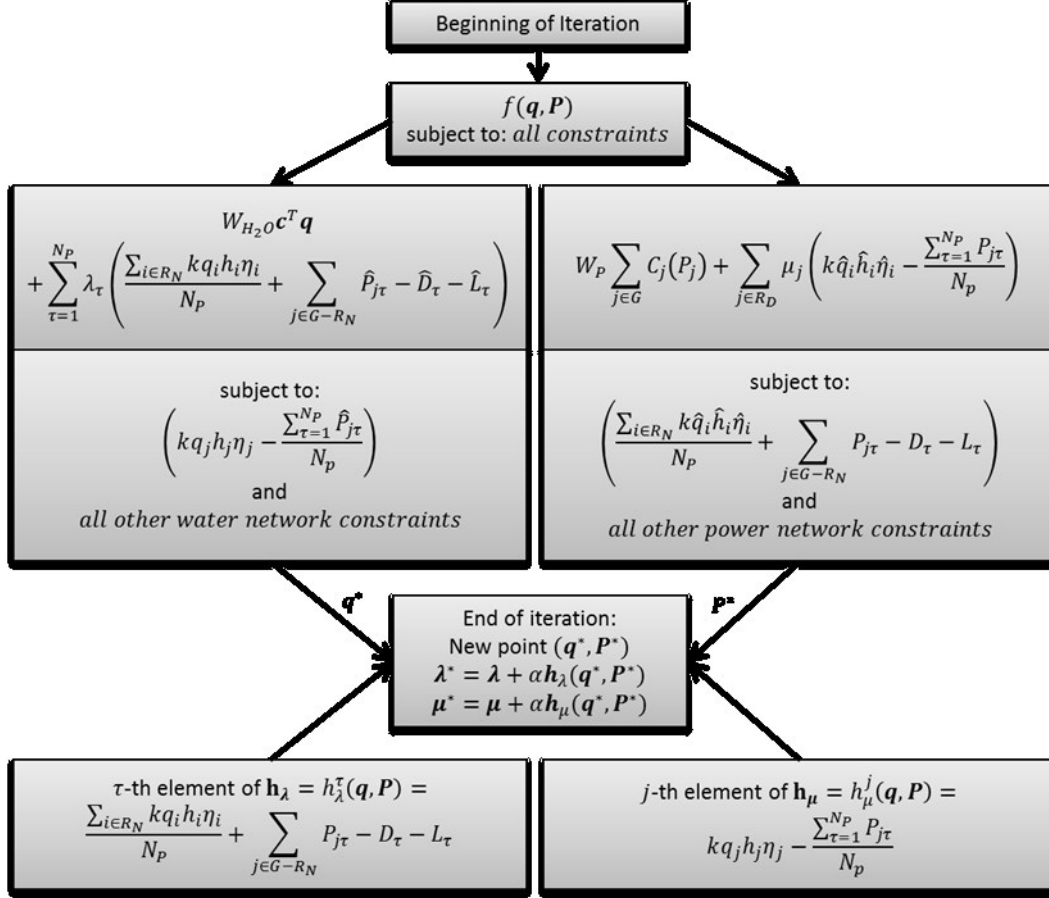


Figure 8: Solution flow of the optimality condition decomposition procedure as applied to the IWPM problem

This formulation allows the water network and power network to be solved in parallel as illustrated in both Figure 7 and Figure 8. Weights W_{H_2O} and W_P provide a means to perform multi-objective analysis between water system priorities and the cost of power production. An overarching dynamic optimization can be used to explore the Pareto optimal curve while considering time-varying factors, but is not included in this research.

Lagrange multipliers are updated using a simple gradient ascent where $\mathbf{h}_{\lambda}(\mathbf{q}, \mathbf{P})$ is the gradient of the Lagrangian function $L(\mathbf{q}, \mathbf{P})$ with respect to λ as shown by taking the derivative of the following Lagrangian function:

$$L(\mathbf{q}, \mathbf{P}) = f_{H_2O}(\mathbf{q}) + f_P(\mathbf{P}) + \lambda^T \mathbf{h}_{\lambda}(\mathbf{q}, \mathbf{P}) + \mu^T \mathbf{h}_{\mu}(\mathbf{q}, \mathbf{P})$$

The gradient of $L(\mathbf{q}, \mathbf{P})$ with respect to λ is shown by the following:

$$\nabla_{\lambda} L(q, P) = h_{\lambda}(q, P)$$

and with respect to μ :

$$\nabla_{\mu} L(q, P) = h_{\mu}(q, P)$$

At the end of each timestep, the Lagrange multipliers will have achieved an “optimal” value, which corresponds to an imputed value of water for that particular reservoir with respect to electric power production. This value can be used to optimally select bidding prices within a deregulated electricity environment as well as assess the economic tradeoffs of other criteria, such as flood control, water supply, irrigation, navigation, environmental, water quality, and other important economic considerations. Due to its relatively rapid convergence, computational efficiency, and parallelizability, Lagrangian relaxation is the selected method to be used to connect water and power system models at each timestep, but this in its full form has not yet been fully implemented within the IWPM.

5 **Artificial intelligence**

Since all details and objectives cannot be accurately incorporated into mathematical models, simplifications have to be made. Evolutionary programming techniques, however, can include a wide variety of integer and continuous variables; any constraints; and optimize over nonlinear, nondifferentiable, nonsmooth, and nonconvex objective function surfaces. In general, artificial intelligence (AI) techniques such as fuzzy set theory, artificial neural networks (ANNs), evolutionary programming (EP), genetic algorithms (GAs), particle swarm optimization (PSO), simulated annealing (SA), function optimization by learning automata (FOLA), reinforcement learning (RL), and ant colony optimization (ACO) are suitable methodologies for multiobjective studies because they can provide many nondominated solutions in one optimization run. This is in contrast mathematical programming approaches requiring many optimization runs (Pandya

and Joshi 2008). Also, AI methods are often shown to achieve near *global* optimum rather than simply local optima, in which mathematical techniques often become trapped while optimizing over multimodal or nonsmooth objective functions (Warsono et al. 2008). Thus, many AI methods will outperform some of the more popular mathematical techniques in finding optimal solutions as exemplified in the comparison between GA and LR unit commitment techniques by Kazarlis et al. (1996).

Some disadvantages of AI techniques in general are that they can suffer from long computation times and lack of theoretical convergence proofs, in contrast with mathematical programming. Also, OPF studies incorporating security and contingency constraints have not yet been performed using AI techniques (Pandya and Joshi 2008; Capitanescu et al. 2011).

Computer time can be reduced in AI techniques by reducing the search space. Chen and Chen (2001a; 2001b), Chen (2005), Chen et al. (2006), Chen (2007), Chen and Lee (2007), Chen (2008), Chen et al. (2008), Lu et al. (2008), Chen et al. (2011), Lin et al. (2011), and Tsai et al. (2011) suggested using the so-called direct search method (DSM), which reduces the search space to only feasible solutions, and therefore reduces the computational requirements while still claiming to reach global optimum answers to the economic dispatch problem given certain parameters. Results of using direct search to enhance stochastic search within economic dispatch problems have shown superiority over other artificial intelligence methods in achieving global optimum with significantly less computer time and faster convergence (Lin et al. 2011; Tsai et al. 2011). Also, most evolutionary methods lend themselves well to computer parallelization which can decrease computation time. Xia and Elaiw (2010) and Belede et al. (2009) discussed hybrid methods that might decrease computation time by linking the AI model with a mathematical method.

Due to the flexibility and capabilities of AI techniques to provide Pareto optimal curves with ease, an AI or hybrid technique could be used to determine optimal power dispatch considering multiple objectives and criteria. PSO techniques have relatively fast convergence speed compared to other AI techniques with respect to the number of iterations to achieve the global optimum (Pandya and Joshi 2008). The PSO technique could incorporate many different criteria such as economic and environmental criteria for both the water system and the power system. Thus, the optimal dispatch tool within the IWPM tool could potentially serve as a platform to study cap-and-trade scenarios for both air and water pollution control, to provide economic dispatch for both power sales and water sales, or to analyze tradeoffs between economic operation of power systems and water efficiency of irrigation systems. PSO interactions with the water and power network solutions would provide a wide range of nondominated solutions, from which feasible solutions could be selected. For example, a simulated “nondominated” solution describing environmental and economic criteria may not satisfy all water system priorities according to historical water rights due to some numerical issue in the optimization. However, since AI techniques can give a wide range of nondominated solutions, all infeasible solutions may be discarded.

The amount of computational resources required for AI techniques to be used at each timestep to optimally select flows and dispatch power injections in the water and power systems respectively outweigh the benefits of having globally optimal solutions. For many water systems, the operation is so highly constrained that a solution that simply satisfies constraints is often considered sufficient in practice. Therefore, the Lagrangian relaxation was selected as the preferred method for static optimization between water and power system simulations. An AI

technique was selected, but not yet implemented, for solving an overarching dynamic optimization.

6 Dynamic Optimal Policies

Although dynamic optimal policies have not been implemented for this research, the full formulated three-level model structure is discussed herein. In this third level of the IWPM structure, dynamic hydropower unit commitment is solved. In terms of electric energy storage, hydropower charging and discharging decisions may be determined based on power system requirements at each timestep but considering dynamic factors such as ramp rates, cost of lost generation, startup costs, and lagged water routing. Since water and power systems modeling and optimal dispatching present such challenging problems, a sophisticated dynamic programming algorithm should be used that can dynamically optimize reservoir system operations under uncertainty. Therefore, a simulation-based dynamic optimization algorithm called reinforcement learning could be formulated that can potentially shape optimal reservoir guide curves or another type of release strategy while incorporating realistic water and power system constraints, evaluation of both multiple objectives, and input and forecasting uncertainties. Such a dynamic optimization routine would not be extremely complicated to insert into the model structure. Figure 9 displays the flow diagram for the dynamic optimization routine. The only difference between Figure 9 and Figure 7 is the inserted Q-function update after the Lagrangian converges.

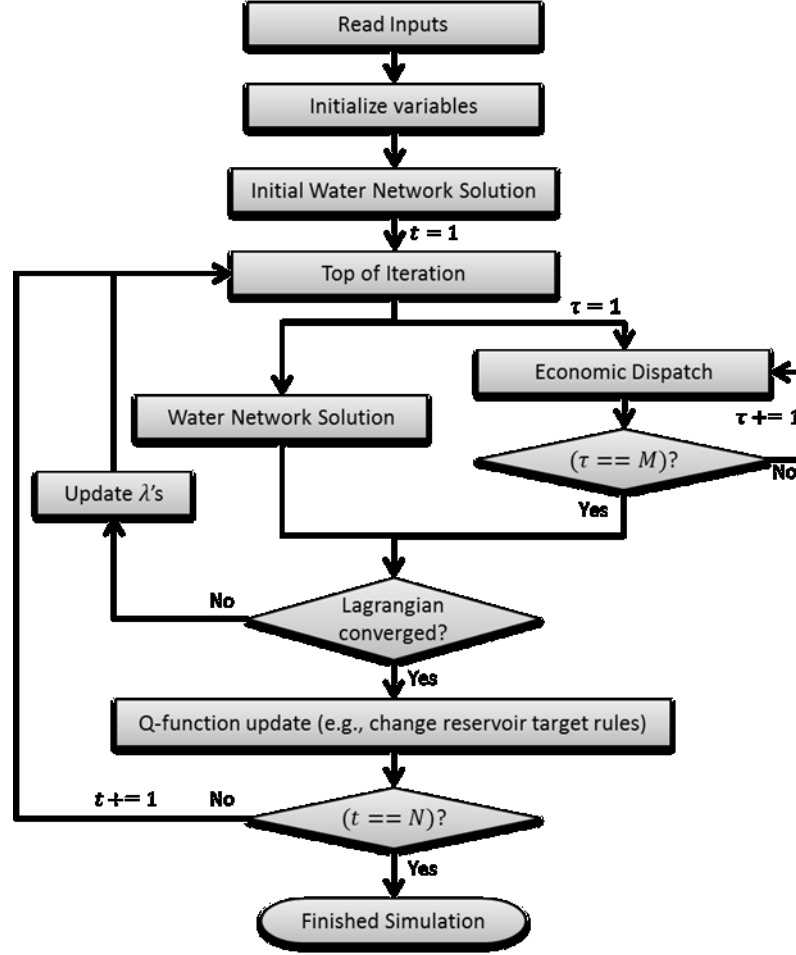


Figure 9: Flow diagram for implementation of the reinforcement learning algorithm with other two levels of the IWPM structure

Reinforcement learning is used to provide optimization over multiple timesteps, and is essentially solved during the simulation procedure by balancing greedy and exploratory decisions. Greedy decisions are determined by previous knowledge of the system. Exploratory decisions allow the solution algorithm to explore potentially new areas of the solution space. In order for the reinforcement learning algorithm to work, it should be simulating for long enough to be able to see many possible states of the system. Even with large historical datasets, the amount of data is not enough for the RL technique. Therefore, historical data can be reproduced a number of times and stacked on itself sequentially or in parallel. Additionally, data can be

synthesized in order to explore uncertainty in measurements and predicted variables such as inflow, wind power production, and load estimates.

Optimal policies can utilize practically anything (e.g., a function, a table, fuzzy rules, neural network, etc.) that provides operating decisions as a function of the state of a system, which might include current reservoir levels or release decisions, current inflow, inflow forecasts, current wind power production, and wind power forecasts. Operating decisions could be release decisions or target reservoir levels. Target reservoir levels are typically used and are recommended in an IWPM application, because the reservoir storage component is explicitly defined which is useful for both water and power system challenges. Storage can mitigate irregularity of flows to water supply systems and floods in river networks, and can also help firm uncertain power production from intermittent RESs. Figure 10 displays the flow of the procedure in a more conceptual way.

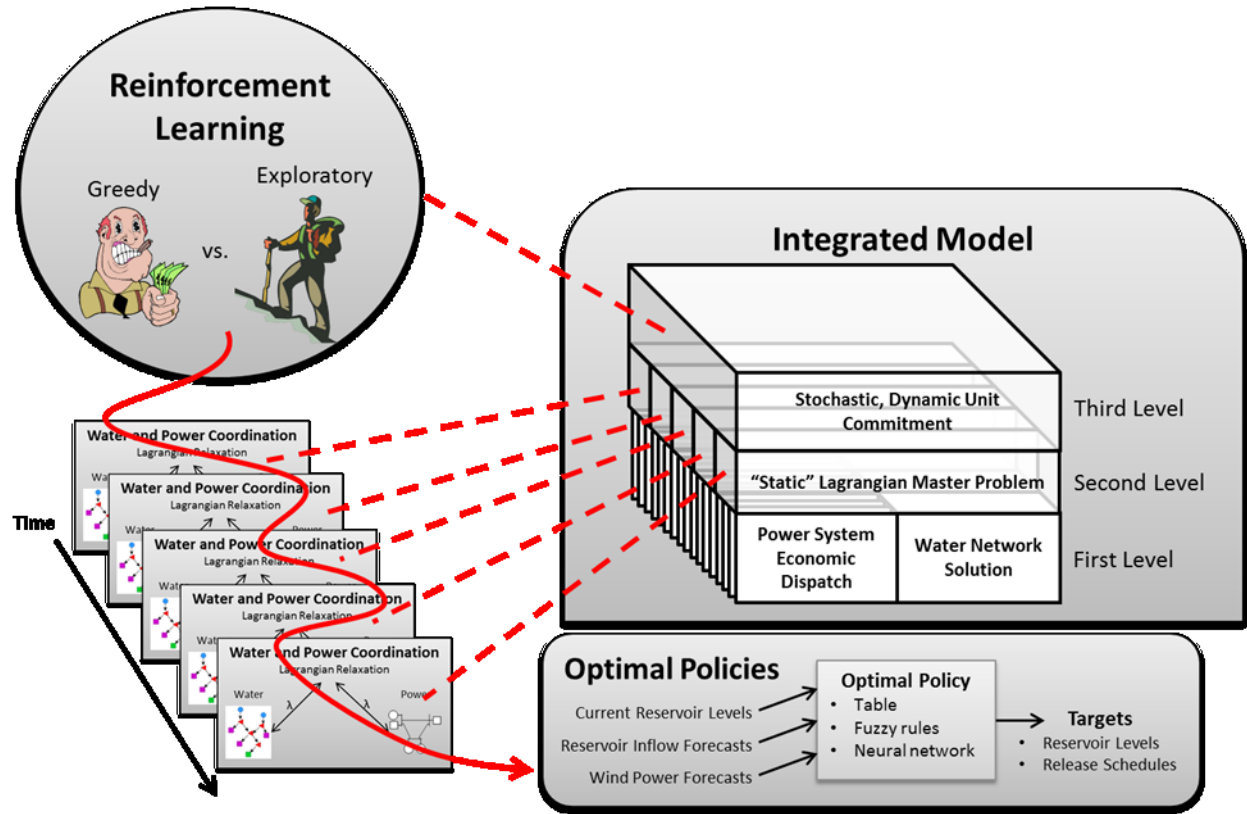


Figure 10: Conceptual diagram of the reinforcement learning procedure applied to the IWPM and optimizing dynamic policies

A benefit to reinforcement learning is that it lends itself well to parallel processing and distributed computing since optimal dynamic policies are updated at each timestep within the solution process. Essentially, at the end of a timestep for each individual parallel reinforcement learning “worker,” the optimal policy can be updated, which is not a process that requires any type of sequential ordering. Transitional matrices for optimization problems with multiple state dimensions (e.g., for water systems this occurs when there is more than one reservoir in the system) are extremely difficult to estimate because historical datasets are too small, and therefore stochastic dynamic programming algorithms would require a lot of simplification and extra work. RL learns to cope with uncertainty in the system as it progresses through the simulation. This can be done by penalizing states that make the system vulnerable or by rewarding decisions that put the system into a less vulnerable state. Uncertainty can be taken into account by using a

variety of stochastic generation methodologies (Salas 1993) to generate a lot of different possible forcings (e.g., inflow, wind speed, temperature, or other climatic unknowns) and run separate reinforcement learning workers along all of these generated forcing datasets. Each worker shares the current estimate of the optimal policies with all the other workers. The parallelized RL model produces implicitly-created optimal policies, which require no more post-processing. Figure 11 illustrates this parallelized model structure.

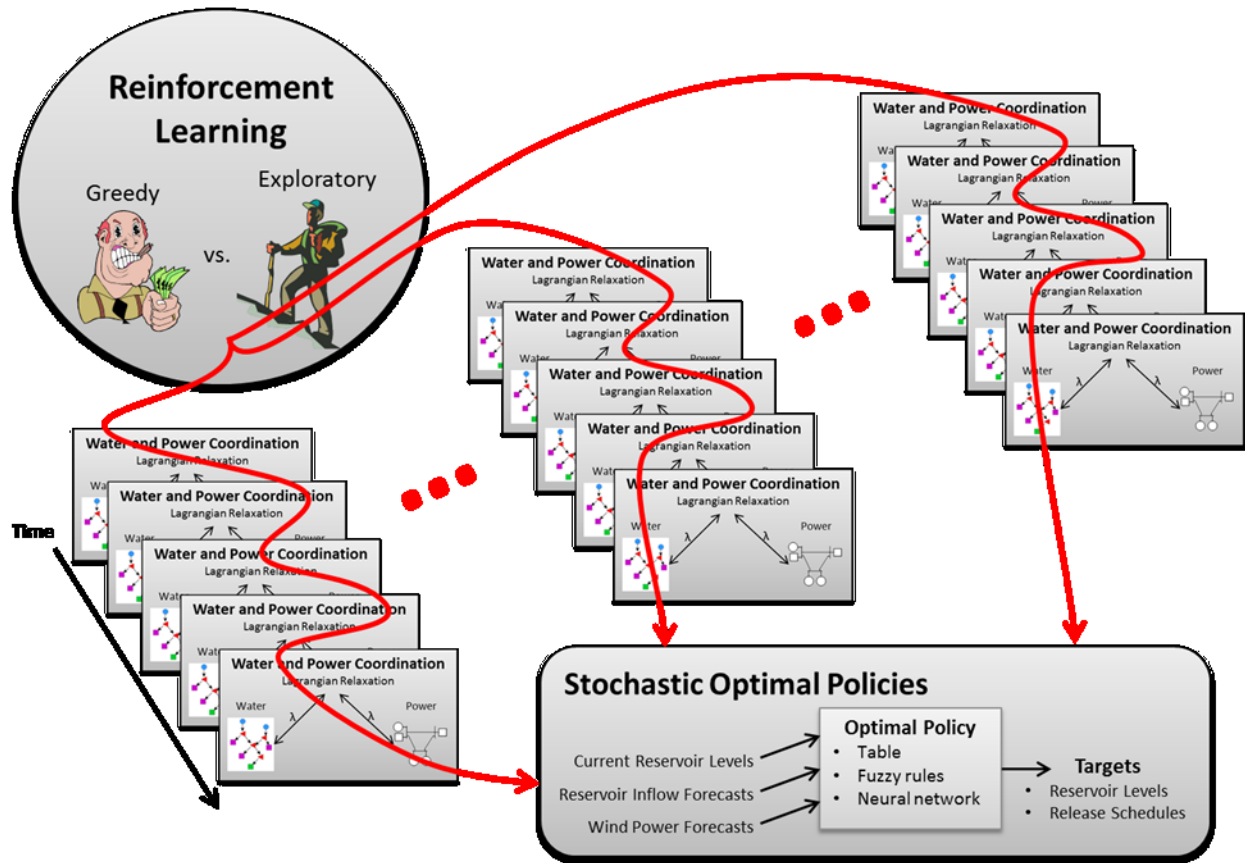


Figure 11: Reinforcement learning in parallel to determine optimal policies for stochastically generated sample input sets

Although RL can be used in highly distributed settings, the complexity of the problem requires significant computing resources even with careful design of program architecture. Therefore, the third level of the IWPM has not yet been implemented, and should only be

implemented following satisfactory results in terms of computational efficiency and convergence characteristics of optimization and simulation within the first two levels of the model structure.

IV Implementation of Water Network Model

MODSIM has been a useful research tool for river and reservoir operations modeling since 1978. Its applications as a generalized river basin management decision support system are widespread. In the past, MODSIM has been heavily used in dealing with regional scale water rights issues and water modeling. However, hydropower has not been a major consideration within its development history. MODSIM, rather, has incorporated hydropower similar to the industry has incorporated it. That is, hydropower is generally treated as a “side-effect” of other reservoir operations, but it is extremely important in justifying the feasibility of reservoir projects. Recently, with a seemingly wide-spread interest of renewable energy integration into the power grid, additional hydropower considerations have been confronting water managers because of its large operating ranges and capabilities. However, the flexibility of hydropower operations highly depends on non-power considerations within the water system. As discussed in the previous chapter, requirements for an integrated water and power model include optimization routines that allow for analysis of multiple objectives, and to do so in a way that exploits the capabilities of the hydropower system to mitigate operational challenges within the power system.

The first level of the three level structure discussed previously includes water and power network solvers. A generalizable, interconnected water and power network model is ideal, but of the generalized water network models, none utilize a structure suitable for the proposed model structure. Therefore, additional tools have been incorporated into MODSIM in this research in order to make it suitable for participation multi-level model structure. Object-oriented hydropower considerations that include reusable hydropower unit efficiencies, flexibly-defined hydropower units, pumped storage hydropower, and hydropower targets were added to the

MODSIM core. Dialogs in the MODSIM GUI interface allow the user to define power plant efficiencies, hydropower units, and hydropower targets within MODSIM's easy-to-use graphical user interface.

In its previous structure, MODSIM utilized hydropower within reservoir nodes. Only one efficiency table, power capacity, generating hours timeseries, and forebay and tailwater elevations could be identified within a reservoir node. However, as seen in many cities and irrigation districts, turbines need not exist only within a reservoir, but may reside within a pipeline or aqueduct. Although it is possible to simulate such behavior and run-of-river projects with 0 capacity reservoir nodes in MODSIM, some constraints limit the behavior and amount of hydropower units that can be defined. Pumps had to be represented in a roundabout way, by defining a number of generating hours that exceed the total number of hours within any particular timestep, which produces at runtime a "power production" value that really represents power consumption from the pump. Additionally, and perhaps most importantly, elevations of another reservoir could not be used to help define head within the turbines.

Instead of associating hydropower units directly with reservoirs, the new hydropower unit representation within MODSIM associates hydropower units with any set of links in the network as connections between nodes. Therefore, multiple hydropower units can now be defined for any particular reservoir, and each hydropower unit can use forebay or tailwater elevations of two different reservoirs to calculate head.

A new optimization routine using the conditional gradient method and an associated golden line search was connected with MODSIM for solving the nonlinear power equations. The routine was developed as a generalized procedure where users can create custom code to interact with the model and even construct a customized nonlinear objective function. The routine

designed to be compatible with the second and third levels within the selected model structure, although much of the second level and all of third level have not yet been developed and connected to MODSIM. An overarching Lagrangian relaxation master problem between the water and power models, as discussed in the previous chapter, requires a nonlinear optimization routine to simultaneously solve a nonlinear problem and smooth all-or-nothing solutions given by the MODSIM network solver, which are characteristics of linear programming (LP) solutions describing the tendency to give solutions at the vertexes within the solution space which may be sensitive to very small changes in input parameters. The conditional gradient method provides a convenient solution to that problem.

1 New Hydropower Objects

Three new “objects” have been added to aid user interaction with the tool and separate modeling tasks within the MODSIM solver. These three objects are turbine (or pump) efficiency tables, hydropower units, and hydropower targets, with each object building off of the previous. An efficiency table, one or more links, one or two reservoir nodes, and a few other properties, together define a hydropower unit. One or more hydropower units, one or two demand nodes, a timeseries of power demands, and a few other properties define a hydropower target object. As an illustration of the new hydropower unit and hydropower targets structure currently within MODSIM, consider the network shown in Figure 12.

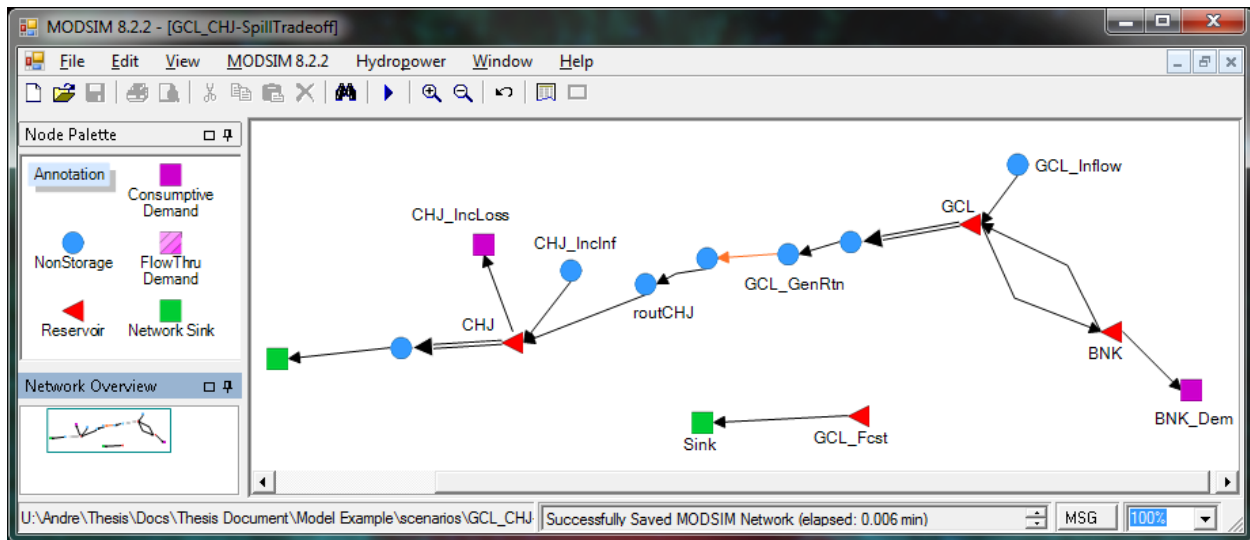


Figure 12: An example MODSIM network to display the use and application of the new hydropower unit structure

The network has three reservoirs, Grand Coulee (GCL), Banks Lake (BNK), and Chief Joseph (CHJ). Four hydropower “units,” or rather power plants, are defined to represent hydropower production from CHJ, GCL, and BNK, as well as the electric power consumption from pumps that convey water from GCL to BNK. Right-clicking the links below CHJ, GCL, and BNK opens up the context menu shown in Figure 13.

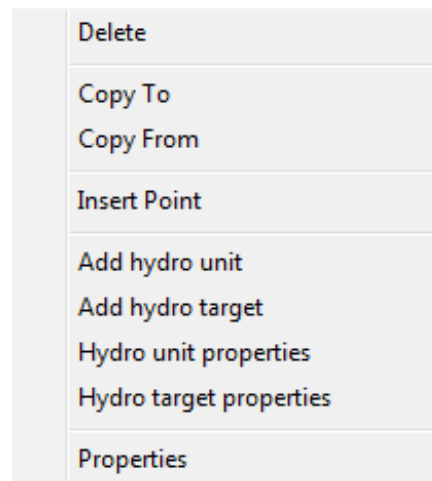


Figure 13: Context menu shown when right-clicking on link with hydropower unit defined

When selecting “Add hydro unit” or “Hydro unit(s) properties” to add a hydropower unit or view information of an already existent hydropower unit respectively, the form shown in Figure 14 is displayed. The hydropower unit has a name and description associated with it so that

the user can identify the object. A unit type can be specified as either Turbine or Pump. The selected convention within MODSIM is that power consumption (from pumps) is a negative value, and power production (from turbines) is a positive value. The maximum power that the hydropower unit can produce is also specified. It is important to note here that the name-plate capacity of a power generation unit is not always the maximum power that can be produced from that unit. The forebay and tailwater levels are defined from Grand Coulee as the elevation definitions for this particular hydropower unit. A unit can be defined as peak generation only, which means that the recorded value of power production from the unit is that produced during the peak generating hours as defined by Labadie (2010). Multiple links can be used to define discharge through the unit if desired. Efficiency tables can be created, saved, and deleted from the updated MODSIM model. These tables can be named, and contain information about the efficiencies defined at multiple heads and flows with user-specified units. After a table is defined for a particular power efficiency, it can be reused at another hydropower unit. Reservoir forebay and tailwater elevations are defined at reservoir nodes using the “A/C/E/Hydraulic Capacity” tab as shown in Figure 15 and the Power tab under “Power Plant Elevation” as shown in Figure 16, respectively.

Hydropower Unit(s) ID: 1

Unit Name:

Unit Description:

Unit Type:

Max. Power (kW): ☐ Peak Gen. Only

Elevation Definitions

From: at

To: at

Link(s) that defines unit discharge:

- BNK_BNK_Dem
- BNK_GCL
- CHJ_CHJ_IncLoss
- CHJ_IncInf_CHJ
- CHJ_PwrOut
- CHJ_Spill
- GCL_BNK
- GCL_Dwn_GCL_GenRtn
- GCL_Fcst_Sink
- GCL_GenRtn_NonStorage15
- GCL_Inflow_GCL
- GCL_PwrRel**
- GCL_Spill
- NonStorage15_routCHJ
- NonStorage16_Sink1

Efficiency Table Name:

Head Units: Flow Units: /

of Heads: # of Flows:

Power Plant Efficiency Table		
Head (ft)/Flow	0	1000000
0	0	0
100	1.105	1.105
150	0.996	0.996
200	0.942	0.942
---	---	---

Figure 14: A form used for building the conventional hydropower unit below Grand Coulee

Reservoir Node Properties (2)

Node Name: GCL

Description:

General | **Power** | **Targets** | **Evaporation** | **Groundwater Seepage** | **A/C/E/Hydraulic Capacity** | **Runoff Forecast**

Area Units: acres

Capacity Units: acre-ft

Hydraulic Capacity Units: ft³ / second

	Area	Capacity	Elevation (ft)	Hydraulic Capacity
▶	0	0	1208	0
	0	50000	1209.073	0
	0	300000	1214.411	0
	0	600000	1220.514	0
	0	900000	1226.293	0
	0	1200000	1231.788	0
	0	1700000	1240.436	0
	0	2000000	1245.353	0
	0	3000000	1260.67	0
	0	4000000	1274.716	0
	0	5000000	1287.725	0
	0	5185388.4	1290	0
*				

OK **Cancel** **Apply**

Figure 15: Stage-storage relationship for the reservoir behind Grand Coulee (GCL)

Reservoir Node Properties (2)

Node Name:

Description:

A/C/E/Hydraulic Capacity | **Runoff Forecast**

General | **Power** | **Targets** | **Evaporation** | **Groundwater Seepage**

Ignore

Power Plant Elevation

Elevation Type:

Plant Elevation:

	Outflow	Elevation
1	0	951.76
2	4132.231	956.23
3	8264.463	960.69
4	12396.69	965.16
5	16528.92	969.62

Add tailwater elevations here

Power Plant Efficiency

Ignore (this is for the old type of hydropower unit)

OK **Cancel** **Apply**

Figure 16: Tailwater elevation curve defined at power plant elevation

Tailwater elevations must either be fixed or vary with reservoir outflow, where reservoir outflow can either be defined by a particular link or by all links flowing out of the reservoir. If not all links flowing out of the reservoir should be used in the tailwater elevation calculation, then a single outflow link should be defined, which can be found in the reservoir node dialog in the General tab when the storage right extension is active (Labadie 2010). It is highly

recommended that a reservoir outflow link is selected that defines the flow exiting the reservoir downstream.

Pumping units are defined differently than turbine units in that a user simply changes the unit type to Pump within the hydropower unit form as shown in Figure 17. When defining hydropower targets for these hydropower units, power consumption targets are defined as negative values. Otherwise, the user need not be concerned about any of the other calculations performed in the background.

The screenshot shows the 'Hydropower Unit(s)' dialog box. The 'Unit Name' is 'BNK_PumpUnit' and the 'Unit Type' is 'Pump'. The 'Max. Power (kW)' is 570000. The 'Elevation Definitions' section shows 'From: Forebay at GCL' and 'To: Forebay at BNK'. The 'Link(s) that defines unit discharge:' list includes 'GCL_BNK'. The 'Efficiency Table Name' is 'BNK_PumpEff'. The 'Head Units' are 'ft', 'Flow Units' are 'ft³ / second', '# of Heads' is 2, and '# of Flows' is 2. The 'Power Plant Efficiency Table' is shown below.

	Head (ft)/Flow	0	1
0	0.88	0.88	
100	0.88	0.88	

Figure 17: The hydropower unit form after creating a new efficiency table

MODSIM uses a sign convention that treats electric power injected into the grid as positive values and electric power consumed (exported from the grid) as negative values. Thus, MODSIM must use efficiencies differently in calculating power consumption than in calculating power production. For pumping units, electric power consumption is power input P_{in} , and power

output P_{out} refers to power applied to the discharging water. For turbines, electric power production is P_{out} , and P_{in} refers to the power of the flowing mass of water. Therefore, both Eqs. (6) and (7) are required to distinguish between turbines and pumps in power calculations, and efficiency η is defined as the ratio of P_{out} and P_{in} .

$$\eta = \frac{P_{out}}{P_{in}} \quad (16)$$

Efficiency tables are constructed as individual objects, and can define efficiencies of a single hydropower unit or of an aggregate number of units such as in a power plant. Efficiencies should include both efficiencies of turbines and generators unless post-processing is performed prior to use within a power flow model. If a user desires to change the efficiency table after defining it, an existing table can be selected from the drop down box or a new efficiency table can be created. Selecting a different efficiency table name will automatically fill out the form with information about the selected efficiency table.

To create a new unit, the user can simply click New Unit, or right-click on a link and select “Add hydro unit”, and another copy of the same form will appear. Additionally, a multi-hydropower unit dialog view can be seen by selecting Hydropower → Hydropower Units. After this hydropower unit is added and saved, the form shown in Figure 18 is displayed. Double-clicking on a row that defines a particular hydropower unit opens the single-view dialog for that unit.

The screenshot shows a software window titled "Hydropower Unit(s)". At the top is a text input field labeled "Enter Query String Here" and a "Run Query" button. Below this is a table with the following columns: HydroUnitID, HydroUnitName, Description, Power Capacity, Hydro Unit Type, Flow Link, From Elev Type, From Reservoir, and To Elev Type. The table contains four rows of data. Below the table is a list box labeled "Link(s) that defines unit discharge:" containing various links, with "GCL_PwrRel" selected. To the right of the list box is a section for "Efficiency Table Name:" set to "GCL_Eff", with buttons for "New", "Save", and "Delete". Below this are input fields for "Head Units:" (ft), "Flow Units:" (ft³ / second), "# of Heads:" (15), and "# of Flows:" (2). At the bottom right is a "Power Plant Efficiency Table" with columns for Head (ft)/Flow and efficiency values. The table has five rows of data. At the bottom left is a "New Unit" button, and at the bottom right are "OK" and "Cancel" buttons.

HydroUnitID	HydroUnitName	Description	Power Capacity	Hydro Unit Type	Flow Link	From Elev Type	From Reservoir	To Elev Type
1	GCL_PowerPlant		6735000	Turbine	GCL_Pw...	Forebay	GCL	Tailwa...
2	BNK_PumpUnit		570000	Pump	GCL_BNK	Forebay	GCL	Forebay
3	BNK_GenUnit		314000	Turbine	BNK_GCL	Forebay	BNK	Forebay
4	CHJ_hydroUnit		2607000	Turbine	CHJ_Pw...	Forebay	CHJ	Tailwa...

Head (ft)/Flow	0	1000000
0	0	0
100	1.105	1.105
150	0.996	0.996
200	0.942	0.942
250	0.909	0.909

Figure 18: The form displaying multiple hydropower units defined within the network

Data can be copied from this form to a spreadsheet for analysis, and many hydropower units can be easily created using this form by copying from a spreadsheet and pasting into it. For example, if seven new pumping units are to be added between Grand Coulee and Banks Lake, the spreadsheet shown in Figure 19 can be constructed for aiding in creating the new units. Copying the table of units as shown in Figure 19 and within the multi-hydropower unit form, right-clicking on a column or row header of the table, causes the context menu shown in Figure 20 to appear. Clicking “Paste Table” adds the copied rows of hydropower unit definitions into the table and automatically creates the hydropower units. However, the only component of a hydropower unit remaining to be defined is generating hours unless the user wants the

hydropower unit to remain on during each timestep. Figure 22 shows the default form for defining generating hours that is created.

	A	B	C	D	E	F	G	H	I	J	K	L
	HydroUnitID	HydroUnitName	Description	Power Capacity	Hydro Unit Type	Flow Link	From Elev Type	From Reservoir	To Elev Type	To Reservoir	Efficiency Table	Peak Gen. Only
1												
2	1	GCL_PowerPlant		6735000	Turbine	GCL_PwrRel	Forebay	GCL	Tailwater	GCL	GCL_Eff	FALSE
3	2	BNK_PumpUnit		570000	Pump	GCL_BNK	Forebay	GCL	Forebay	BNK	BNK_PumpEff	FALSE
4	3	BNK_GenUnit		314000	Turbine	BNK_GCL	Forebay	BNK	Forebay	GCL	BNK_GenEff	FALSE
5	4	CHJ_hydroUnit		2607000	Turbine	CHJ_PwrOut	Forebay	CHJ	Tailwater	CHJ	CHJ_effCurve	FALSE
6	5	BNK_PumpUnit1		300000	Pump	GCL_BNK	Forebay	GCL	Forebay	BNK	BNK_PumpEff	FALSE
7	6	BNK_PumpUnit2		300000	Pump	GCL_BNK	Forebay	GCL	Forebay	BNK	BNK_PumpEff	FALSE
8	7	BNK_PumpUnit3		300000	Pump	GCL_BNK	Forebay	GCL	Forebay	BNK	BNK_PumpEff	FALSE
9	8	BNK_PumpUnit4		300000	Pump	GCL_BNK	Forebay	GCL	Forebay	BNK	BNK_PumpEff	FALSE
10	9	BNK_PumpUnit5		300000	Pump	GCL_BNK	Forebay	GCL	Forebay	BNK	BNK_PumpEff	FALSE
11	10	BNK_PumpUnit6		300000	Pump	GCL_BNK	Forebay	GCL	Forebay	BNK	BNK_PumpEff	FALSE
12	11	BNK_PumpUnit7		300000	Pump	GCL_BNK	Forebay	GCL	Forebay	BNK	BNK_PumpEff	FALSE

Figure 19: Spreadsheet containing data for copying 7 new identical pumping units into the hydropower controller.

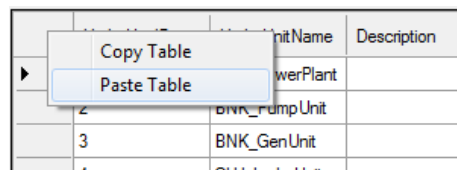


Figure 20: Context menu that allows users to copy and paste the table of hydropower units to and from the form

Hydropower Unit(s)

Run Query

	HydroUnitID	HydroUnitName	Description	Power Capacity	Hydro Unit Type	Flow Link	From Elev Type	From Reservoir	To Elev Type
▶	1	GCL_PowerPlant		6735000	Turbine ▼	GCL_Pw...	Forebay ▼	GCL ▼	Tailwa... ▼
	2	BNK_PumpUnit		570000	Pump ▼	GCL_BNK	Forebay ▼	GCL ▼	Forebay ▼
	3	BNK_GenUnit		314000	Turbine ▼	BNK_GCL	Forebay ▼	BNK ▼	Forebay ▼
	4	CHJ_hydroUnit		2607000	Turbine ▼	CHJ_Pw...	Forebay ▼	CHJ ▼	Tailwa... ▼
	5	BNK_PumpUnit1		300000	Pump ▼	GCL_BNK	Forebay ▼	GCL ▼	Forebay ▼
	6	BNK_PumpUnit2		300000	Pump ▼	GCL_BNK	Forebay ▼	GCL ▼	Forebay ▼
	7	BNK_PumpUnit3		300000	Pump ▼	GCL_BNK	Forebay ▼	GCL ▼	Forebay ▼
	8	BNK_PumpUnit4		300000	Pump ▼	GCL_BNK	Forebay ▼	GCL ▼	Forebay ▼
	9	BNK_PumpUnit5		300000	Pump ▼	GCL_BNK	Forebay ▼	GCL ▼	Forebay ▼
	10	BNK_PumpUnit6		300000	Pump ▼	GCL_BNK	Forebay ▼	GCL ▼	Forebay ▼
	11	BNK_PumpUnit7		300000	Pump ▼	GCL_BNK	Forebay ▼	GCL ▼	Forebay ▼

Link(s) that defines unit discharge:

- CHJ_InclInf_CHJ
- CHJ_PwrOut
- CHJ_Spill
- GCL_BNK
- GCL_Dwn_GCL_GenRtn
- GCL_Fcst_Sink
- GCL_GenRtn_NonStorage15
- GCL_Inflow_GCL
- GCL_PwrRel**
- GCL_Spill
- NonStorage15_routCHJ

Efficiency Table Name: GCL_Eff

New Save Delete

Head Units: ft Flow Units: ft³ / second

of Heads: 15 # of Flows: 2

Power Plant Efficiency Table

Head (ft)/Flow	0	1000000
0	0	0
100	1.05	1.05

New Unit OK Cancel

Figure 21: Multi-hydropower unit table after pasting new units into the table

Generating Hours

Data | Plot

☒ Varies By Year ☐ Interpolate Units: hours / hour

	Start Date	
▶	10/01/2010 00:00:00	1
*		

OK Cancel Apply

Figure 22: Default generating hours associated with any new hydropower unit pasted into the multi-hydropower unit table

Hydropower targets are defined in similar ways as hydropower units, with both single and multi-view dialogs aiding the user in defining hydropower targets. A single-view dialog is displayed in Figure 23 where a name and description can be given to the hydropower target to aid identification. Hydropower units used to meet the hydropower target are displayed in the bottom left of the form, and timeseries data for hydropower production or consumption targets are displayed in the bottom right area. For ease of use, timeseries data can be copied and pasted from a spreadsheet by right-clicking on the row or column headers of the table. Multiple hydropower units can be selected to match a specified power target, which allows the user to build a combined pump-generating unit that will follow a specified target that may be either positive (producing power) or negative (consuming power).

Hydropower Target ID: 3

Name: Save Delete

Description:

Hydropower unit(s):

- BNK_GenUnit
- BNK_PumpUnit
- CHJ_HydroUnit
- GCL_PowerPlant**

☒ Varies By Year ☐ Interpolate Units: /

Power_Target Timeseries (m/d/yr)

Start Date	Value
10/01/2010 00:00:00	721
10/01/2010 01:00:00	820
10/01/2010 02:00:00	729

New Target OK Cancel

Figure 23: Single hydropower target dialog that defines a hydropower target

As in the case with hydropower units, hydropower targets also have a multi-view dialog that allows the user to view a list of all hydropower targets, as well as to copy and paste hydropower targets from a spreadsheet. Copying and pasting hydropower target definitions is performed in a similar way as hydropower units described above. However, pasting hydropower targets is not as useful since the timeseries of hydropower targets needs to be filled even after the pasting operation. Figure 24 displays the multi-view hydropower target dialog.

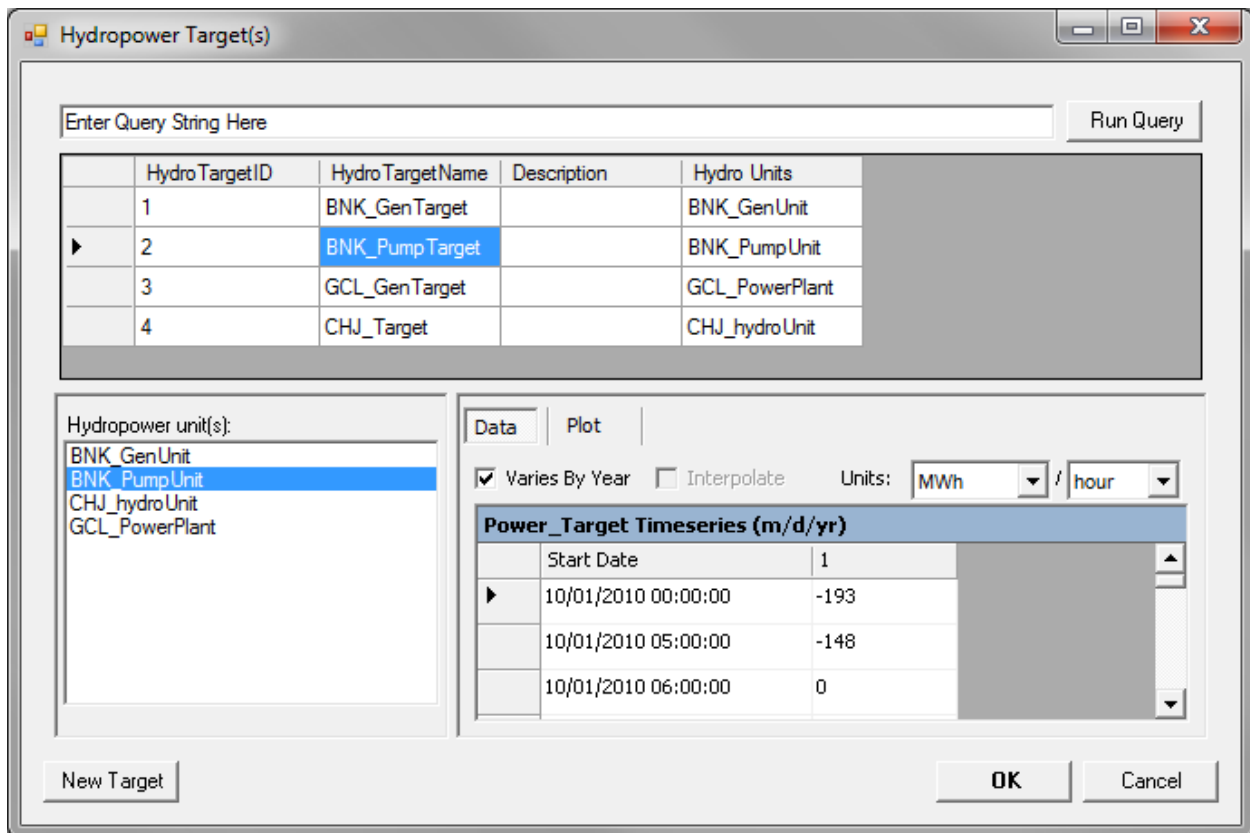


Figure 24: Multi-hydropower target dialog that defines multiple targets

2 Hydropower Output

MODSIM output is stored in comma separated value (*.csv) files that are then copied into a Microsoft Access database (*.mdb format). Although previously, output was only defined for links and nodes, there is now an option to produce output from hydropower units and targets. Hydropower output can be turned on using the MODSIM Extensions dialog box found in the main menu at MODSIM 8.X.X → Extensions. Figure 25 displays the extensions manager with the hydropower extension turned on.

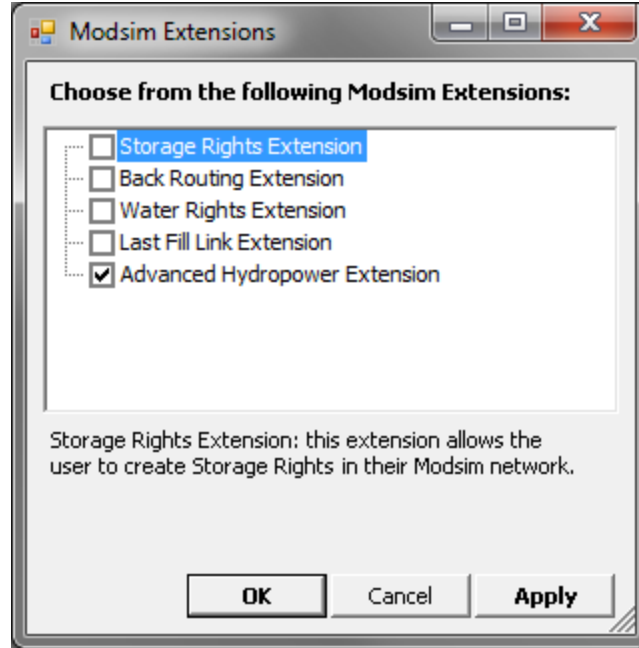


Figure 25: Extension manager to turn hydropower controller on

The output structure for hydropower units and targets is reasonably simple and easy to understand. Within the output database, information used to define a hydropower unit are found in the table *HydroUnitsInfo*, and *HydroUnitOutput* stores output information of the hydropower unit for each timestep such as amounts of discharge through the unit, head, efficiency, power produced, energy produced, the downtime factor ($t_{unit,off}/t_{timestep}$) and the number of generating hours during that timestep. These tables are related by using the *HydroUnitID* attribute of the hydropower units.

Hydropower targets information and output data is also housed in two separate tables *HydroTargetsInfo* and *HydroTargetOutput*, respectively, and connected to each other through the *HydroTargetID* attribute. Each hydropower unit and target output have output at each timestep which are indexed by the *TSIndex* attribute within the *Timesteps* table. Figure 26 displays a diagram of the structure of the output database.

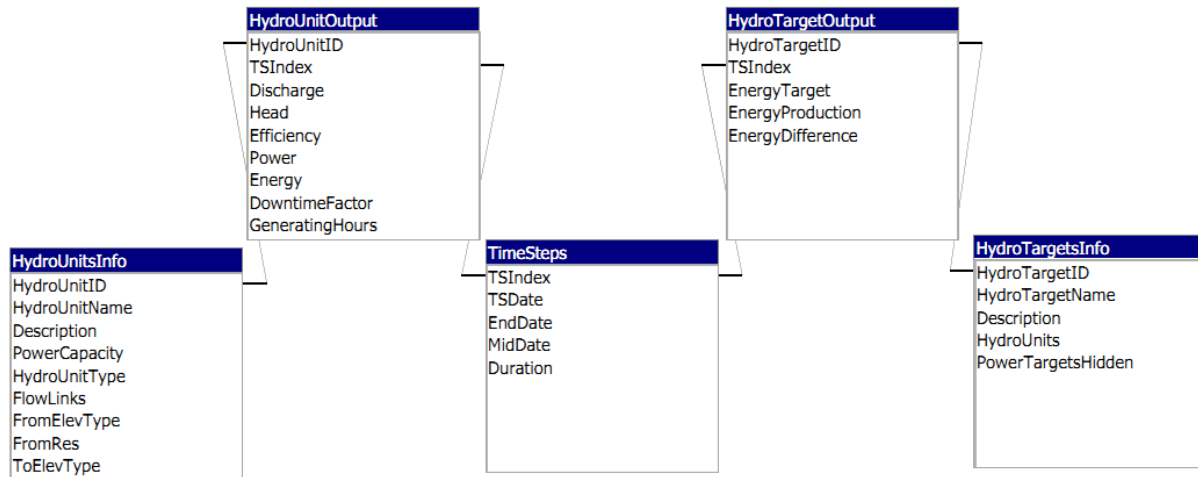


Figure 26: Hydropower unit and target output structure within output database

After simulation of a MODSIM network, the user is able to view output for these hydropower units in the same way other simulated output is viewed within MODSIM. That is, right-click on a link or a reservoir node that contains a hydropower unit or target, and click “Graph” from the context menu. If the option “Graph” is not displayed, an error likely occurred during network simulation that prevented the output from being created properly. Click on MSG in the lower right of the MODSIM graphical user interface (GUI) to see the messages that occurred during simulation. Figure 27 displays a sample graphing dialog within MODSIM once a MODSIM network is successfully completed.

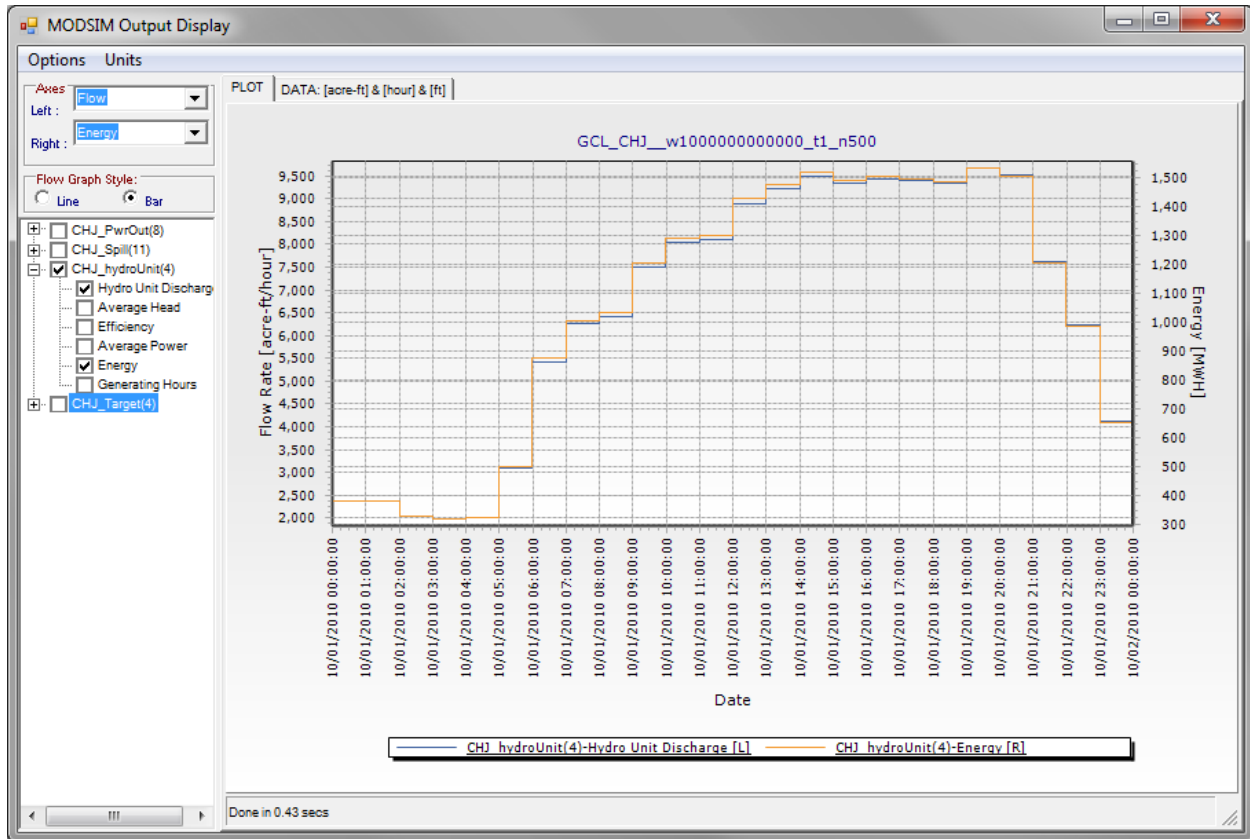


Figure 27: A sample hydropower unit output showing energy and hydropower unit discharge

By selecting various parameters to be displayed along the left or right axes (in Figure 27, shown as Flow and Energy respectively), a user can view other hydropower unit outputs such as Average Head, Efficiency, Average Power, or Generating Hours. Hydropower targets can be displayed as well as the difference between energy produced and the targets, as illustrated in Figure 28. Graphs can be exported and manipulated in various ways, colors changed, and when multiple MODSIM files are open simultaneously, output from all of the files can be plotted on the same figure using the option from the main menu: MODSIM 8.X.X → Scenarios Analysis.

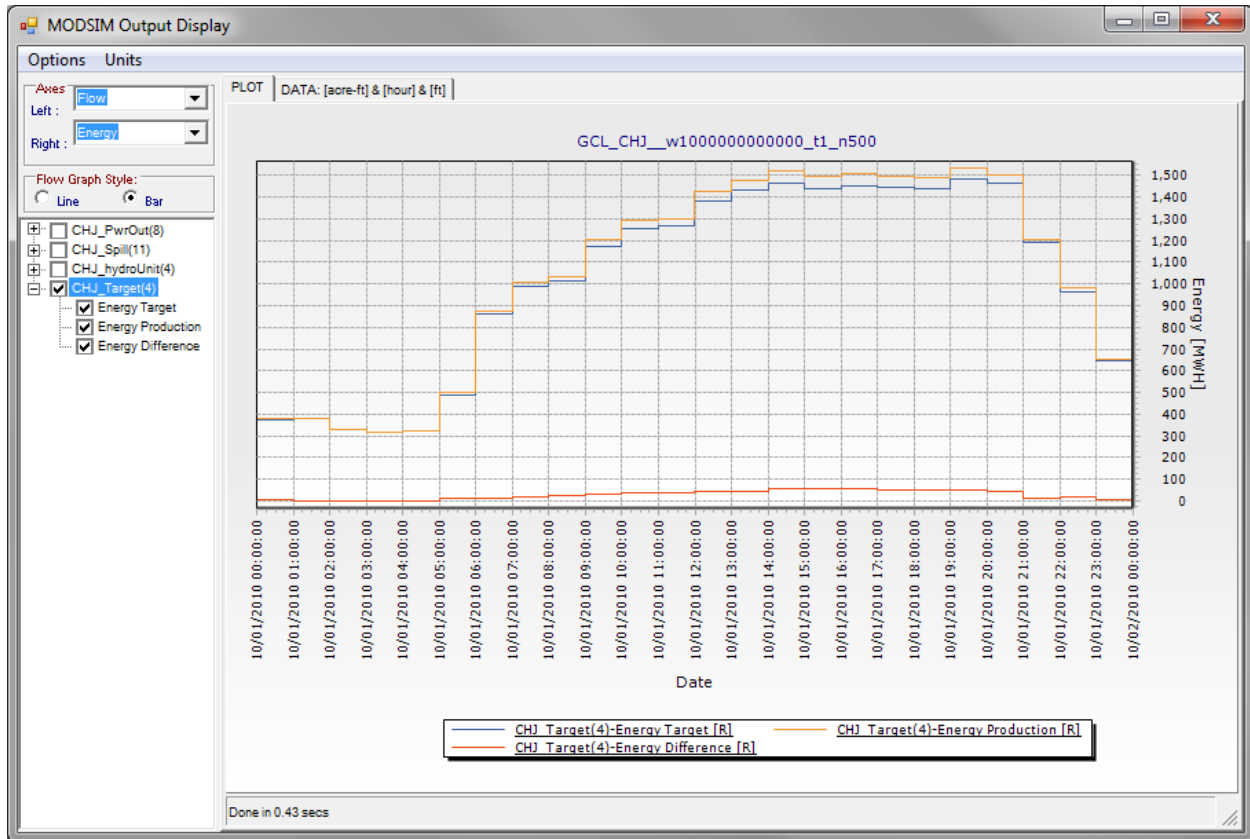


Figure 28: Hydropower targets displayed in the graphical output

3 Successive Approximations

MODSIM utilizes an iterative solution process, i.e., successive approximations, to solve parts of water networks that are nonlinear, such as routing, evaporation from reservoirs, and therefore reservoir storage itself. Hydropower production is represented by a highly nonlinear equation, and can also be solved using an iterative process with limitations as described in Chapter III. Upper bounds on links that define hydropower unit discharge are set according to Eq. (4). For application of successive approximations in MODSIM, hydropower units must be constructed as in Section 1, and in addition, the link should be given a large negative cost (generally, $|c| > 50,000$), where costs are ordered according to priority with the rest of the network. In order to use the successive approximations technique in the MODSIM GUI, the hydropower extension must be selected prior to running the network. After clicking to simulate

the network, several choices are presented to the user: an option to run the network as a normal run without any attempt to match hydropower targets, several options used to match a hydropower target using successive approximations, steepest descent, the conditional gradient method or a combination of the methods. The dialog presented to the user is displayed in Figure 29.

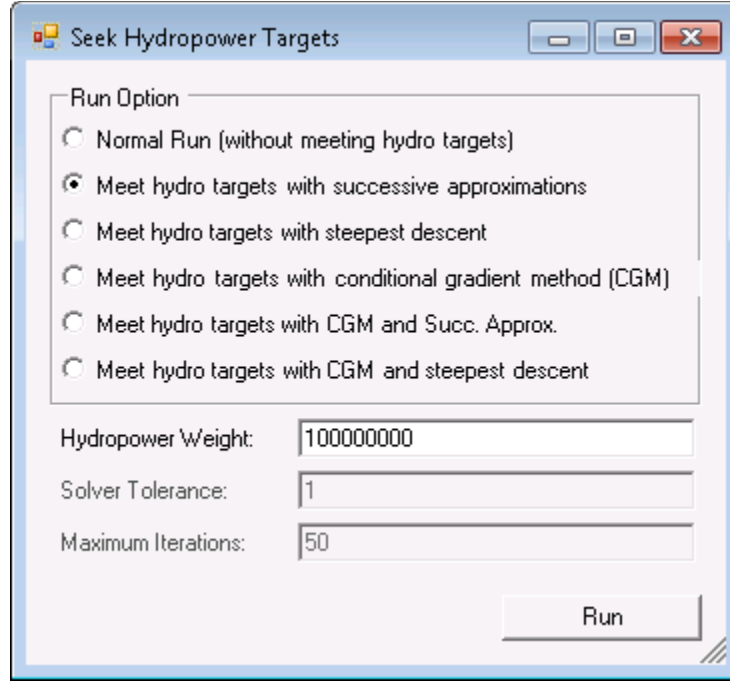


Figure 29: Simulation options presented to the user at runtime when hydropower targets are present in the system

In order to ensure that hydropower production from a hydropower unit could deviated from the hydropower target according to priority within the solution methodology, an artificial node and two artificial links are added to the system that essentially add an absolute term to the objective function shown in the following equation:

$$\min_{q_i} c|q_i - u_i^*| \quad \forall i \in H$$

where H is the set of all links associated with a hydropower target, c is the cost associated not meeting a hydropower target i , q_i is the discharge through the hydropower link i , and u_i^* is the “optimal” discharge through the hydropower turbine that matches a specified hydropower energy

target, which is estimated using Eq. (4). By setting up the artificial link structure as seen in Figure 30, this objective can be accomplished where the “DEM” and “INF” nodes are the artificial demand and inflow nodes described by Labadie (2010). Lower and upper bounds as well as link costs are displayed in the picture for each of the links. All links (including spill links) were detached from the downstream node in order for this technique to be compatible with the routing algorithm described by Labadie (2010).

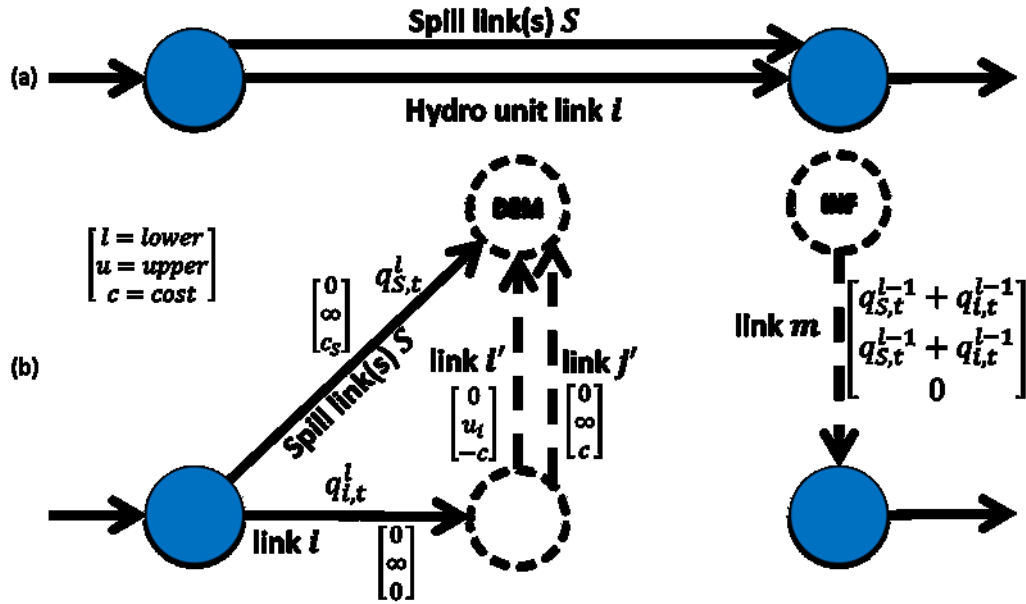


Figure 30: Hydropower target link structure of routing link before (a) and after (b) initialization of the model at runtime

At each iteration, the upper bound u_i on link i' is set according to Eq. (4). Flow typically converges on optimal values within seven iterations, which is the number of iterations within which other nonlinear features of MODSIM generally converge as well. Solution time for MODSIM to match hydropower targets using successive approximations requires about an extra 50% of the solution time over a normal MODSIM run, depending on network setup. Sometimes, when the constraints on the successive approximations approach described in Chapter III are not satisfied, the algorithm converges to the wrong powerplant outflow, which is a disadvantage of using this method. Additionally, when used with an overarching optimization routine such as

Lagrangian relaxation, the method will likely produce “bang-bang” or unstable behavior when new Lagrange multipliers update MODSIM link costs, which is the motivation behind adapting MODSIM to implement the conditional gradient method to provide stable answers.

4 Conditional Gradient Method Implementation

A network flow algorithm lies at the core of the MODSIM solver, which is discussed in more detail in Labadie (2010). However, the network solver will often give all-or-nothing, or “bang-bang” solutions when priorities conflict with each other and can only solve network flow problems that can be described by equations (1), (2), and (3); that is, other nonlinear objective functions cannot be solved. When integrating MODSIM with a power system model and optimizing over objective functions that include the hydropower equations, a nonlinear objective function with a solver that provides more stable solutions with small changes to inputs is required since hydropower calculations are highly nonlinear. This reduces the adverse effects on the convergence properties of an overarching optimization technique such as the Lagrangian relaxation. Therefore, the conditional gradient method, or Frank-Wolfe method, was utilized to minimize the generalizable nonlinear objective functions. A general flow diagram of the conditional gradient method is presented in Figure 4, and mathematical description is presented in Chapter III. This section describes the implementation of the algorithm within the water network flow model, MODSIM.

At the core of the MODSIM software packages lies a data object called *Model* that houses all of the basic information about a MODSIM river and reservoir network. Throughout the model solution, various “events” take place within the code. When an event is “raised,” it can be handled by any subscribers interested in that particular event. The conditional gradient method only handles three *Model* events: *Init*, *Converged*, and *ConvergedFinal*, and does so

using an interface called *IConditionalGradientSolvableModel*. The interface defines the attributes of any object that make it solvable by the conditional gradient algorithm, which is implemented in a class called *ConditionalGradientSolver*. A new class called *OptiModel* was created as an interface between *Model* and the *ConditionalGradientSolver*. Figure 31 illustrates the mapping of events from the *Model* object to the *OptiModel* object.

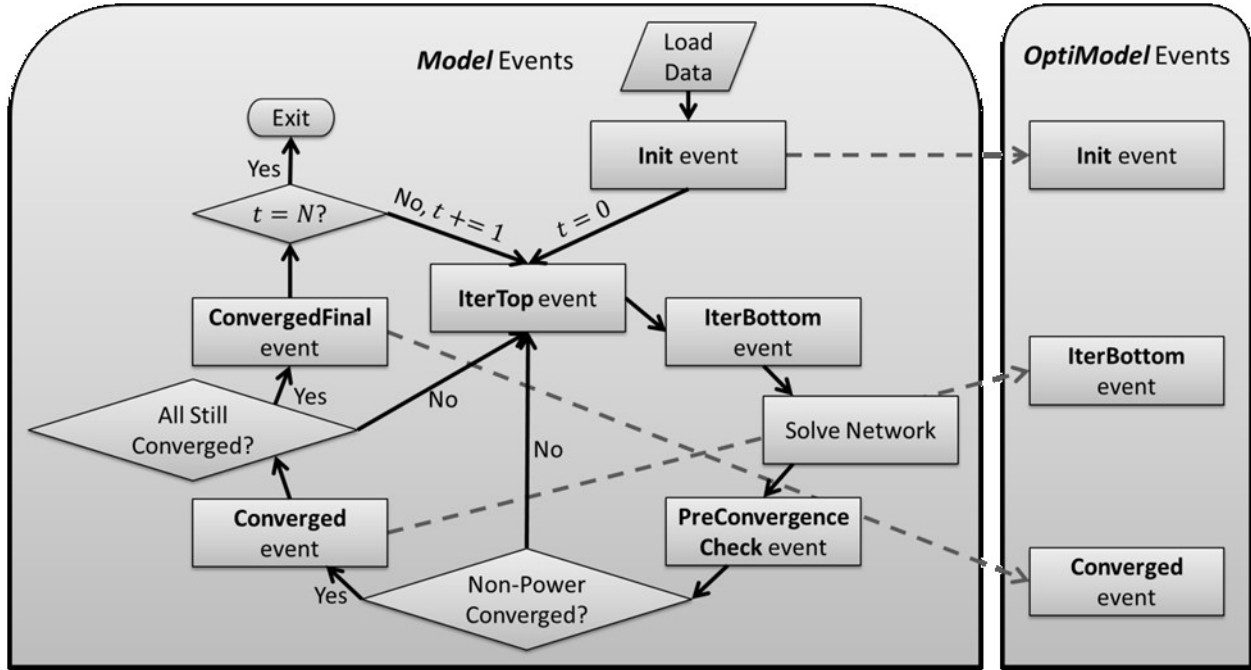


Figure 31: Mapping of event occurrences from a MODSIM *Model* object to a *OptiModel* object

At model runtime, the *Init* event is raised when all data structures within the model have been filled with data prior to entering the timestep loop. At the top of each iteration before any data structures are updated, the *IterTop* event is raised. After all data structures have been updated for a particular iteration just before the network is solved, *IterBottom* is raised. After non-hydropower convergence criteria (i.e., groundwater return flows, routed flows, and end-of-period storage levels) have been met the *Model* object raises the *Converged* event. Another event called *ConvergedFinal* has been added to the newest version of MODSIM since the development

of the MODSIM 8.1 user's manual (Labadie 2010). The *ConvergedFinal* event is raised after convergence of all criteria and just before the timestep is incremented.

The Conditional Gradient Solver handles three events called *Init*, *IterBottom*, and *Converged*. These events correspond to something slightly different than as defined within the *Model* object. Instead of referring to the time just prior to network solution, *IterBottom* from *OptiModel* refers to events just after a linear optimization has taken place. Since MODSIM actually solves a nonlinear problem using successive iterations, *OptiModel IterBottom* occurs after all non-power criteria have converged, which is why the *Model Converged* event is mapped to *OptiModel IterBottom*. *OptiModel Converged* refers to the time when the entire nonlinear programming problem has converged on a solution, which is why the *ConvergedFinal* event was added to *Model* because all other non-power criteria only converge after the *Model Converged* event is raised.

Additional mapping was required for a MODSIM *Model* to be suitable for the conditional gradient method. All this mapping is stored within the *OptiModel* class which implements the *IConditionalGradientSolvableModel* interface. This interface is given in the code segment below.

```

using System;

namespace ASquared.ModelOptimization
{
    public interface IConditionalGradientSolvableModel
    {
        // Events
        event EventHandler Init;
        event EventHandler IterBottom;
        event EventHandler Converged;

        // Running the model
        void Run();
        void Reset();

        // Properties to interact with during model solution
        Int32 Iteration { get; }
        IConditionalGradientSolvableFunction objective { get; set; }
    }
}

```

As seen in the interface, the three events *Init*, *IterBottom*, and *Converged* are required by the *ConditionalGradientSolver*, but two methods and two properties are also required. When a user calls the *Solve()* method within the *ConditionalGradientSolver*, the *Run()* method within the *IConditionalGradientSolvableModel* object (i.e., *OptiModel* in the case of MODSIM) is called. At the beginning of each new timestep, the *Reset()* method is called which resets the variables for the conditional gradient method. The *Iteration* property defines the current iteration within the MODSIM model. The *objective* property is another interface that defines the objective function and constraints.

In the case of MODSIM, costs are reset to original values within this method in order to ensure that original priorities are maintained as the user originally specified and do not migrate away, which is required since the conditional gradient method will change link costs of variables within its objective function. Since link costs are iteratively changed through the solution of the conditional gradient method, a change in priorities could potentially result, which can be dealt with by changing the cost or weights associated with the objective function and with conflicting

priorities in the water system network to reflect true priorities. This is true because the conditional gradient method will converge on the closest solution possible before a conflicting priority surpasses the gradient of the objective function in priority, which is depicted in Figure 46 and discussed in more detail in surrounding paragraphs. To ensure priorities remain ordered appropriately, the user will need to ensure the gradient of the objective function does not produce costs that outweigh costs associated higher priority links. For example, if an off-stream water demand $D = 1000 \text{ kcf/s}$ is to be attained even if a hydropower target cannot be attained, a cost of c_D is assigned to the link diverting water to the demand. If flow q_D flowing to demand D was equivalent to $5000 - q_H$ according to mass balance constraints for the simple link structure displayed in Figure 32.

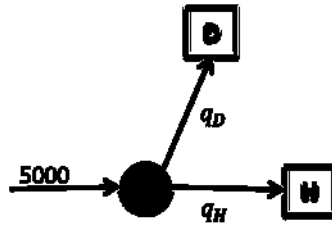


Figure 32: Link structure for simple example

Then, a squared term minimizing the deviation of hydropower production $k\eta q_H h$ (simplified to $k'q_H$ for this simple example even though head h and efficiency η depend on q_H) from a hydropower target $P_{targ,H}$:

$$\min_{q_H} M(k'q_H - P_{targ,H})^2 + c_D q_D$$

or

$$\min_{q_H} M(k'q_H - P_{targ,H})^2 + c_D(5000 - q_H)$$

solved by conditional gradient method will attempt to converge on the solution:

$$q_H^* = \frac{1}{k'} \left(\frac{c_D}{2M} + P_{targ,H} \right)$$

and will fail to satisfy the condition that $D = 5000 - q_H = 1000$ if:

$$q_H^* = \frac{1}{k'} \left(\frac{c_D}{2M} + P_{targ,H} \right) \geq 4000$$

Therefore, in order to ensure that the condition is satisfied, M should be sized so that $q_H^* \leq 4000$ for any feasible combination of $P_{targ,H}$ and k' . In mathematical terms,

$$M \leq \frac{c_D}{2(4000k' - P_{targ,H})}$$

or, if $P(q_H)$ represents the hydropower equation for a discharge of q_H :

$$M \leq \frac{c_D}{2(P(4000) - P_{targ,H})}$$

Objective functions within the conditional gradient solver are defined as an interface to the solver using the *IConditionalGradientSolvableFunction* interface found in the following code segment. Users can define custom objective functions by implementing this interface and passing their new objective function into *OptiModel*.

```

using System;
using ASquared.SymbolicMath;

namespace ASquared.ModelOptimization
{
    public interface IConditionalGradientSolvableFunction
    {
        // Initialization
        void Initialize();

        // Nonlinear function
        Symbol fxn { get; }
        Matrix nonlinearMask { get; }

        // Linear optimization interaction
        Matrix costs { get; set; }
        Matrix decisions { get; set; }
        String[] variables { get; }
        Matrix A { get; }
        Matrix b { get; }
        VariableType[] VariableTypes { get; }
        ConstraintType[] ConstraintTypes { get; }

        // Convergence
        bool IsConverged { get; set; }
    }
}

```

Not used with
IConditionalGradientSolvableModel

The *IConditionalGradientSolvableFunction* interface can be used as standalone without having the *IConditionalGradientSolvableModel* interface. When doing so, the constraints need to be defined using variables *A*, *b*, *VariableTypes*, and *ConstraintTypes*. These are required when another linear optimization solver is not provided to the *ConditionalGradientSolver* since a generalized linear optimization solver (Microsoft 2012) will be used to solve the LP subproblem, which requires additional information in order to define the feasible space. Using the *IConditionalGradientSolvableModel* interface implies that the user is providing another linear optimization routine during its own iterations, and therefore defines the constraint matrices for itself and solves the LP problem itself, as is the case with MODSIM that utilizes its own network solver. Therefore, the objects defining constraints must be within a class implementing *IConditionalGradientSolvableModel*, but they are unused properties; all other methods and

properties will be used. In this way, the conditional gradient solver provides a generalized interface that allows any objective function or model to be solved using the conditional gradient solver, not just water network solutions as in the case of MODSIM.

The *Initialize()* method is used to initialize data structures that will be in continual use throughout the solution of the conditional gradient procedure. For a MODSIM *Model* object, *Initialize* is used to build an array pointing to the links within the MODSIM network, and also build symbolic math objects that house the variables assigned to each link in the network. For example, the symbolic math variable for the first link in the network (a link with *Link.number* equal to 1) is “q_1”, for the fifth link “q_5”, and so forth. The *Initialize()* method is also used to set all the hydropower unit link costs to a nonzero value so that a false solution is not attained right away, and the *variableMask* property to distinguish between hydropower unit links and non-hydropower unit links.

All the other interface attributes of the *IConditionalGradientSolvableFunction* are properties. Two properties *fxn* (“Function”) and *variableMask* help to define the nonlinear function over which *ConditionGradientSolver* performs a line search. The *fxn* property defines the full nonlinear objective function using a symbolic math representation discussed in detail subsequently. The *variableMask* property is a vector that contains ones at indices for all variables that are used within *fxn* and zeros for all other variables. The *variableMask* property is required because not all variables are required to participate in the objective function, but all must be included when linear combinations of two LP solutions are calculated, which is performed within the *ConditionalGradientSolver*. Note that the *Matrix* class that makes up the *variableMask* property, and a few of the other properties, is sufficiently generic to define both matrices and vectors.

Three of the properties *costs*, *decisions*, and *variables* help to define interaction between an LP model or function and the conditional gradient solver. The *costs* property is a vector of costs that are multiplied by the vector of *decisions* that define the LP objective function. In the case of MODSIM, *costs* and *decisions* are equivalent to \mathbf{c} and \mathbf{q} in (1) respectively. MODSIM houses a built-in class that defines the *costs* and *decisions* properties in order of link number. Link numbers are one-based, but these matrices are zero-based. Therefore, link 1 costs and flows can be retrieved or set in *costs*[0] and *decisions*[0], and link 10 in *costs*[9] and *decisions*[9]. There are no gaps in link numbers, so the costs and decisions associated with a link l can be accessed as follows: *costs*[*l.number* – 1] and *decisions*[*l.number* – 1]. The string array *variables* defines the name of each variable. In MODSIM, the variable names of links 1 and 10 are *variables*[0] = “q_1” and *variables*[9] = “q_10” respectively.

Properties *A*, *b*, *VariableTypes*, and *ConstraintTypes* define the constraints for the LP subproblem within the conditional gradient method. Since MODSIM uses its own solver to perform the LP optimization during the iterations, these properties need not be defined. When a user does not provide a model that performs LP optimization itself, *ConditionalGradientSolver* utilizes its own LP solver. When this is the case, *A*, *b*, *VariableTypes*, and *ConstraintTypes* must be defined. The property *A* is the constraint matrix that defines the coefficients that multiply variables. The property *b* is the right-hand side of the constraints. The property *VariableTypes* define the types of variables for each variable, and *ConstraintTypes* define the types of constraints.

Properties and methods of an object implementing the interface *IConditionalSolvableModel* are called and manipulated in the order shown in Figure 33. As events are raised within the *IConditionalSolvableModel* object, the solver performs various tasks

required for each of those events. In this way, code used to build the conditional gradient solver can be completely separate from the core MODSIM code.

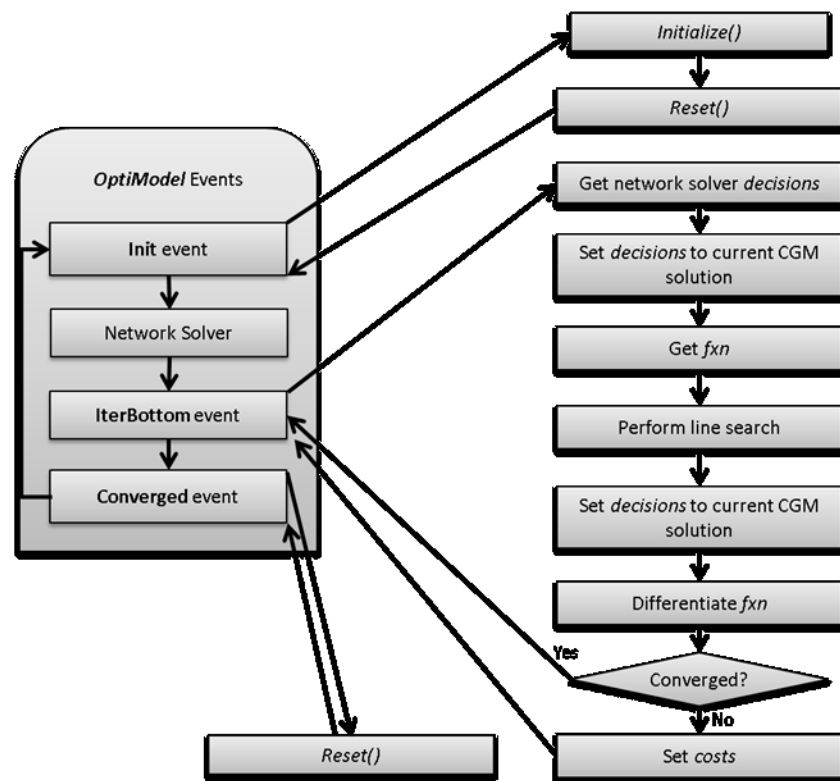


Figure 33: Flow diagram of interaction that the conditional gradient solver has with a class implementing the *IConditionalGradientSolvableModel* interface using event subscribers

A simple example will help to clarify how to build these properties. Consider the linear programming formulation:

$$\min_x -x_1 + 2x_2 - 0.5x_3$$

subject to:

$$-2x_1 - x_2 + x_3 \leq 2$$

$$x_1 + 2x_2 \geq -7$$

$$x_1 \leq 3$$

$$x_1 \geq 0$$

$$x_2 \leq 0$$

x_3 free

Then, the properties should be set up according to the following code snippet:

```
Matrix A = "[-2 -1 1; 1 2 0; 1 0 0]";
Matrix b = "[2; -7; 3]";
VariableType[] VariableTypes = new VariableType[]
{
    VariableType.NonNegative,
    VariableType.Negative,
    VariableType.Free
};
ConstraintType[] ConstraintTypes = new ConstraintType[]
{
    ConstraintType.LeftLessThanRight,
    ConstraintType.LeftGreaterThanRight,
    ConstraintType.LeftLessThanRight
};
```

The last property *IsConverged* is used to determine whether the LP model has converged and to specify whether the conditional gradient method has converged so that the LP model is aware of the convergence of the conditional gradient method. Using this interface attribute provides a way for the conditional gradient solver to be completely separated from MODSIM, or any other LP model, and yet inform MODSIM that it has converged. For example, in Figure 31 above, after the *Model Converged* event, the convergence is checked again. An instance of *ConditonalGradientSolver* will use the *IsConverged* property of the interface *IConditionalGradientSolvableFunction* to set a convergence property in the MODSIM *Model* object so that it does not proceed to *ConvergedFinal* unless a maximum number of iterations was reached.

4.1 Customizing the objective function

A custom objective function for the network can be constructed by creating a new class in C# that implements *IConditionalGradientSolvableFunction*. In order to simplify the amount of coding required by a user, a base class called *OptiFunctionBase* was created that defines most of

the required interface attributes to be able to use the conditional gradient method. Thus, the custom class should inherit *OptiFunctionBase* and implement *IConditionalGradientSolvableFunction*, as well as define *fxn*, *variableMask*, and *Initialize()*. *OptiFunctionBase* defines all other required interface attributes for *IConditionalGradientSolvableFunction*.

Within *OptiFunctionBase*, the *fxn* property defines the objective function as a symbolic math object of type *Symbol*. The *Symbol* class recursively contains information about its own type as well as operands and operators within it. So, a *Symbol* object could refer to a variable “*x*” or it could refer to an expression “*-x*”. For example, let *f* be a particular instance of *Symbol* that defines the equation $2x + 5^{x-1}$. Several other *Symbol* instances actually make up *f*. In fact, there are nine individual *Symbol* instances within *f*. At the lowest level, there is one *Symbol* for each number and each variable ‘2’, ‘x’, ‘5’, ‘x’, and ‘1’. There is a *Symbol* that performs the *minus* operation on ‘x’ and ‘1’. There is also a *Symbol* that performs the power operation between ‘5’ and $x - 1$, and so on. The top-level *Symbol* instance *f* refers to the addition operator between the multiplication *Symbol* containing $2x$ and the power *Symbol* containing 5^{x-1} . Regular mathematical operations (i.e., addition, subtraction, multiplication, division, powers, logarithms, etc.) are supported along with derivatives and partial derivatives (Meyer and Dozier 2012). Users can create custom functions simply by setting the value of *fxn*. For instance, to set *fxn* equal to the function in the previous example, $2x + 5^{x-1}$, but with an added term $3y$, the following code would be used:

```
Symbol x = "x";
Symbol y = "y";
Symbol fxn = 2 * x + (5 ^ (x - 1)) + 3 * y;
```

The *Symbol* class performs an unconventional operation by overloading the bitwise OR operator ‘^’ to make it represent a power term, which does not have precedence over addition, subtraction or multiplication. Therefore, whenever ‘^’ is used, it should be used with parentheses around it as shown in the example above. In this simple example, ‘x’ and ‘y’ were used as the variables. However, in MODSIM, ‘q_X’ is used and the *fxn* is a property of the class instance implementing *IConditionalGradientFunction*.

So, for a more realistic example, let *OptiModelInstance* be the instance of *OptiModel* that will be used to minimize flow through a link named “Releases” in a MODSIM network representing flood flows. Link numbers in MODSIM can be determined by opening a link Properties dialog box, and in the upper left next to “Link Properties” are parentheses with a number inside (e.g., “Link Properties (3)”). Link numbers can also be accessed through custom code by retrieving the value of the *number* attribute from a *Link* instance. Progressing through an example should clear up any confusion. Create a network such as the one shown in Figure 34 with the default timestep, timeperiod, and units.



Figure 34: Simple network to illustrate customizability

Within the multilink under the reservoir, define a link called “Releases” with maximum capacity of 2500 acre-feet/month, and one other link to have no capacity but a cost of 100000. Name the link with a set capacity “Releases.” Name the link going from NonStorage to the reservoir “Inflows.” Within the NonStorage node, define the inflows as follows in Figure 35. Within the reservoir node, define the maximum volume, initial volume, and target volume as 5000 acre-feet, 2500 acre-feet, and 5000 acre-feet respectively. Finally, save the network to a file.

NonStorage Node Properties (1)

Node Name: **NonStorage**

Description:

Data | Plot

☐ Varies By Year ☐ Interpolate Units: **acre-ft** / **month**

Inflow Data (m/d)

	Start Date	Flow Rate
▶	01/01 00:00:00	500
	02/01 00:00:00	750
	03/01 00:00:00	1500
	04/01 00:00:00	3000
	05/01 00:00:00	4500
	06/01 00:00:00	2500
	07/01 00:00:00	1000
	08/01 00:00:00	500
	09/01 00:00:00	400
	10/01 00:00:00	350
	11/01 00:00:00	400
	12/01 00:00:00	450
*		

OK Cancel Apply

Figure 35: Inflows to the reservoir in the simple network

For this example, a release schedule will be defined and the conditional gradient method will be used to minimize the difference between the release schedule and the actual releases. The link with a high cost is used to maintain problem feasibility if the reservoir becomes full and is unable to pass all the required flow through the “Releases” link. Let the release schedule from the reservoir be defined as in Figure 36.

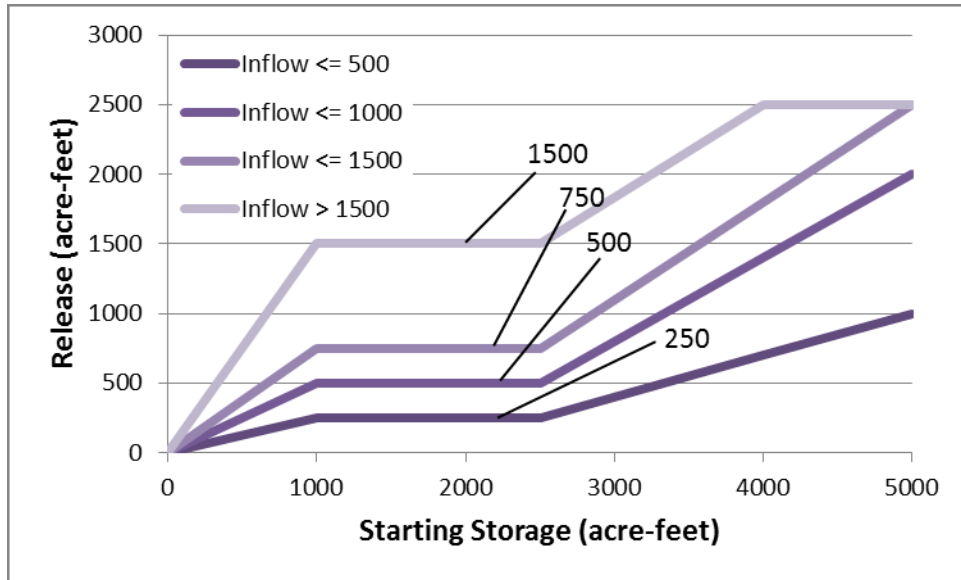


Figure 36: Release schedule for simple example network

For this simple example problem, the code is relatively simple. As mentioned above, the attributes *Initialize()*, *fxn*, and *variableMask* need to be defined. The *Initialize()* method and *fxn* property are overridden in the *OptiFunctionBase* derived class, and *variableMask* property of the *OptiFunctionBase* derived class is simply assigned within *Initialize()* because in this example it only needs to be defined once. The code sample below displays the new objective function.

```
using System;
using Csu.Modsim.ModsimModel; // from libsim.dll
using Csu.Modsim.ModsimOptimization; // from ModsimOptimization.dll
using ASquared; // from A2CM.dll
using ASquared.SymbolicMath; // from A2CM.dll
using ASquared.ModelOptimization; // from ModelOptimization.dll

namespace SimpleExampleApplication
{
    public class SimpleExampleFunction :
        OptiFunctionBase,
        IConditionalGradientSolvableFunction
    {
        private Model _model;
        private Link _inflows, _releases;
        private Node _reservoir;
        private double _a = 1000.0, _b = 2500.0, _c = 4000.0, _d = 5000.0;

        public SimpleExampleFunction(Model model)
            : base(model)
        {
            _model = model;
        }
    }
}
```



```

public override void Initialize()
{
    // Get the links and nodes used in calculations
    _inflows = _model.FindLink("Inflows");
    _releases = _model.FindLink("Releases");
    _reservoir = _model.FindNode("Reservoir");

    // Make sure to start with a nonzero cost
    _releases.mInfo.cost = -100;

    // Initialize OptiFunctionBase
    base.Initialize();

    // Create the mask
    base.variableMask = new Matrix(_model.Links_All.Length, 0.0);
    base.variableMask[_releases.number - 1] = 1;
}

public override Symbol fxn
{
    get
    {
        double inflow = _inflows.mInfo.flow;
        double resStorage = _reservoir.mnInfo.start;

        Symbol q = base.SymbolVariables[_releases.number - 1];
        double stepSize, end;

        if (inflow <= 500)
        {
            stepSize = 250.0;
            end = 1000.0;
        }
        else if (inflow <= 1000)
        {
            stepSize = 500.0;
            end = 2000.0;
        }
        else if (inflow <= 1500)
        {
            stepSize = 750.0;
            end = 2500.0;
        }
        else
        {
            stepSize = 1500.0;
            end = (2500.0 - 1500.0) / (_c - _b) * (_d - _b) + 1500.0;
        }

        // Get the release schedule
        double releaseSchedule;
        if (resStorage <= _a)
            releaseSchedule = resStorage / _a * stepSize;
        else if (resStorage <= _b)
            releaseSchedule = stepSize;
        else
            releaseSchedule = Math.Min(2500.0,
                (resStorage - _b) / (_d - _b) * (end - stepSize) + stepSize);

        // Return the squared difference between the release schedule
        // and the flow through "Releases"
    }
}

```

```

        return 1000000*(q - releaseSchedule) ^ 2;
    }
}
}
}

```

The code above defines the objective function for the simple example network. A large weight (1,000,000) is required on the penalty term, since target storage volumes in reservoirs have a large negative cost (of -49,000 by default). If the penalty term is not sufficiently large, the solution of each network flow problem will favor the links that meet the target storage volume instead of the release schedule. The penalty cannot be too large since the magnitude may exceed the size of *long* data types, which is the data type used at the core of the MODSIM solver. For this same reason, the magnitude of the values within the water network flow solution cannot be scaled down to allow for more reasonably sized penalty terms. Attempting to scale MODSIM network solutions up requires that they be multiplied in orders of 10 per extra degree of accuracy. For example, if a user desires to have an accuracy of three decimal places, MODSIM will multiply all link lower bounds, flows, and upper bounds by 10^3 because the network solver requires integers (of *long* data type). Scaling down, however, decreases the precision of the solution to less than integer and is highly undesirable since users may have a large range of flows throughout the network that require more precision. To utilize this objective function during the solution of a MODSIM network, create a new class that starts the solver as follows in the code segment below.

```

using System;
using Csu.Modsim.ModsimOptimization; // from ModsimOptimization.dll
using Csu.Modsim.ModsimModel; // from libsim.dll
using Csu.Modsim.ModsimIO; // from XYFile.dll
using ASquared.ModelOptimization; // from ModelOptimization.dll

namespace SimpleExampleApplication
{
    public class SimpleExample
    {
        public static void Main(string[] args)
        {
            // Read the MODSIM network from file

```

```

        string networkfile = args[0];
        Model model = new Model();
        model.OnMessage += new Model.OnMessageDelegate(OnMessage);
        model.OnModsimError += new Model.OnModsimErrorDelegate(OnMessage);
        XYFileReader.Read(model, networkfile);

        // Build the OptiModel instance with the user-defined function
        OptiModel optModel = new OptiModel(model, ObjectiveFormulation.UserDefined, null);
        optModel.objective = new SimpleExampleFunction(model);

        // Build the conditional gradient solver
        ConditionalGradientSolver solver = new ConditionalGradientSolver(optModel);
        solver.MaxIterations = 100;
        solver.Tolerance = 1;

        // Start solving
        solver.Solve();
    }

    static void OnMessage(string message)
    {
        Console.WriteLine(message);
    }
}

```

Results can be viewed by opening the MODSIM network and graphing the output as seen in Figure 37. Viewing the results using the graphical output helps the user debug the code and, in this simple example, storage-release relationships. As seen in the figure, releases from the reservoir increase as inflow increases and storage volumes increase, according to the rules defined in Figure 36.

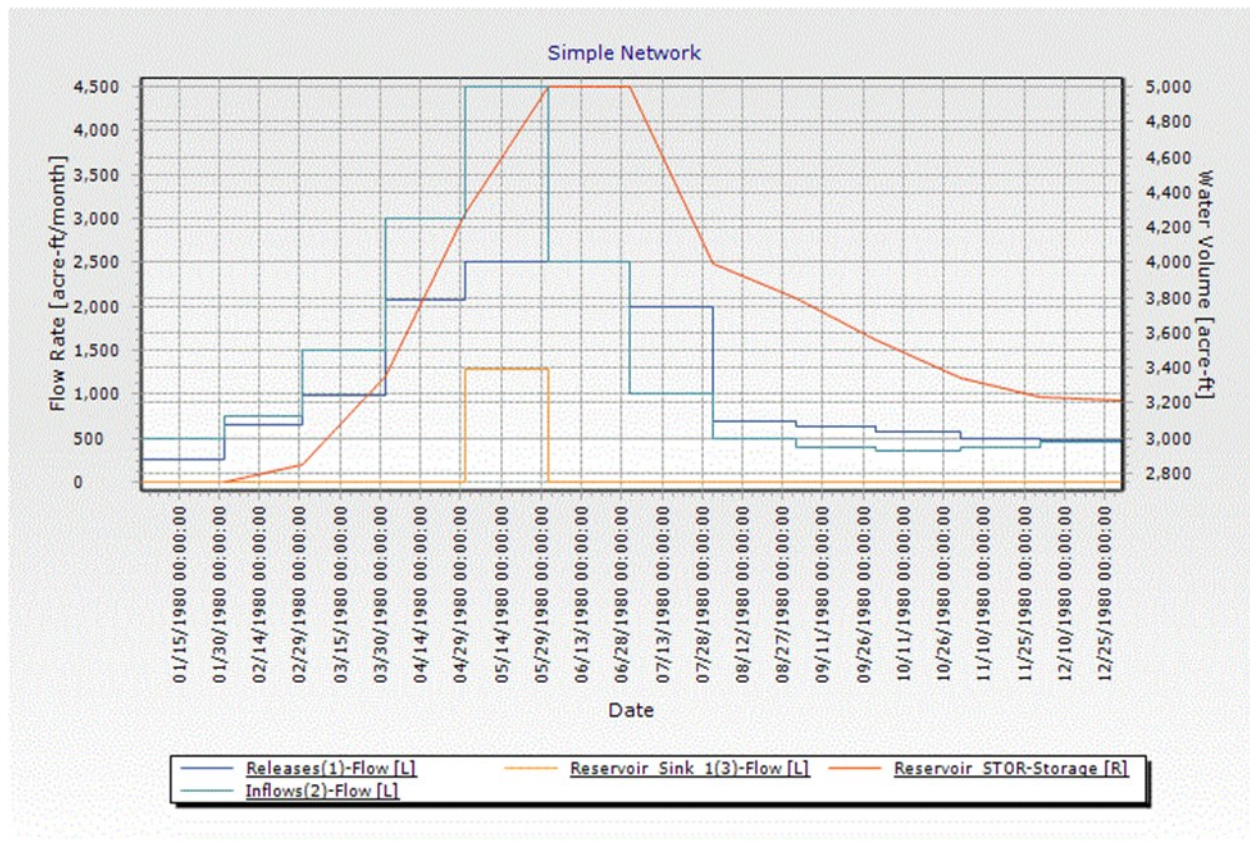


Figure 37: Graphical outputs of simple example network

4.2 Built-in capabilities

Some basic objective function objects have been created that will aid in developing code. These objects can be derived so that a user can modify functionality slightly. Current built-in functions include a function that attempts to match a hydropower target, a function that analyzes tradeoffs between some environmental criteria, and a function that connects MODSIM to a simple two-bus power network via Lagrangian Relaxation, which could be relatively easily adapted to incorporate other configurations of an electric grid. Figure 38 shows that each objective function implements the *IConditionalGradientSolvableFunction* interface and derives originally from *OptiFunctionBase*. The class *EnvVsHydro* analyzes tradeoffs between environmental criteria and meeting a hydropower target, and therefore derives from *HydroTargetSeeker*, because it utilizes the same objective function and adds to it. The

TwoBusSystem class also derives from the *HydroTargetSeeker* class, but it utilizes a new objective function to minimize squared deviation from originally specified hydropower targets while satisfying the complicating constraints, which define constraints that power produced in the water network is also injected into the power system model.

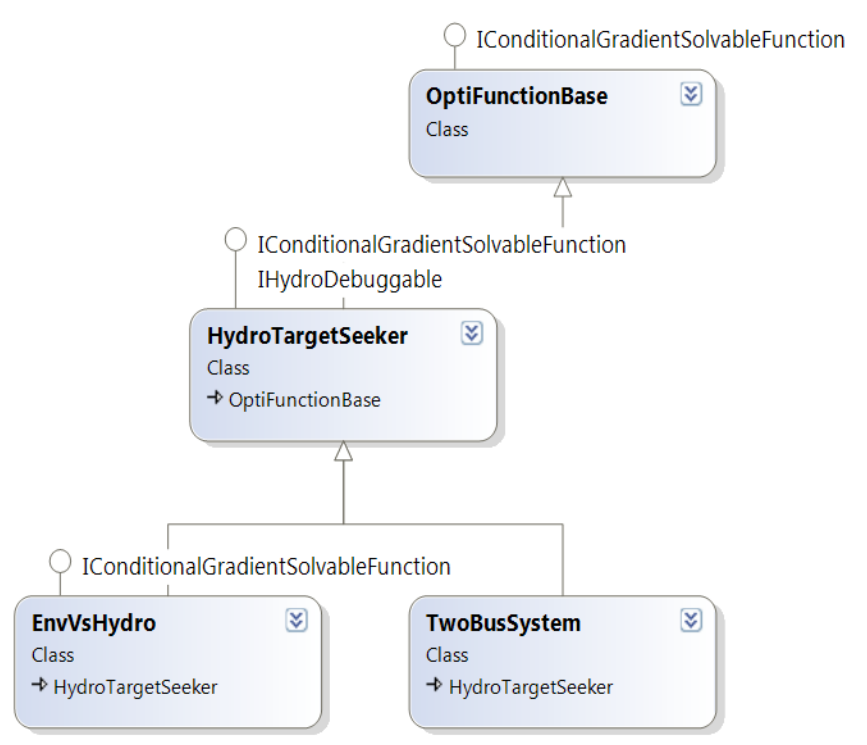


Figure 38: Class diagram of built-in objective functions

The *OptiFunctionBase* class holds most of the useful information that will be used to build any custom objective function. As mentioned above some of the required interface attributes within a *IConditionalGradientSolvableFunction* such as *A*, *b*, *ConstraintTypes*, and *VariableTypes* are not used by MODSIM, so these properties are simply empty. Within *OptiFunctionBase* there are a few attributes that are not fully defined, but a derived class needs to define. Both *fxn* (the symbolic representation of the full objective function) and *variableMask* (a vector that masks variables that are not included in the objective function or that the user does not want to use in determining convergence of the conditional gradient method) require a derived

class to define. The properties *costs*, *decisions*, and *SymbolVariables* retrieve the costs, flows, and symbolic math representation of the flows through all links in the network ordered by the *number* attribute in the *Link* class. The property *variableMask* must also be order by link number. The *lower* and *upper* attributes get a vector of lower and upper bounds on all links, again ordered by link number. The property *RoutingCompatibility* is another symbolic math variable that should be utilized within the objective function of a network that includes routing, reasoning for this is discussed in detail below. The method *GetModsimObjectiveFunction()* gets a symbolic representation of the MODSIM objective function $\mathbf{c}^T \mathbf{q}$ that can be used within a customized objective function if desired. Figure 39 displays all public attributes of the *OptiFunctionBase*.

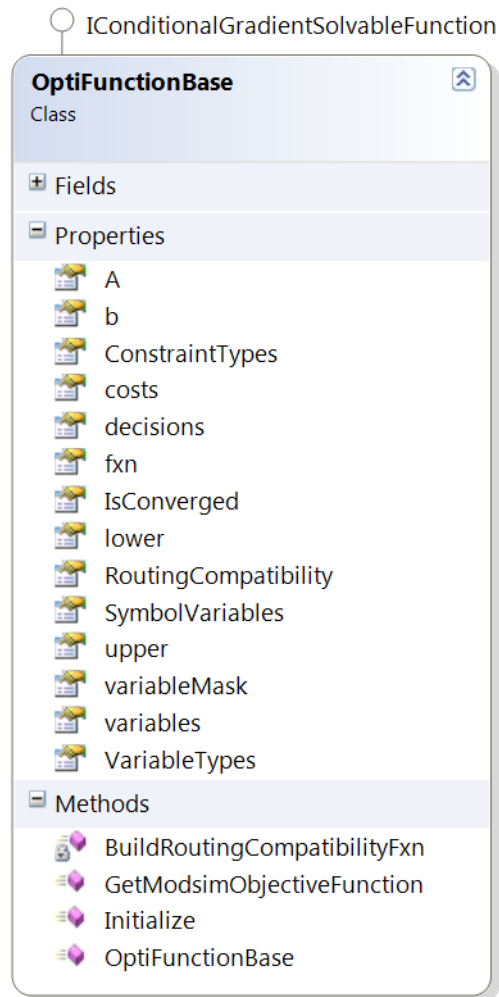


Figure 39: Class diagram of the *OptiFunctionBase* class

When routing exists in the water network, a special penalty within the objective function is required to cope with the routing. Routing places a nonlinear relationship between variables within a single timestep, and therefore a linear combination between one feasible network solution and another (which is performed as a part of the line search in the conditional gradient method) no longer constitutes a feasible network solution. A novel approach is used in making the routing and the conditional gradient method compatible. Routing within MODSIM is handled iteratively by setting up artificial paths as shown in Figure 40 and Figure 41. “Artificial” paths

are represented by the dashed links and nodes, which refer to links and nodes that are automatically generated at the beginning of a network simulation.



Figure 40: Network setup with routing link prior to simulation. Figure adapted from Labadie (2010)

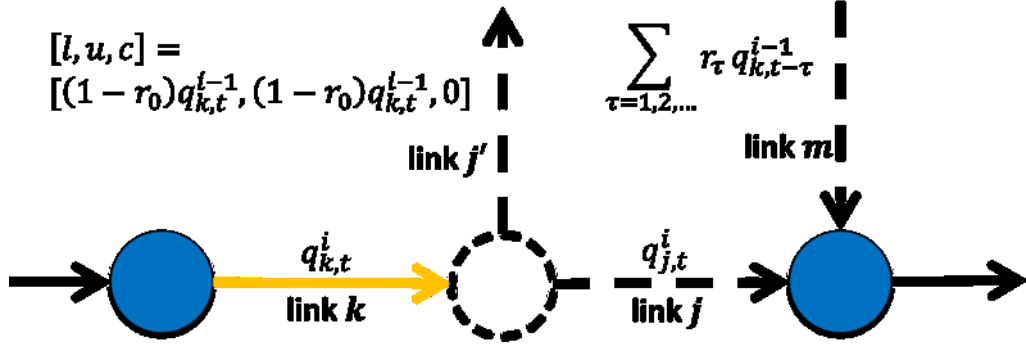


Figure 41: Network setup with routing link after simulation starts. Figure adapted from Labadie (2010)

Artificial paths associated with routing links are designed to maintain mass balance through the network satisfied while iteratively changing return flow until the diverted through link j' equals the flow through link k . Figure 41 illustrates how this is accomplished. At each successive approximation iteration i , flow $q_{k,t}^i$ at link k and time t is to be routed to another node downstream at time $t + \tau$ for $\tau = 1, 2, \dots$. So, the lower and upper bounds on link j' are given as the flow calculated at the previous iteration $q_{k,t}^{i-1}$ multiplied by $1 - r_0$, which represents the amount of flow that does not reach the downstream end of the reach at the current time t , but takes longer to reach the downstream end. Thus, flow $q_{j,t}^i$ through link j at all times t should equal $r_0 q_{k,t}^{i-1}$. When the conditional gradient method is used with MODSIM routing links without additional terms in constraints or objectives, these requirements are violated, most likely because routing does not satisfy mass balance (within a single timestep) as the conditional gradient method expects from the network flow algorithm. Therefore, a term within the objective is used

to rectify routing. This term essentially minimizes the difference between the symbolic math representation of flow through link j , $q_{j,t}$, and the previous estimate of what it should be $r_0 q_{k,t}^{i-1}$. In mathematical terms, the objective function requires an added minimization term with an associated weight as follows:

$$\min_{q_{j,t}} \lambda_k (q_{j,t} - r_0 q_{k,t}^{i-1}) + \frac{\alpha}{2} (q_{j,t} - r_0 q_{k,t}^{i-1})^2$$

where λ is a Lagrange multiplier updated using the same equation given in Eq. (32) except with $h(q_{j,t}) = (q_{j,t} - r_0 q_{k,t}^{i-1})$. The property *RoutingCompatibility* within the *OptiFunctionBase* class, builds all the required penalty terms required to ensure compatibility between the conditional gradient method and flow routing within MODSIM. The following code segment is the actual *RoutingCompatibility* property within *OptiFunctionBase*. When this term is added to the objective function, it effectively decreases the differences between the network solution and routing.

```
Symbol penalize = 0.0;
_lambda.Update(_model.mInfo.Iteration, _routingConstraint);
for (int i = 0; i < _routingLinks.Length; i++)
{
    Link r = _routingLinks[i], rArt = _routingLinks_Art[i];
    Symbol q = _symbolVars[rArt.number - 1] - r.m.lagfactors[0] * r.m.lInfo.flow;
    if (_lambda.UseAugmented)
        penalize += _lambda[i] * q + _lambda.Alpha / 2.0 * (q ^ 2);
    else
        penalize += _lambda[i] * q;
    this.variableMask[rArt.number - 1] = 1;
    _routingConstraint[i] = (double)rArt.mlInfo.flow
        - r.m.lagfactors[0] * (double)r.m.lInfo.flow;
}
return penalize;
```

Without utilizing the routing term in the objective function when using the conditional gradient method, routing does not converge properly. Figure 42 displays flow through the link downstream of the routing link (link j in Figure 41), which should equal zero. When using the term in the objective function, flows through link j are closer to zero than without.

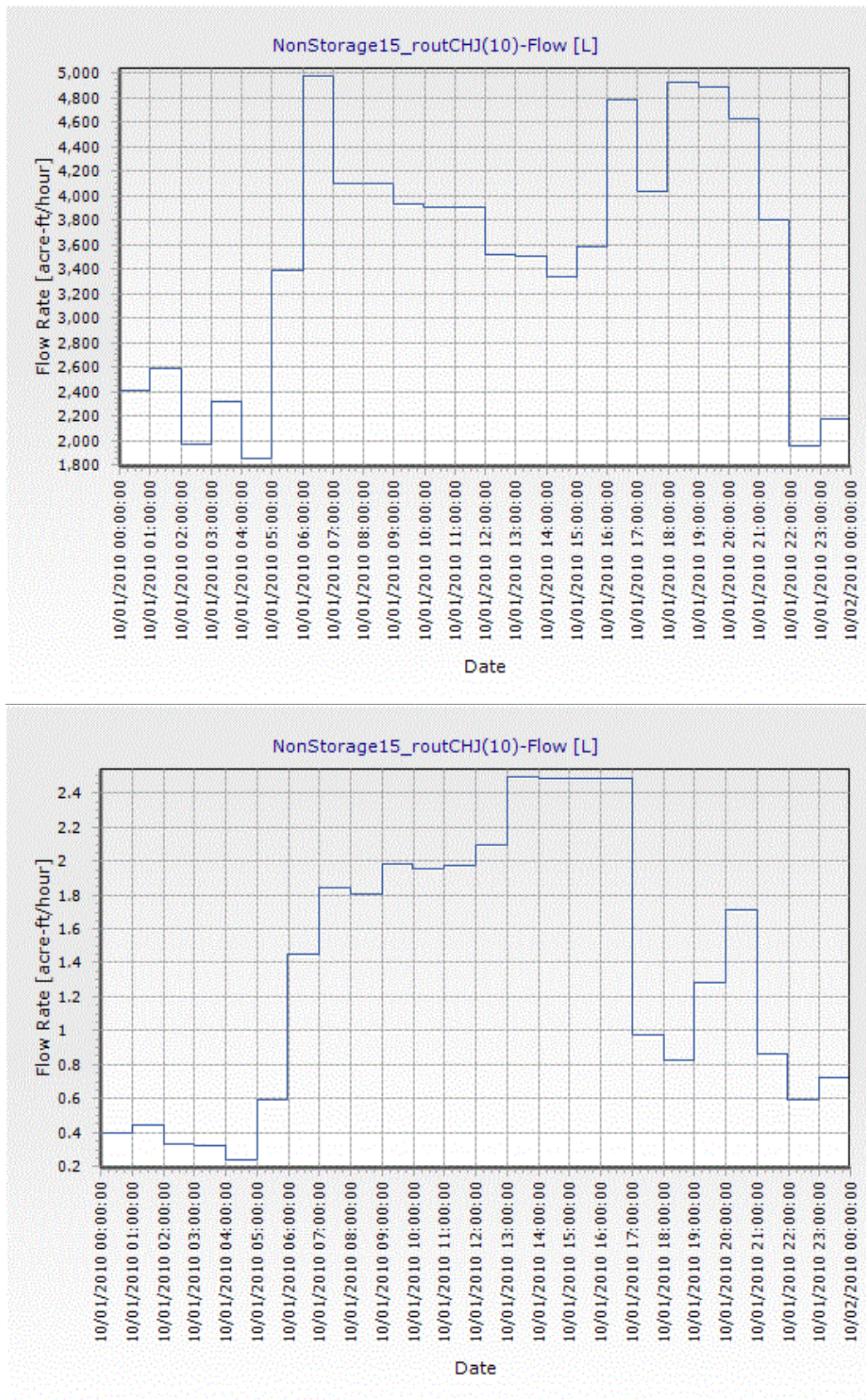


Figure 42: Flow through the zero-flow link with (bottom) and without (top) routing terms in the objective function

Capabilities of the *OptiFunctionBase* class have been explored, which are applicable to any customized objective function within the MODSIM optimization toolkit. New built-in tools specific to the hydropower objectives will now be explored. As mentioned previously, these constitute three classes that are derived from *OptiFunctionBase*: *HydroTargetSeeker*, *EnvVsHydro*, and *TwoBusSystem*.

The *HydroTargetSeeker* class is a relatively simple class containing useful tools for constructing symbolic functions of flow, head, efficiency, and power production of hydropower units as well as defining the penalty terms between hydropower unit power production and hydropower targets. Parameters for the constructor are a MODSIM *Model* instance and a weight associated with the hydropower production target function, which sets the value retrieved by the property *Weight*, which corresponds to the weight associated with the penalty term on hydropower production deviations from hydropower targets. The *HydroPenaltyFunction* property builds the hydropower production target portion of the objective function, and *fxn* property is the interface member containing the full objective function (including the routing compatibility term) that interacts with the *ConditionalGradientSolver* class. *Targets* retrieves all the hydropower target objects throughout the MODSIM network. Perhaps, the most useful property in the class is the *TargetCalculator* which retrieves an instance of the *HydroTargetCalculator* class, which is discussed in more detail subsequently.

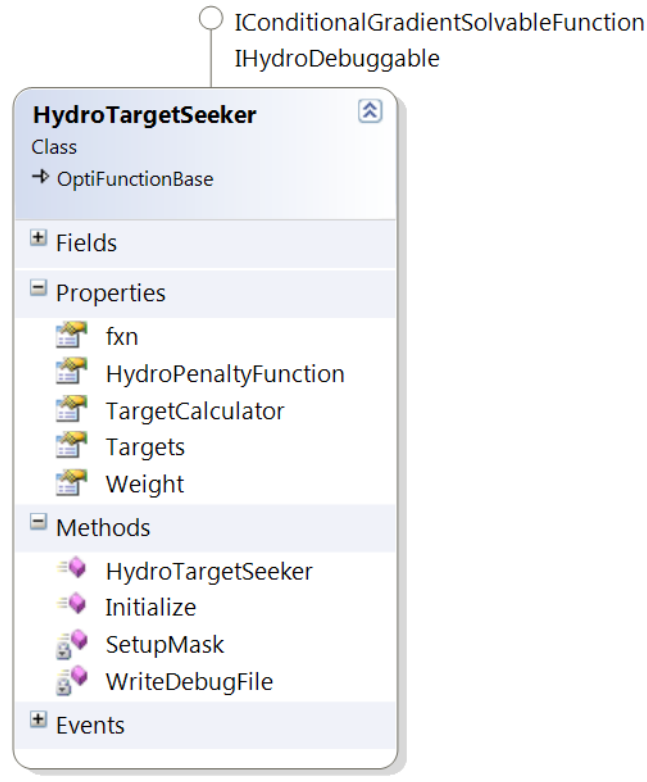


Figure 43: Diagram of attributes within the *HydroTargetSeeker* class

Two classes aid the *HydroTargetSeeker* class in building the hydropower objective function: *HydroCalculator* and *HydroTargetCalculator*. These two classes provide functions to build a symbolic representation of the flow, head, efficiency, and ultimately power and energy production. Each component is ultimately a function of flow through the links, since head and efficiency are functions of discharge through the hydropower unit as shown in Eq. (17). In this way, an instance of the *ConditionalGradientSolver* computes the derivative of the hydropower objective function and it retrieves the gradient of the objective function with respect to the discharge through the hydropower unit(s), which is then passed back into MODSIM as link costs. Eq. (18) shows the derivative of the hydropower function and Eq. (19) shows that the costs c_i within MODSIM are set to the derivative evaluated at the current estimate of the unit

discharge \hat{q}_i at each iteration. Note that these equations are for one particular hydropower unit or hydropower plant i .

$$\hat{P}_i = k q_i \eta_i(q_i, \hat{h}_i) h_i(q_i) \quad (17)$$

$$\frac{d\hat{P}_i}{dq_i} = k \left[\eta_i(q_i, \hat{h}_i) \left\{ h_i(q_i) + \frac{dh(q_i)}{dq_i} q_i \right\} + \frac{d\eta_i(q_i, \hat{h}_i)}{dq_i} q_i h_i(q_i) \right] \quad (18)$$

$$c_i = \left. \frac{d\hat{P}_i}{dq_i} \right|_{(q_i=\hat{q}_i)} \quad (19)$$

The functions of head $h_i(q_i)$ and efficiency $\eta_i(q_i, \hat{h}_i)$ are fitted polynomial equations based on user-provided input data. In MODSIM, users specify reservoir storage-capacity curves and efficiency tables of hydropower units. For reservoir elevations, users fill the A/C/E/Hydraulic Capacity table within the reservoir node as displayed in Figure 15.

A user can specify (only in code at this time) how MODSIM should calculate head (i.e., forebay and tailwater elevations) when being solved using the conditional gradient solver. The value of *HydropowerController.ElevType* can be specified as *ElevationFunctionType.Estimate*, *ElevationFunctionType.PiecewiseLinear*, or *ElevationFunctionType.Polynomial*. When the value of *ElevType* is *Estimate*, head and efficiencies are estimated as constants given a particular flow regime during iterations. When *PiecewiseLinear* is specified, MODSIM will estimate the head function as a line with respect to discharge through the hydropower unit. When *Polynomial* is specified, MODSIM will fit an n -th order polynomial to head and efficiency curves using least squares approximations by iteratively increasing n until the n -th order polynomial simulates head or efficiency attaining a coefficient of determination (R^2) of 0.999, which usually works well with stage-storage relationships since they are generally smooth curves. The least squares approximation for fitting polynomials using matrix notation is accomplished by solving the following linear system in Eq. (20) for weights \mathbf{w} .

$$(X^T X)\mathbf{w} = X^T T \quad (20)$$

where T is a matrix of target values, generally corresponding with measured values and X is a matrix of input values. In the stage-storage example, T is the vector of elevation values for the reservoir, and X is defined as follows with storage capacity $S_{c,i}$ for all data points i :

$$X = \begin{pmatrix} 1 & S_{c,1} & S_{c,1}^2 & \cdots \\ 1 & S_{c,2} & S_{c,2}^2 & \cdots \\ \vdots & \vdots & \vdots & \ddots \end{pmatrix}$$

Using polynomials provides a smooth, differentiable curve that is used to represent head and tailwater equations which is required when calculating the gradient of the nonlinear objective function. Otherwise, the conditional gradient method fails to converge. Figure 44 and Figure 45 display elevation curves fit to polynomial functions for reservoirs along the Columbia River. As illustrated in the figures, polynomial functions fit the curves reasonably well.

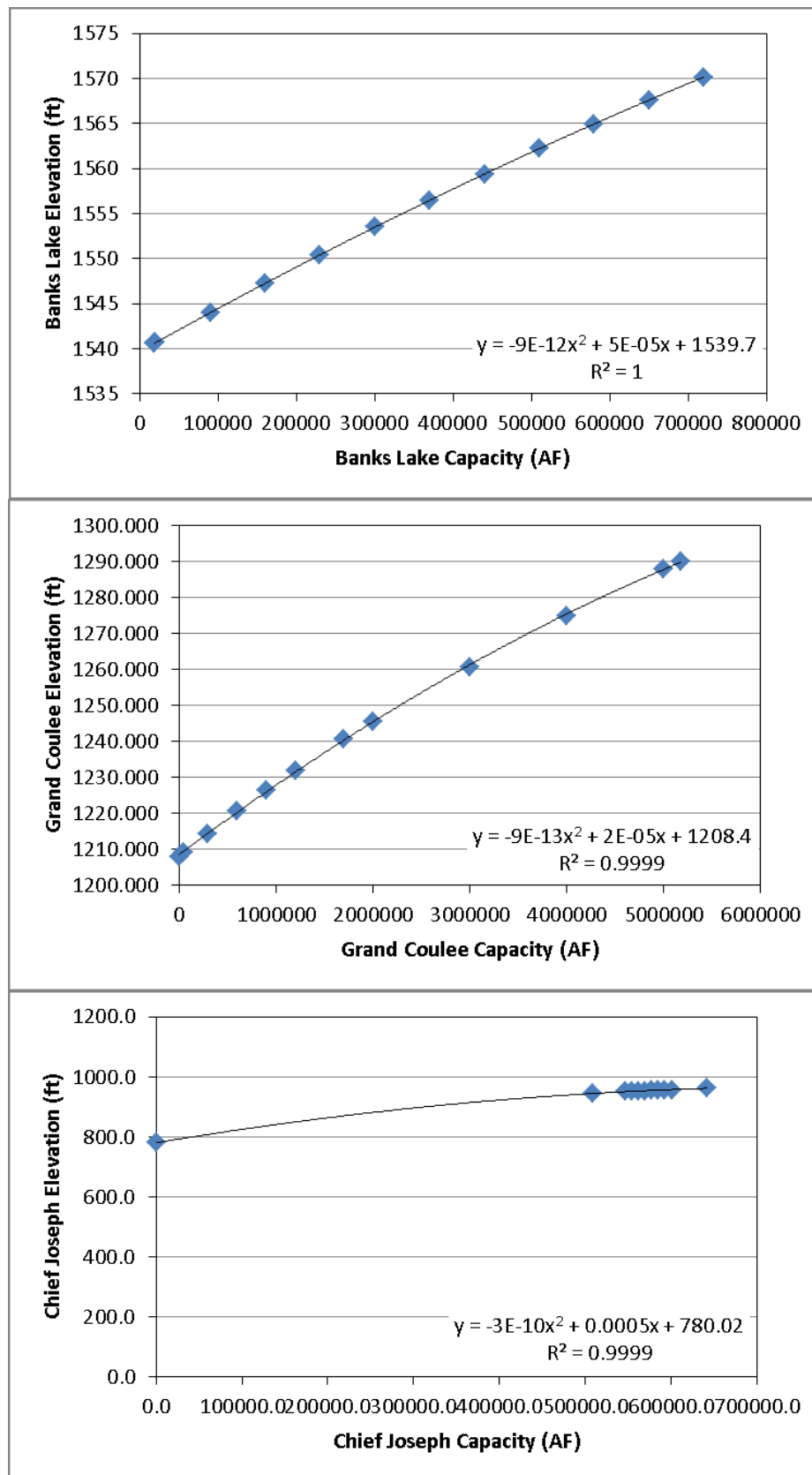


Figure 44: Fitted polynomials for Stage-Storage relationships of Banks Lake, Grand Coulee, and Chief Joseph

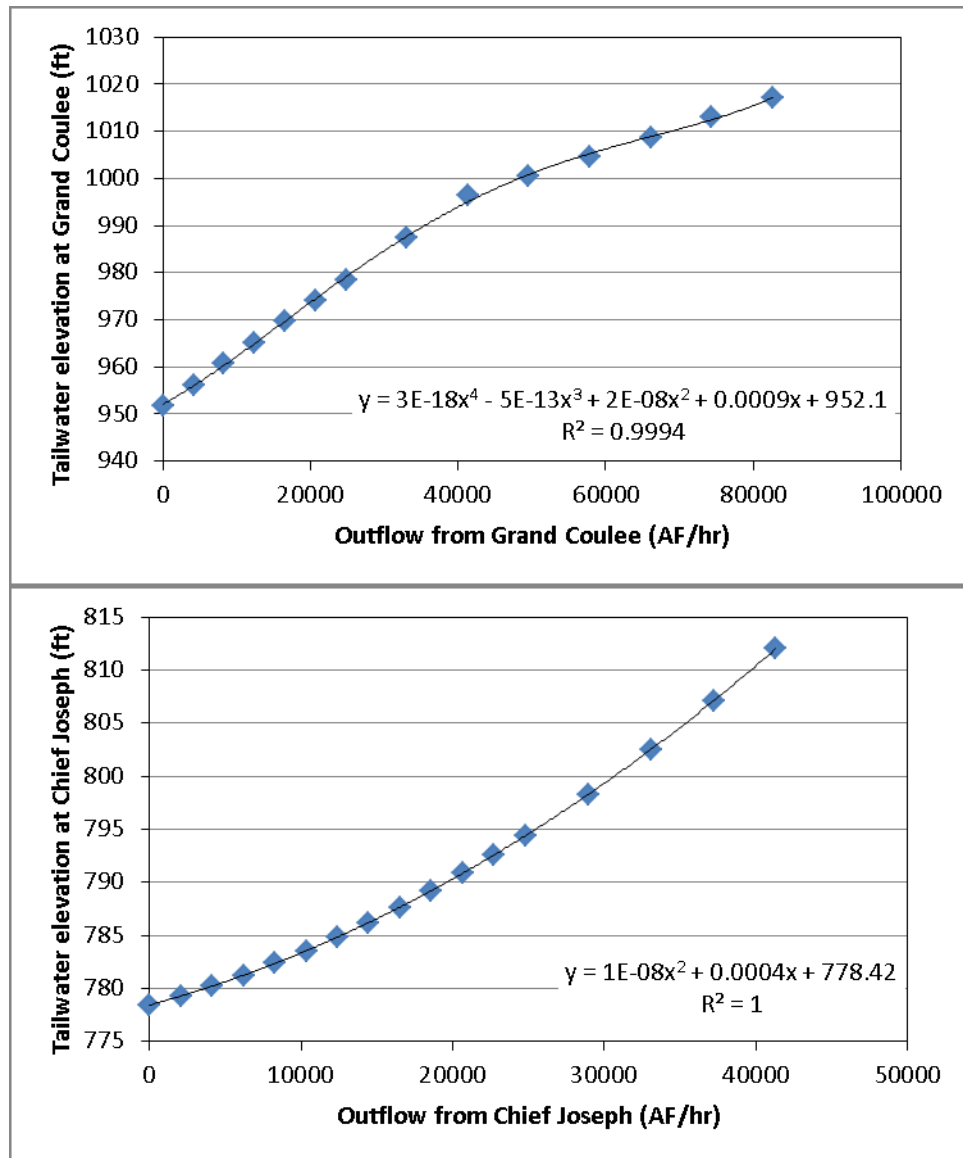


Figure 45: Tailwater elevation curves from Grand Coulee and Chief Joseph

As seen in Figure 44 and Figure 45, fitting polynomial functions to reservoir stage-storage and tailwater elevation curves is a reasonable approach when there are sufficient data points to fill in large gaps or operating agencies have already developed fitted curves to the data (as in the case of the curves displayed in the figures), assuming the data cover the full range from between the minimum storage volume and the maximum storage volume. Caution should be used when the stage-storage data tables have few data points or data that does not cover the full

range of storage capacities, since outside the bounds of fitted data, higher order polynomials tend to extrapolate poorly.

The complexity of equation (18) motivated the use of a symbolic math representation of the full nonlinear hydropower objective function. Additionally, symbolic math allows users to easily modify the objective function to almost any desired objective function. When the symbolic representation of (17) is passed into *ConditionalGradientSolver*, the derivative (18) is automatically calculated using a symbolic math toolbox (Meyer and Dozier 2012), and the *costs* attribute within the instance of *HydroTargetSeeker* is set as in Eq. (20). Essentially, this setup accounts for the full hydropower equation by iteratively updating total outflow (used in estimating tailwater elevations) and elevation head after each iteration of the conditional gradient algorithm.

5 Discussion

Two different solution methodologies have been discussed: successive approximations and the conditional gradient method. Each solution methodology can seek hydropower targets within MODSIM, but has advantages and disadvantages. Depending on the objective of a particular modeling study, either solution methodology or a combination of the two may prove to be preferable.

The successive approximations technique when applied to the hydropower problem solves the problem efficiently, does not require use of any symbolic math objects, and achieves a high precision answer quickly. However, since the successive approximations approach still utilizes the network flow structure, it can give “bang-bang” solutions when priorities change even slightly, and can sometimes converge to a false optimum when Eq. (5) is not satisfied.

Therefore, an overarching optimization problem such as the decomposed water and power algorithm proposed in Chapter IV, convergence problems are likely to occur.

The conditional gradient method (CGM) does not tend toward bang-bang solutions with small changes in input parameters. However, CGM has some major drawbacks as well. CGM generally takes 2 to 10 times longer than the successive approximations routine depending on solver parameters and network setup. This is due to a common problem with the CGM, known as the zig-zagging effect, where linear precision increases in the objective function cause exponential increases in computation time. Precision of the answer in the CGM can also be limited by the integer solver within MODSIM, since MODSIM uses integers within its network flow solver, it cannot be scaled down to have equivalently sized units as the hydropower penalty terms. Therefore, the size of the penalty on the hydropower target equation is limited by the positive size of 64-bit integers divided by the maximum flow that could be conveyed through the MODSIM links. After the CGM computes the gradient, it applies the gradient to link costs within the MODSIM network. In order for solutions to converge to some specified precision, these new link costs need to be larger in magnitude than any conflicting priority as the procedure converges. Otherwise, the solution process will terminate prematurely since the MODSIM solver ceases to respond to changes in link costs when they are of less magnitude than the conflicting link cost. This would not be an issue if the MODSIM objective function and variable sizes could be scaled appropriately to allow for sufficiently large penalties in the hydropower target objective function, but the integer-based solver in MODSIM prevents this. Figure 46 displays these limitations of the CDM with two possible conflicting costs of links other than link i in the MODSIM network.

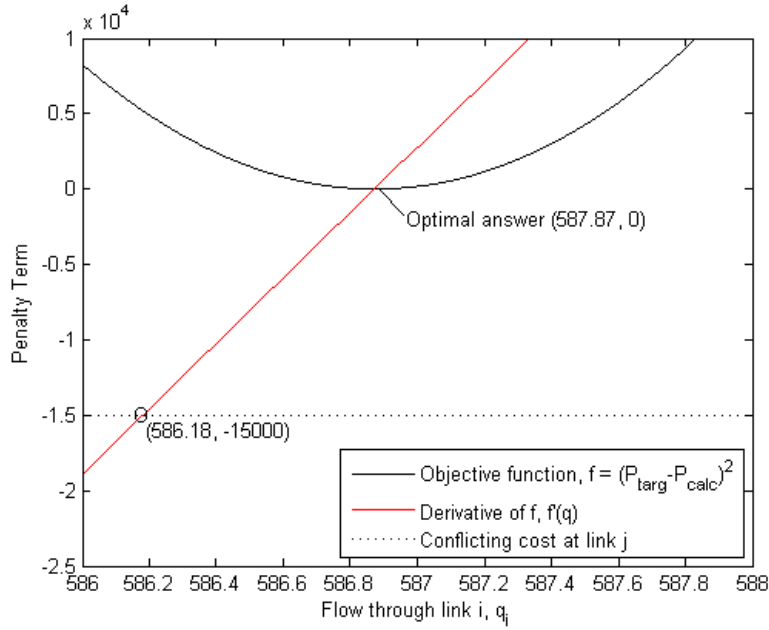


Figure 46: Convergence limitations

In Figure 46, an example hydropower target penalty function is defined so that MODSIM attempts to find the optimal flow through link i to $q_i^* = 587.87$. However, another link j with cost -15000 may restrict the flow through link i even if link j *should* have less priority. For example, if MODSIM places flow through link k when the cost of link i is greater than -15000 , then if the solution starts at $q_i^0 > 586.18$, the next cost set to link i will be within $(-15000, \infty)$. Then, the MODSIM solver will place flow through link k . If the objective function is convex and the derivative of f is therefore monotonically increasing, the next iteration produces $q_i^1 = 0$, and the next iteration or a few iterations later, the CDM will produce $q_i^l > 587.18$ again. The process will repeat itself until MODSIM converges on 586.18 (not 587.87). Within a MODSIM network, this type of example is not an uncommon occurrence. Therefore, proper setting of penalty magnitudes is actually a large part of the model calibration.

As an example of the differences between the successive approximations and CDM techniques, a MODSIM network for Grand Coulee, Banks Lake, and Chief Joseph was setup

with historical hydropower production as targets. A snapshot of hydropower production using successive approximations in a day within the simulated time period for each of the hydropower facilities (Banks Lake pumping, Grand Coulee generating, and Chief Joseph generating) are displayed in Figure 47 and Figure 48. The CGM seems to consistently converge on a local minimum during this period as shown by its poor performance at the Banks Lake pumping station. Separating weights to the various parts of the hydropower equation may help to mitigate this issue.

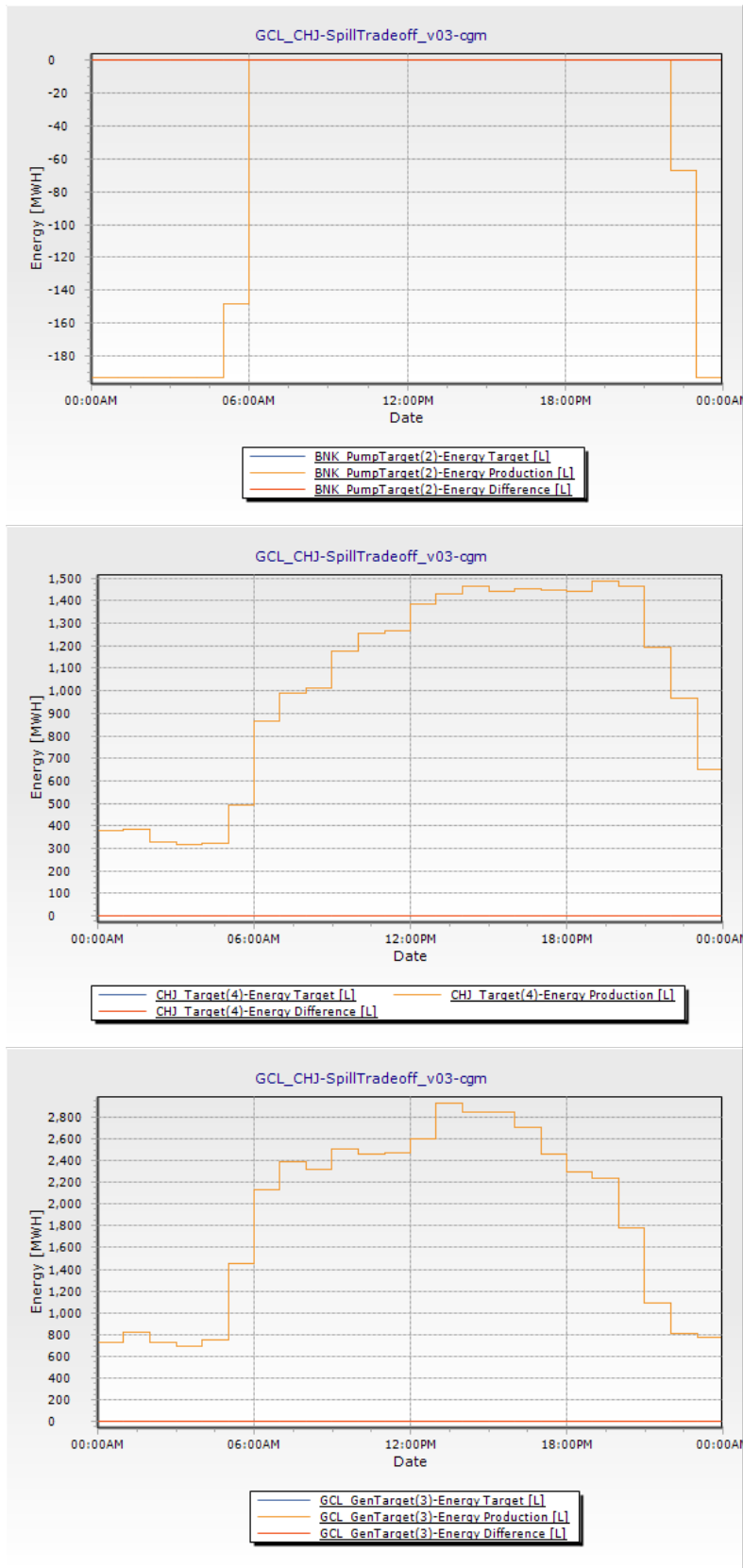


Figure 47: Simulated and observed hydropower production from Banks Lake (top), Grand Coulee (middle), and Chief Joseph (bottom) using the successive approximations approach

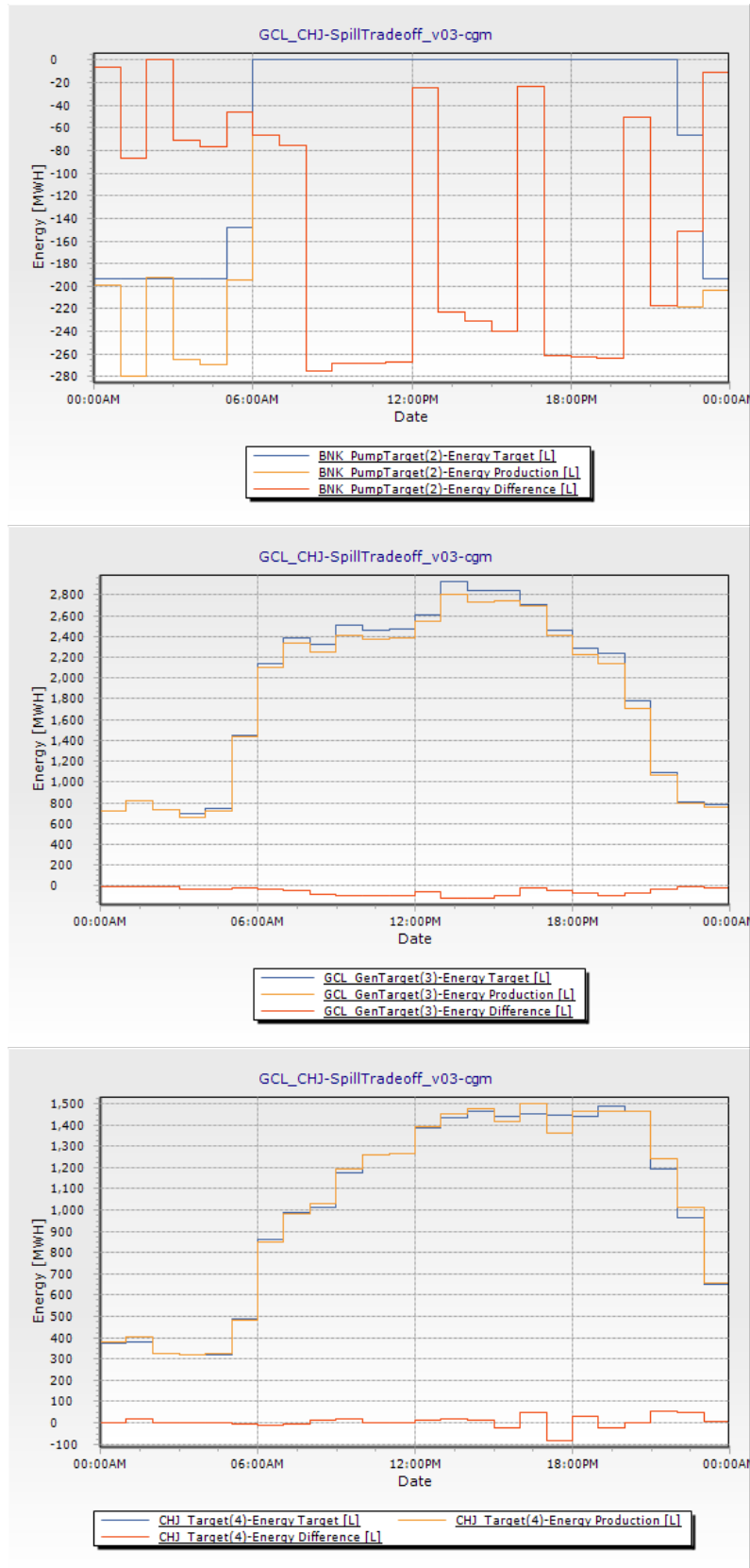


Figure 48: Simulated and observed hydropower production from Banks Lake (top), Grand Coulee (middle), and Chief Joseph (bottom) using the conditional gradient method

V Implementation of Simplified Integrated Model

The second level of the three level integrated water and power model (IWPM) structure as formulated in Chapter III describes a fully decomposed Lagrangian Relaxation technique to the IWPM problem. However, in order just to test the additional nonlinear modeling capabilities of the water network model, a simpler implementation of the second level has been developed. In order to do this, a linear programming formulation of a DC power flow was implemented to represent the power system and solve for optimal hydropower injections while satisfying transmission constraints. Optimal hydropower injections as deemed appropriate by the DC power flow model are then introduced into the water network model as hydropower targets.

The power network subproblem is formulated as a linear programming (LP) problem to minimize the absolute difference between hydropower injections and historical power production, which is essentially given to the model as targets so as to examine operational deviations from the historical scenario. Power network solution simply provides an initial estimate \hat{P}_j of the set of optimal power injections P_j^* to the water network. The use of this power network objective function is to ensure that a feasible set of hydropower targets are passed into the water network solver in order to provide transmission-constrained hydropower injections to the grid. Let $f_P(\mathbf{P})$ be defined as follows in Eq. (21):

$$f_P(\mathbf{P}) = \sum_{j \in R_{all}} |P_j - P_{targ,j}| \quad (21)$$

However, in order to define this problem as a linear programming problem, large costs are assigned to nonnegative variables that define positive and negative deviations from the power target $P_{targ,j}$. Therefore, the objective function is formulated as Eq. (22) with the subsequent

additional constraint shown as Eq. (23) where M is a large weight and the \mathbf{s} vectors are slack (-) and excess variables (+) that represent a positive distance from a specified power target.

$$\min_{\mathbf{p}} M \cdot \mathbf{s}^+ + M \cdot \mathbf{s}^- + 100 \cdot M \cdot S_{imp} + 100 \cdot M \cdot S_{exp} \quad (22)$$

subject to (9), (10), (25) and (26) as well as the following constraint (23):

$$P_i - P_{targ,i} + s_i^- - s_i^+ = 0 \quad (23)$$

The energy balance equation (9) is updated to include a “swing” power importer S_{imp} and exporter S_{exp} that specify an excess or deficit of power within the balancing area (the portion of the grid being modeled) as follows in Eq. (24):

$$\sum P_i + S_{imp} - S_{exp} = P_{load} + P_{losses} \quad (24)$$

This linear programming problem defines the simple power dispatch algorithm to dispatch power generating resources as a deviation using an absolute norm from pre-specified hydropower targets only when transmission constraints are violated. This objective function aims at minimizing deviations from a specified hydropower target at a particular reservoir without deviating too much, which is essentially a methodology allowing hydro resources to be flexibly operated to mitigate constraints within the power systems such as transmission constraints.

Additional constraints ensure that power flows across branches within the transmission system do not exceed the heat rating for the line. Eqs. (25) and (26) are energy balance as a function of power injections $P_{i,j}$ and power consumption $L_{i,j}$, and limitations on power flows $PF_{i,k}$ between each bus i and k .

$$\sum_{k \in B_i} PF_{i,k} + \sum_{j \in G_i} P_{i,j} - \sum_{j \in D_i} L_{i,j} = 0 \quad (25)$$

$$-PF_{i,k,max} \leq PF_{i,k} \leq PF_{i,k,max} \quad (26)$$

where B_i is the set of all branches connected to bus i , G_i is the set of all power generators at bus i , and D_i is the set of all power demands at bus i . Power flows across a branch from i to k are limited by $PF_{i,k,max}$. Outputs of the power model consist of optimal power injections \mathbf{P}^* dispatched in order to satisfy transmission power flow constraints.

The simplified formulation of the water optimization problem is provided in Eq. (27), which attempts to minimize the squared distance from pre-specified hydropower targets $P_{target,i}$ at hydropower unit i and also satisfies transmission constraints using an Augmented Lagrangian formulation (Conejo et al. 2006; Bertsekas 1995) to relax the constraint that hydropower production calculated within the water network $kq_j h_j \eta_j$ should be equal to the estimated optimal hydropower injection into the power system model \hat{P}_j for a particular reservoir or hydropower unit j . Squared terms penalize large deviations from the power target more than small deviations, and therefore help to avoid bang-bang solutions and the squared (augmented) portion of the Lagrangian term essentially aids the solver in selecting a better estimate of the optimal Lagrange multiplier. Let $f(\mathbf{q})$ be defined by the following equation where $R_{turbines}$ and R_{pumps} are the sets of all turbines and pumps:

$$f(\mathbf{q}) = \sum_{j \in R_{turbines}} \left[(kq_j h_j \eta_j - P_{target,j})^2 + \lambda_j (kq_j h_j \eta_j - \hat{P}_j) + \alpha (kq_j h_j \eta_j - \hat{P}_j)^2 \right] \\ + \sum_{j \in R_{pumps}} \left[\left(\frac{kq_j h_j}{\eta_j} - P_{target,j} \right)^2 + \lambda_j \left(\frac{kq_j h_j}{\eta_j} - \hat{P}_j \right) + \alpha \left(\frac{kq_j h_j}{\eta_j} - \hat{P}_j \right)^2 \right]$$

Then, the conditional gradient solver solves the following optimization problem during MODSIM simulation:

$$\min_{\mathbf{q}} f(\mathbf{q}) \quad (27)$$

subject to (2) and (3). Calculated hydropower production from the water network should equal the power injected into the power network model, which represents the complicating constraints as shown in Eqs. (28) and (29) that are relaxed within the objective function and multiplied by Lagrange multipliers λ :

$$kq_j h_j \eta_j = \hat{P}_j \quad \forall j \in R_{turbines} \quad (28)$$

$$\frac{kq_j h_j}{\eta_j} = \hat{P}_j \quad \forall j \in R_{pumps} \quad (29)$$

After each iteration of the water network model, Lagrange multipliers are updated using Eqs. (30) and (31) in order to maximize the dual problem formulation with respect to lambda values. At the beginning of each timestep, before iterations begin, the Lagrange multipliers are reset to an initial value, and at each iteration v , the Lagrange multipliers are updated according to the following equations:

$$\lambda_j^{(v+1)} = \lambda_j^{(v)} + \frac{1}{a + bv} (kq_j h_j \eta_j - \hat{P}_j) \quad \forall j \in R_{turbines} \quad (30)$$

$$\lambda_j^{(v+1)} = \lambda_j^{(v)} + \frac{1}{a + bv} \left(\frac{kq_j h_j}{\eta_j} - \hat{P}_j \right) \quad \forall j \in R_{pumps} \quad (31)$$

Eqs. (30) and (31) update Lagrange multipliers for the original Lagrangian relaxation method, but in order to speed convergence an augmented Lagrangian formulation was used where the Lagrange multipliers are updated according to Eq. (32) as follows:

$$\lambda_j^{(v+1)} = \lambda_j^{(v)} + \alpha \cdot h(q) \quad \forall j \in R \quad (32)$$

where R is the set of all hydropower targets within the network and $h(q_j) = (kq_j h_j \eta_j - \hat{P}_j)$ for turbines and $(kq_j h_j / \eta_j - \hat{P}_j)$ for pumps. The parameter α can be increased at each iteration to result in even faster convergence, but this often leads to ill-conditioning of the problem as described by Bertsekas (1995) and was therefore not performed in this study.

1 **The Power Model in Code**

The power dispatch algorithm is implemented in code within the *PowerSystemBase* class, which implements the *IConditionalGradientSolvableFunction* interface, which renders the class capable of solving nonlinear objective functions using the conditional gradient method. However, within the class, a linear programming (LP) problem utilizing the objective function as found in Eqs. (21)-(23) is constructed and solved using the *SolveLinear()* method. After solution of the LP problem, the solver updates the P_i variables in the MODSIM model network, which are located in *HydropowerTarget* objects that house the hydropower targets for a particular hydropower unit. Another class that implements the *IConditionalGradientSolvableFunction* is the *TwoBusSystem* class, which defines an objective function and constraints that can be solved using the conditional gradient algorithm specifically for a two-bus system.

Most of the properties within the *PowerSystemBase* class are required by the *IConditionalGradientSolvableFunction* interface, which makes the class compatible with the conditional gradient solver. For this research, only the linear programming approach was used in power system dispatch because it solves the problem more rapidly and precisely. The property value *RunAsLinearProblem* is set to *true* when the linear programming formulation is to be used. It should be noted that squaring the difference between P_i and $P_{tar,g,i}$ could result in better results overall because larger deviations of power injections from power targets are penalized more than small deviations, which likely tends to keep solutions within reasonable operating ranges.

Variables and linear constraints can be added to the power system using the *LinearModel* property of the *PowerSystemBase* class. As mentioned previously, the *SolveLinear()* method can be used to build and run the LP formulation of the power system problem formulated in Eqs. (21)-(23). The total system load is defined by setting the property *Load* using the same units as

all other calculated power values. A vector of the originally specified hydropower targets $P_{targ,j}$ for unit j is stored within the property *OriginalTargets*, which is a nested array containing a one dimensional array where each element refers to a timeseries of hydropower targets contained in a two-dimensional array with timesteps increasing down its first dimension and hydrologic state (Labadie 2010) increasing across the second dimension.

Power flow equations and limitations as defined in Eqs. (25) and (26) are not included directly in the *PowerSystemBase* class because the class aids in defining a generic power system model. On the other hand, the *TwoBusSystem* class is oriented towards a specific single line diagram (the bus-branch structure of a power flow problem set up) and power flow equations can be explicitly determined with some assumptions on the locations of the “swing” generator S_G and load. Figure 49 displays the one-line diagram used within the *TwoBusSystem* class. Power flow constraints can be added to the *PowerSystemBase* constraint set by manipulating the *LinearModel* property according to instructions on how to use Microsoft’s Solver Foundation class library (Microsoft 2012).

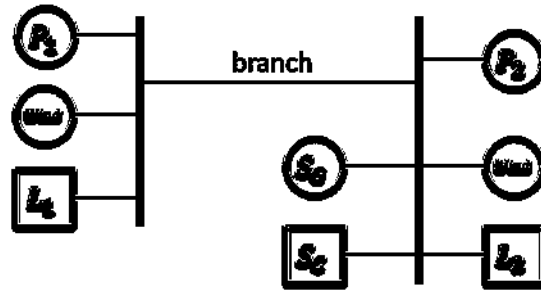


Figure 49: One-line diagram of the generic two-bus system

Although the IWPM within this chapter is more simplistic and in a less generalized form than the long-term goal described in Chapter III, the simple power flow model still demonstrates the capability of an IWPM to address operational challenges of intermittent renewable energy sources such as wind and simulate effects on non-power criteria. Testing of the IWPM was

performed on several reservoirs along the mid-Columbia, and details for this case study can be found in the next chapter.

VI Case Study of Grand Coulee, Banks Lake, and Chief Joseph

Environmental regulations on reservoir and power grid operations such as required integration of renewable energy systems have created many contemporary operational challenges that were not faced before. Integrated water and power systems modeling could potentially provide many benefits to operators and other stakeholders within water and power sectors, because tradeoffs between the two systems can be analyzed and assessed in an integrated fashion. Specifically, within the Pacific Northwest, hydropower is the major source of electric energy within the region. Operations of hydropower facilities are constrained by flood control and environmental criteria, primarily. The Grand Coulee and Chief Joseph dams are located along the Mid-Columbia River, and provide a significant amount of hydropower resources to the region. One particular environmental criterion set by the Clean Water Act that significantly impacts operations at Grand Coulee during periods of high river flows is a total dissolved gas (TDG) threshold of 110%, meaning that TDGs within the water are supersaturated with a 10% larger pressure of TDGs within the water than the ambient atmospheric pressure. Excessive TDG can induce gas bubble disease (GBD) in fish, especially above 120% (Weitkamp and Katz 1980; McGrath et al. 2006). The Environmental Protection Agency (EPA) will grant waivers for dams along the Columbia and Snake Rivers during the fish passage season to allow for TDG levels between 110% and 120%, but restrict it to 110% at other times, simply because dams within the Pacific Northwest are unable to pass all river flow through turbines, and spills are generally desirable in order to promote safer fish passage downstream (since fish passage through turbines often results in high fish mortality).

Discharges through dam spillways increase TDG levels significantly, especially for large dams such as Grand Coulee. Although, spills tend to be avoided, situations occur when spills

must occur for purposes of flood control. Figure 50 displays total dissolved gas, inflow, total outflow, and spillway discharge over the year 2011, which shows levels exceeding 120% for most of the summer, which is when snowmelt runoff tends to peak. As displayed by the figure, high levels of TDG occurred simultaneously with high levels of spillway discharge, but generally close to forebay TDG levels when no spill is occurring.

The Bonneville Power Administration (BPA) (2010) describes the effect that reducing TDG in the river has on power pricing, since avoiding spills means water must be passed through the turbines, even during periods of low demand. Sometimes, when large amounts of hydropower are being generated, wholesale power prices can become negative. In this case, independent power producers (IPPs) must pay to place power on the grid, except in the case of “must-take” agreements with intermittent renewable energy sources, which are agreements that force balancing authorities to accept any power generated from intermittent renewable energy sources. This negative price condition can persist as long as TDG levels and river flow levels are too high. When there is insufficient power load to match the generated power, constraints on the magnitude of spillway discharge and minimum generation requirements through the hydropower turbine units may force grid operators to curtail other power sources, which is mainly wind powerplants in the case of the Pacific Northwest. Consequently, “must-take” agreements and contracts between BPA and independent power producers have been compromised in light of environmental regulations, resulting in large amounts of lost revenue and significant loss to global welfare, a term in economics describing benefits to producers and consumers.

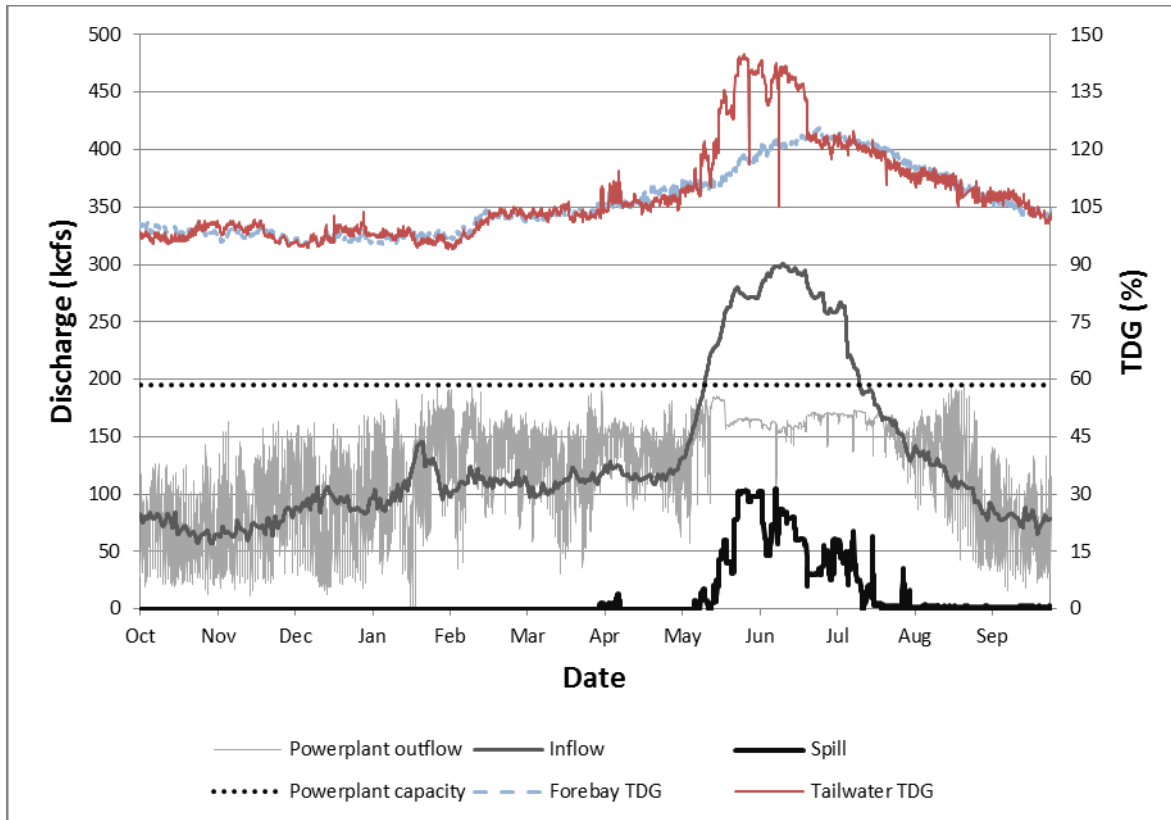


Figure 50: Total dissolved gas (TDG), inflow and outflow at Grand Coulee

In practice, environmental regulations are generally considered operational constraints since they are prescribed by law, whereas contracts and power purchase agreements are slightly more flexible. Global welfare may benefit if environmental regulations are also considered are objectives that have associated tradeoffs with other reservoir operational objectives such as hydropower generation. As seen in Figure 50, outflow from the powerplant at Grand Coulee was lower than capacity for this example, which forced an increase in spillway discharge and TDG levels. Such operations were likely due to excessively high amounts of power generation throughout the rest of the Columbia River System (i.e., exceeding the electric load). This illustrates the potential for tradeoffs between environmental criteria such as TDG and the reliability of electric power production, both of which have significant impacts both financially and culturally across the Pacific Northwest region.

A case study analysis of operations between Grand Coulee, Banks Lake, and Chief Joseph was performed to understand potential tradeoffs between the TDG criteria when transmission constraints and increasing unscheduled power flows due to wind penetration require hydropower re-dispatching. Actual layouts of power transmission systems are not available publicly within the U.S., but can be requested from the Western Electricity Coordinating Council (WECC). However, the balancing area within the Pacific Northwest would have to be essentially “cut out” of the full WECC grid, which requires measured transmission power flows at the cut planes at the edges of BPA’s balancing area. Additionally, generation at individual wind farms would need to be considered in order to mitigate effects of geospatially diverse wind farms on transmission of power with a geospatially diverse set of cascaded reservoirs. Individual wind farm data however is proprietary and is generally not available, especially for recent years. For these reasons, a simple model is applied to demonstrate the capabilities of the IWPM using a simple 2-bus DC system with variable amounts of transmission capacity. The time period of interest is the summer of year 2011, when high spring runoff required curtailing of wind power generation.

1 Model Calibration

Water system model calibration helps ensure that local inflows and outflows between reservoirs are accounted for at hourly timesteps. Inflows are provided in daily timesteps for both Chief Joseph and Grand Coulee, whereas outflows are provided in hourly timesteps. Since local inflows and outflows, or incremental flows, are needed to be calculated in hourly timesteps, both historical daily inflows and historical hourly outflows were used in estimating the incremental flows. Incremental flows can be calculated using a network flow formulation that also incorporates routing features. For the system with Grand Coulee and Chief Joseph, MODSIM

was used to calculate local inflow and outflows by setting up the model as in Figure 51. This network setup provides sufficient amounts of incremental inflows and losses for the model to match historical river flows and reservoir storage volumes. After calibration, a simulation network was constructed that executes the network model with the calculated local inflows and losses while attempting to achieve a specified hydropower target. The simulation network displayed in Figure 52 illustrates the schematic of the MODSIM model that was used to simulate operations at Chief Joseph, Banks Lake, and Grand Coulee.

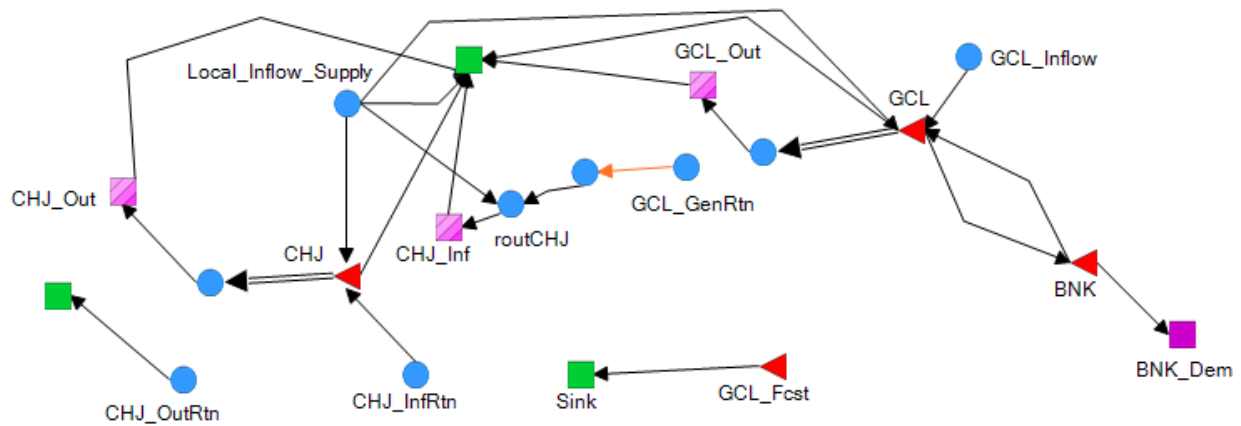


Figure 51: Schematic of MODSIM calibration model used to calculate local inflows

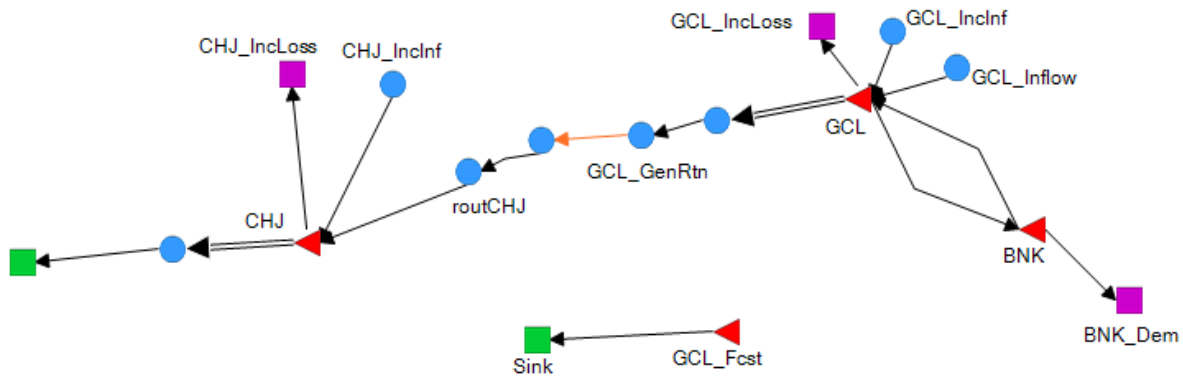


Figure 52: Schematic of MODSIM simulation model

Total outflow from Grand Coulee and Chief Joseph are controlled by nodes *GCL_Out* and *CHJ_Out* with priorities such that discharges through the reservoirs are favored above maintaining storage in the reservoirs. Inflows to Chief Joseph are controlled partially by both

CHJ_Inf and *CHJ_Out* since inflows are daily values and outflows are hourly. Local inflows and losses for Chief Joseph provide the estimated hourly inflow above or below the daily inflow, which is returned from *CHJ_Inf* to *CHJ_InfRtn*. Historical pumping and generating discharge to and from Banks Lake were not used in the calibration since these flows are negligible in comparison with flows along the Columbia River. Local inflows are supplied by *Local_Inflow_Supply* and losses are taken by the green sink node next to it. The link connecting the two nodes is assigned a negative cost in order to ensure that local inflows are not too high. Reservoirs are provided historical storage volumes as targets, which provides MODSIM with sufficient information to establish local inflows and losses.

The link connecting *GCL_GenRtn* to its downstream node is a routing link in which lag factors are specified. Columbia River flows generally require about 1.5 hours to travel downstream from Grand Coulee to Chief Joseph. Therefore, lagged routing factors as shown in Table 5 were used to simulate half of the discharge from Grand Coulee at the current timestep as reaching Chief Joseph at the next timestep, and the other half arriving at the timestep following, which simulates flow reaching at 1.5 hours.

Table 5: Lagged routing factors between Chief Joseph and Grand Coulee

Timestep from current	Fraction of current flow
0	0
1	0.5
2	0.5

Results from the calibration network are placed as estimates of the real inflows and losses placed in the simulation network, which attempts to match hydropower targets. Simulated energy production at each reservoir from the calibration network are used as energy targets within the simulation network, since actual turbine efficiencies as functions of flow and head are inexact and tend to be conservative, resulting in the model producing less energy than measured

historically. Simulated energy production performed reasonably well when compared with historical energy production, except during the summer when energy production within the reservoir fell below its potential, which was not placed in the model as a consideration. Actual energy production in the model corresponds to potential production, but this is not always the case in reality as discussed above. Figure 53 displays the timeseries representation of energy production and energy targets from Grand Coulee. As seen in the figure, electric energy production targets, which are equivalent to measured energy production, are below the simulated production between May 15 and July 15. At Chief Joseph, the same operational phenomenon occurred as shown in Figure 54.

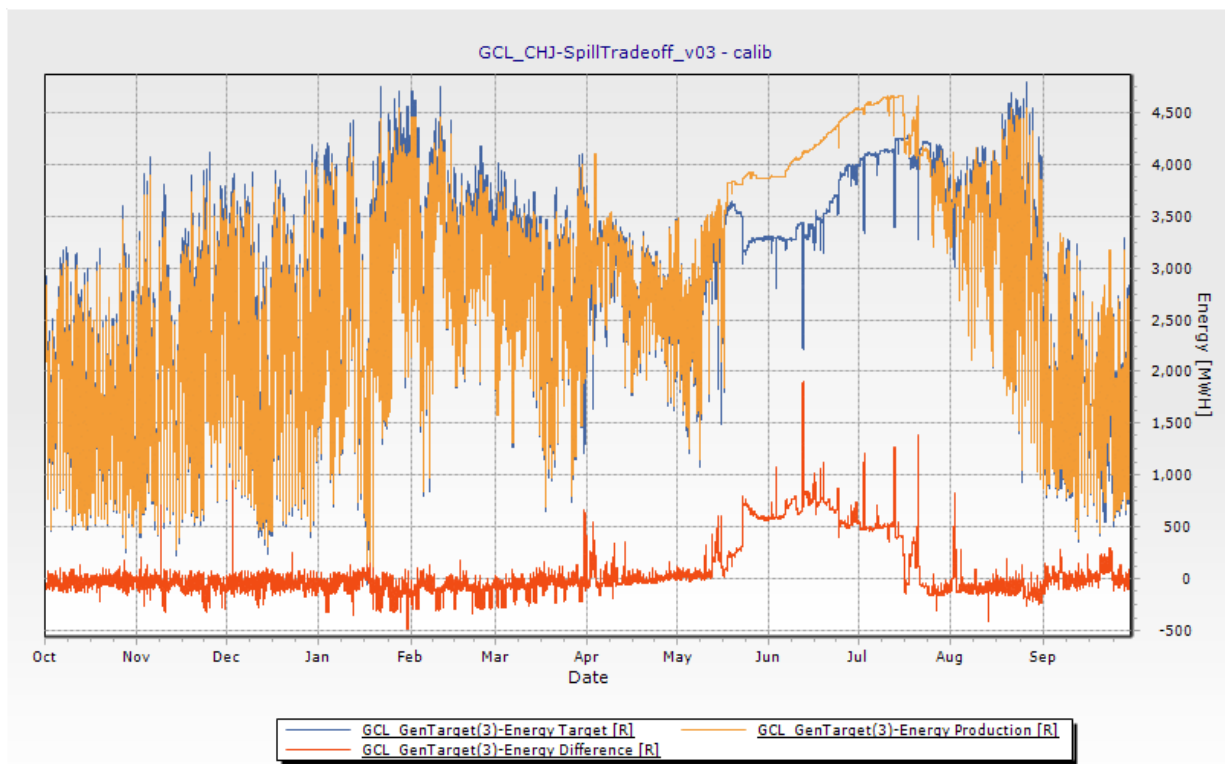


Figure 53: Simulated energy production, energy targets, and production minus targets at Grand Coulee

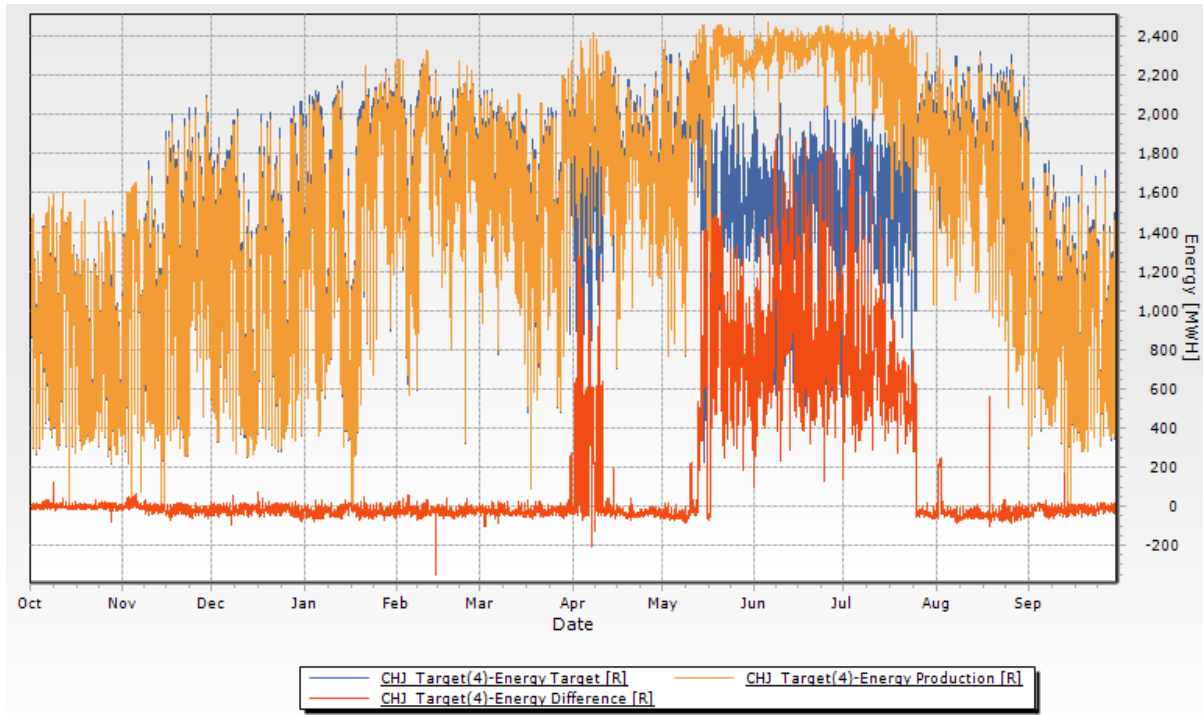


Figure 54: Simulated energy production, energy targets, and production minus targets at Chief Joseph

1.1 *Linear Model of Total Dissolved Gas (TDG)*

A linear regression model of total dissolved gas (TDG) was developed in order to simulate TDG levels given several other variables along with spill. Spill can generally be used as the only input to some TDG models, but Grand Coulee spills do not explain much of the variability of TDG within the Columbia River downstream of Grand Coulee, although some visible relationship can be seen between TDG and spillway discharge at Grand Coulee as shown in Figure 55.

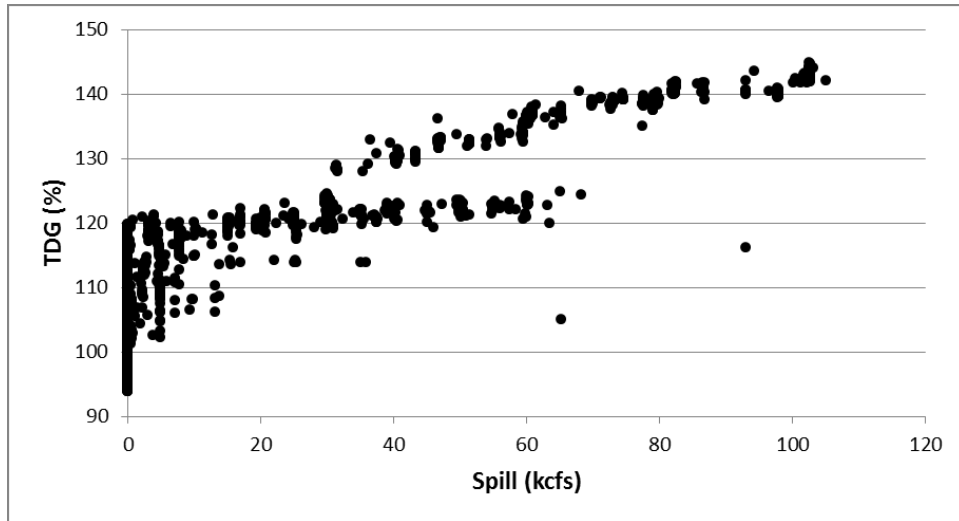


Figure 55: Total dissolved gas (TDG) at Grand Coulee as a function of Spill

Other parameters such as forebay elevation, tailwater elevation, tailwater air temperature, tailwater water temperature, forebay water temperature, forebay air temperature (max and min), barometric pressure, inflow, total outflow, the squared value of spillway discharge, and forebay total dissolved gas were used within the linear regression model. Figure 56 displays the performance of the simulated values when compared to measured values of tailwater TDG (TW_TDG) for two separate datasets (“training” and “testing”). Testing data was not used to build the linear model, but only to simulate TDG with new data to observe its performance on the new data. As shown in the figure, there is good performance in both datasets, where root mean squared error (RMSE) was 2.1 % for testing and 2.4 % for training and the coefficient of determination (r^2) was 0.963 for testing and 0.965 for training. The same “break” in the data can be seen in the fit of the linear model shown in Figure 56.

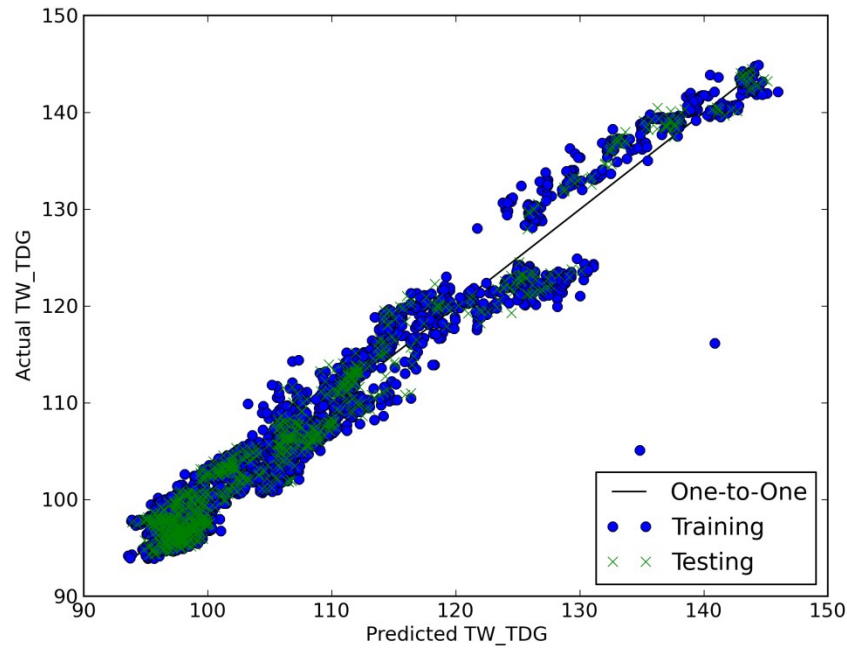


Figure 56: Simulated tailwater TDG versus measured tailwater TDG at Grand Coulee

The TDG model needs to be able to correctly represent changes in TDG given perturbations in the inputs. TDG is expected to increase with increasing spillway discharge. A positive weight value multiplied by spillway discharge terms would be expected when fitting a linear model to TDG levels given spillway discharge. Weights were solved using the regularized least squares method, and the bootstrapping method (Fox 2008) was employed to generate 95% confidence intervals for optimal weight values, which are displayed in Figure 57 as red lines. As shown by the figure, a positive weight value is associated with the spillway discharge variable as well as the squared value of spillway discharge. When more spill occurs, higher TDG levels are produced in the tailwater, and vice versa. Figure 58 displays a perturbed simulation where spillway discharge was set to zero and total outflows were decreased by the amount of missing spill, which may not be a feasible solution, but the positively correlated relationship between spillway discharge and outflow is illustrated. When spillway discharge decreases to zero, then TDG levels decrease from about 145% to 130%, which is a significant improvement, but again

might be at an infeasible solution. The simple linear TDG model works as expected, but has not been thoroughly tested on other years of data, which is a potential improvement to this environmental modeling aspect.

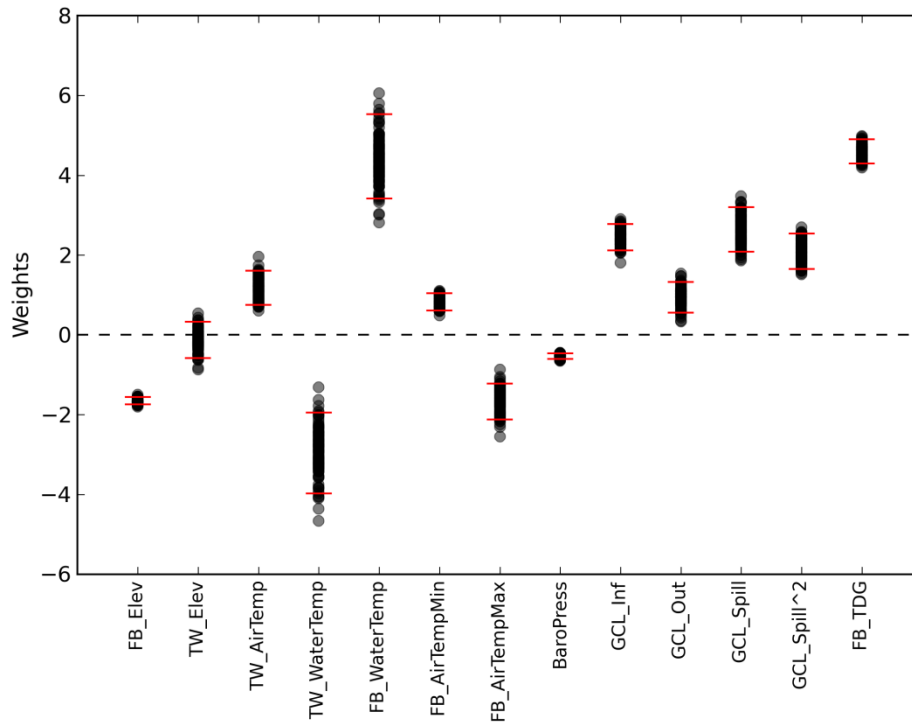


Figure 57: Weights associated with each variable in the linear TDG model

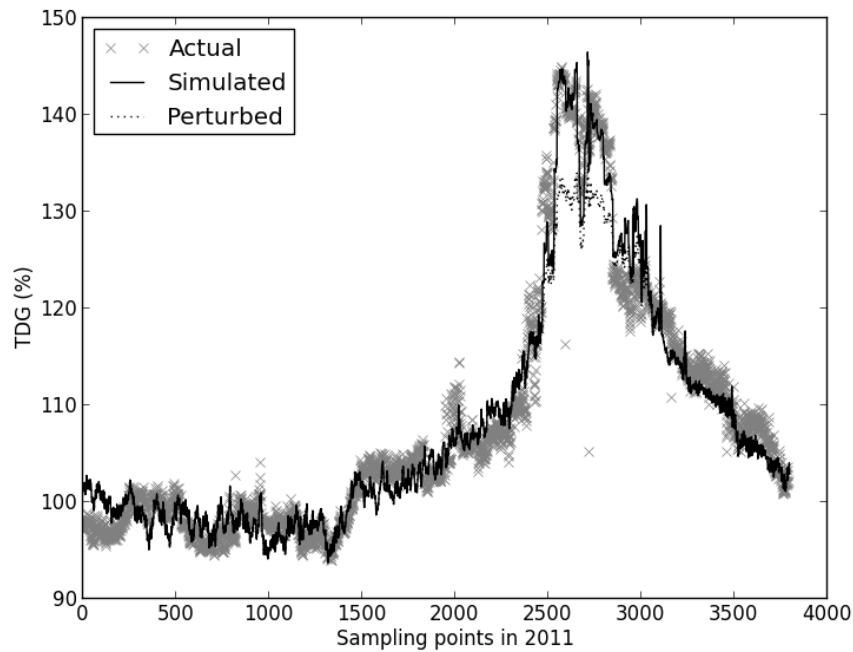


Figure 58: Simulated total dissolved gas using historical reservoir information along with a “perturbed” simulation where spills were set to zero

Penalty on high total dissolved gas (TDG) in the water network model is simulated by using the relationship of spillway discharge and TDG. A large cost on the spillway discharge is used to penalize large spills and therefore also penalizes high TDG levels.

2 **Scenario Setup**

Four major criteria compose the tradeoff space of the model setup for this case study: transmission capacity, capability or flexibility of hydropower facilities to meet specified hydropower targets, increased wind penetration, and TDG. A model of Grand Coulee, Banks Lake, and Chief Joseph was built to load follow, or firm, intermittent wind penetration. Transmission capacity is changed amongst various simulations to analyze the amount of wind that can be integrated into a grid with limited transmission.

A set of simulations were performed with varying amounts of transmission capacity, unscheduled flow using wind farm generation data, and hydropower target deviation penalty weights. The transmission system was modeled as a simple 2-bus DC system as illustrated in Figure 59 where Eqs. (9), (10), (25), (26) apply as constraints and the solution methodology described in Chapter V is used to integrate this system with the model of the mid-Columbia river and reservoirs.

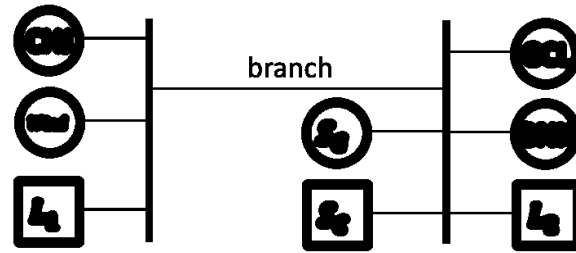


Figure 59: Schematic of two-bus system used to test systems model of mid-Columbia dams

As shown in Figure 59, wind is injected into the left bus and any deviations of power produced or consumed are extracted or injected by the “swing” generator S_G and consumer S_C on the right bus so power flows PF across the branch are simply calculated as the difference between wind production plus production at Chief Joseph and the first load L_1 :

$$PF = P_{CHJ} + P_{wind} - L_1 - S_G + S_C$$

Using this equation for power flow PF , positive values represent flow from left to right and negative values represent flow from right to left. This power flow equation is constrained by the heat capacity of the transmission lines that make up the branch. Thus, a constraint is placed into the LP problem according to Eq. (26). Total load ($L = L_1 + L_2$) is calculated as the initially specified hydropower targets plus the wind generation at each timestep. In this case study, hydropower targets are set to simulated hydropower production using historical inflows, outflows and reservoir storage volumes as described in Section 1. Total load is split in between L_1 and L_2 using the following equation:

$$L_1 = \alpha L$$

where α represents the fraction of the total load that is apportioned to the left bus. A fraction of 0.31 was used in this study, because this value for α centers baseline power flows about zero. Figure 60 displays the calculated power flows across the branch without any wind in the system, where minimum and maximum values lie about -1100 and +1100 MW.

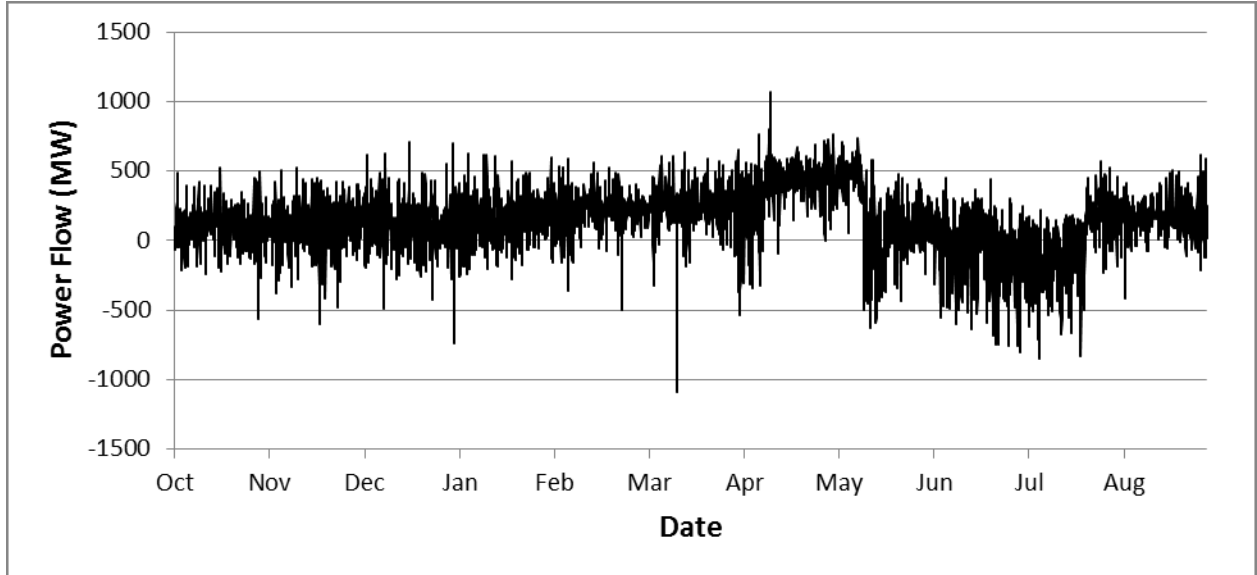


Figure 60: Power flows across 2-bus system for year 2011 when L_1 load on the left bus is represented using 31% of total load at each timestep

Wind data from a single wind farm in Taylor County, Texas was injected into the left bus at each timestep. The wind farm was selected because data was obtainable from Wan (2011) and has a large enough (> 100 MW) capacity to make an impact on hydropower operations. The amount of wind penetration from this wind farm was changed simply by multiplying the injected wind power magnitudes at each timestep by a scalar. A sample of wind data for a couple days is displayed in Figure 61, which displays how wind data was scaled within the testing scenarios. Scaling was performed in this manner due to restrictions on realistic (proprietary) wind data at the farm scale within the Pacific Northwest region. Better methods of estimating more penetration of renewables would have a smoother curve as wind penetration increases since

geographic diversity amongst wind power production in a region will provide diverse wind conditions and therefore wind power penetration levels across the grid. However, this is compounded by the fact that wind regimes vary from region to region and could actually present worse problems for the transmission system. Thus, in order to test the capabilities of the model, the simple scaling technique was deemed sufficient for increasing or decreasing wind power penetration levels at the left bus. Additionally, this technique will produce more conservative, less risk prone results than naturally “smoothing” increases in penetration.

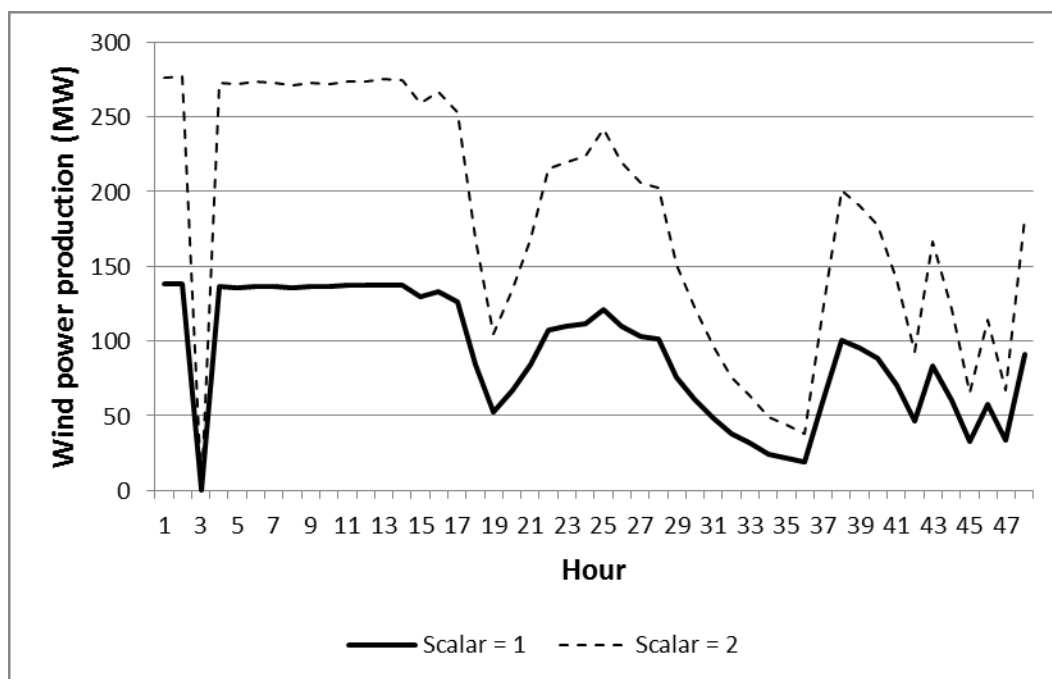


Figure 61: Increasing wind data penetration modeled using a scalar multiplier

Scenarios were defined in terms of hydropower weight, transmission capacity, and wind penetration with values as summarized in Table 6 below for a combined total of 84 scenarios.

Table 6: Transmission capacity and wind penetration scenarios	
Term	Scenarios
Hydropower target deviation penalty	1e+5, 1e+6, 1e+8
Transmission capacity	500 MW, 750 MW, 1000 MW, 1500 MW
Wind penetration scalar value	0, 5, 10, 15, 20, 25, 30

Hydropower penalty terms were selected to span a range of weights so as to have a greater priority than reservoir levels, except at Chief Joseph when storage levels fall below 95% of its capacity. Transmission capacity scenarios were selected in order to provide a range from low or no restrictions to significant restrictions. Wind penetration levels were also selected to give a wide range of low penetration to very high penetration to evaluate the flexibility of the hydro system even in extreme conditions. Wind power production at each timestep was multiplied by scalars ranging from 0 to 30 in increments of 5, which presents the two-bus system with a maximum of about 4200 MW of *additional* power generation from wind. This magnitude of wind penetration lies just above the average remaining capacity of all hydropower plants in the model during the simulated period and a little less than 50% of the total power generating capacity (9656 MW). This is an extreme case of wind penetration in this system, but shows the capabilities of the hydropower system to mitigate transmission problems up to a particular threshold. Since the wind farm is placed on the left side of the bus and the “swing” generator and consumer are on the right, increases in wind production results in imported power to the right bus when hydropower resources and transmission capacities are limited. Thus, reliance on third-party power resources to balance not only wind power penetration but also mitigate transmission line flow can be assessed using the IWPM.

3 Results

The integrated water and power model (IWPM) serves as an engine to make operational decisions between water and power sectors based on effects of transmission capacity and intermittent renewable penetration. Magnitudes of imported and exported power from outside the local balancing area are shown to increase with increases in wind power penetration and a threshold on the amount of wind penetration that the hydropower facilities can accommodate is

determined. Total dissolved gas (TDG) at the tailwater of Grand Coulee is also simulated using water network model output and effects on TDG levels of wind power penetration and transmission capacity are determined.

A major benefit of the IWPM is that it dispatches sets of power resources that are located in different areas within a transmission-constrained grid. Hydropower targets are changed at each timestep by the power dispatch model, and the water network attempts to meet these (or rather, constraints) using the Lagrangian relaxation formulation given in Eq. (27). For a scenario with transmission capacity set to 750 MW, wind penetration was increased up to a factor of 4, showing the effect of the transmission capacity on operations of re-dispatched hydropower units at Chief Joseph. Resulting energy production targets are shown in Figure 62, which shows that as wind power production increases, the target hydropower production at Chief Joseph needs to decrease in order to avoid excessive power flows across the transmission line. Wind penetration had the opposite effect at Grand Coulee, which was required to increase generation in order to decrease the amount of flows across the line as well as balance the wind power resource.

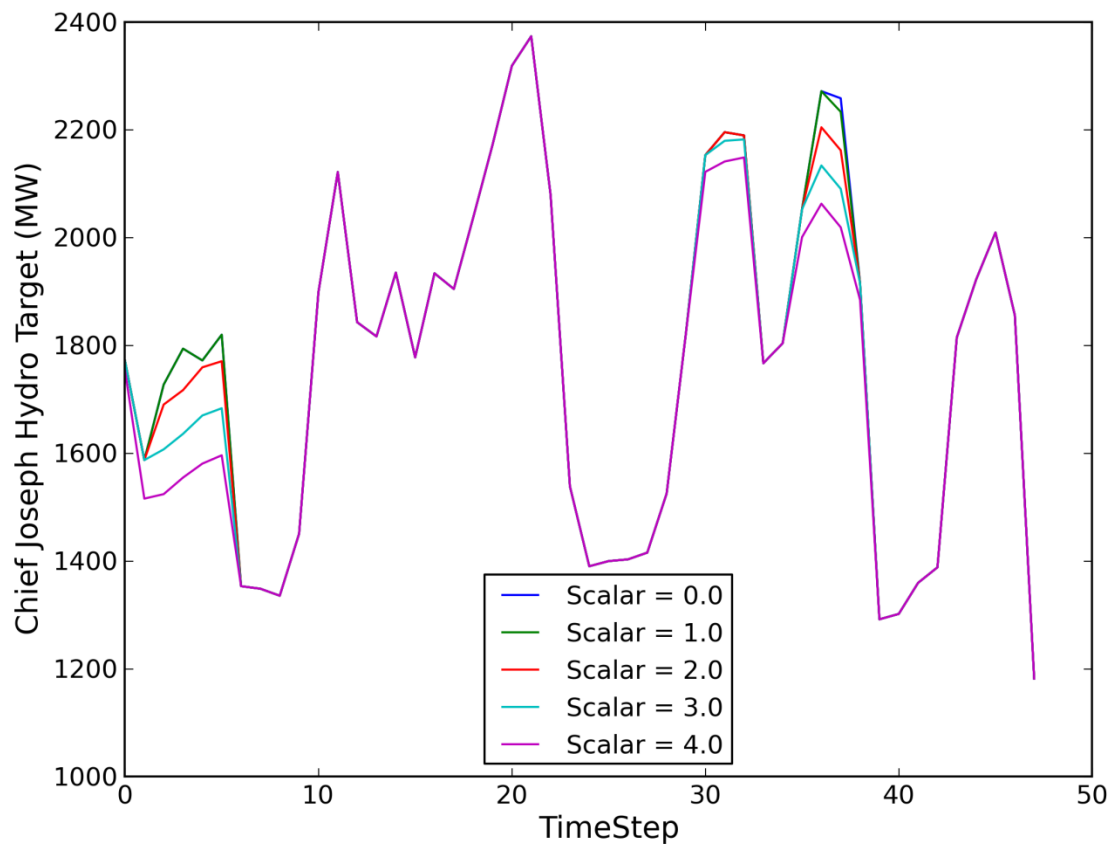


Figure 62: Effect of transmission capacity with increasing wind penetration on dispatched hydropower energy targets at Chief Joseph

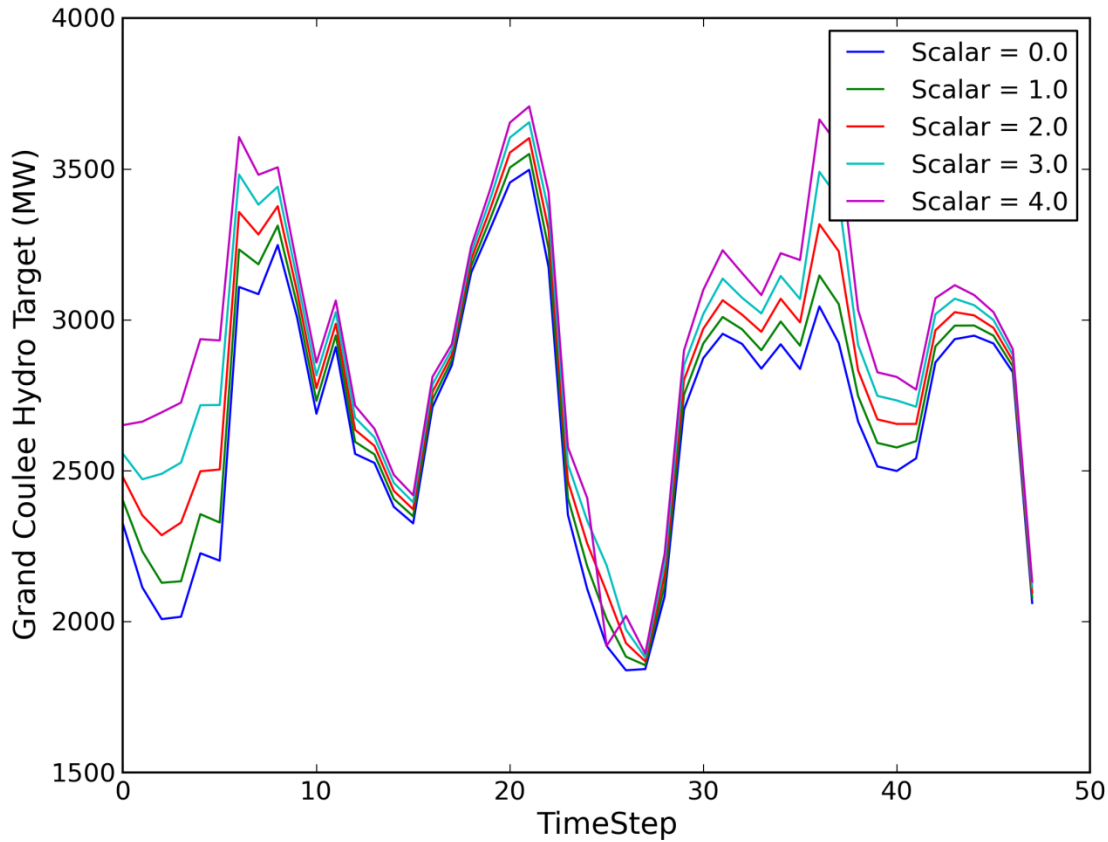


Figure 63: Effect of transmission capacity with increasing wind penetration on dispatched hydropower energy targets at Grand Coulee

Dispatching hydropower resources in order to ensure transmission lines are not overloaded produces power flows across the transmission line as displayed in Figure 64 for various scenarios of transmission capacity and small increases in wind penetration (corresponding to scalar multipliers ranging from 0 to 5). Figure 65 displays power flows as a function of small wind penetration increases with a transmission capacity of 1500 MW. With 1500 MW of transmission capacity, the system does not require operational changes. However, when transmission capacity decreases to 750 MW, power resources are re-dispatched to cap power transmission over the line as seen in Figure 66. Without any additional wind generating capacity, the system can handle limited transmission capacity down to 500 MW with integrated

operations, where over the simulated time period power flows are regulated below transmission constraints as shown in Figure 67.

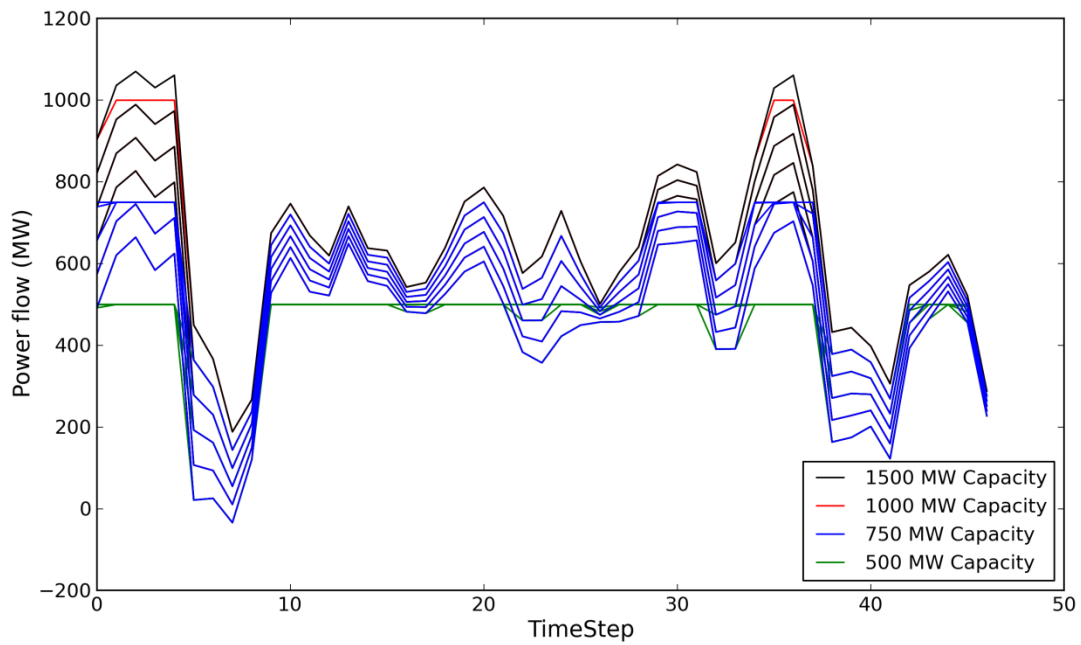


Figure 64: Power flows as a result of dispatched hydropower resources resulting from various scenarios of transmission capacity and wind penetration

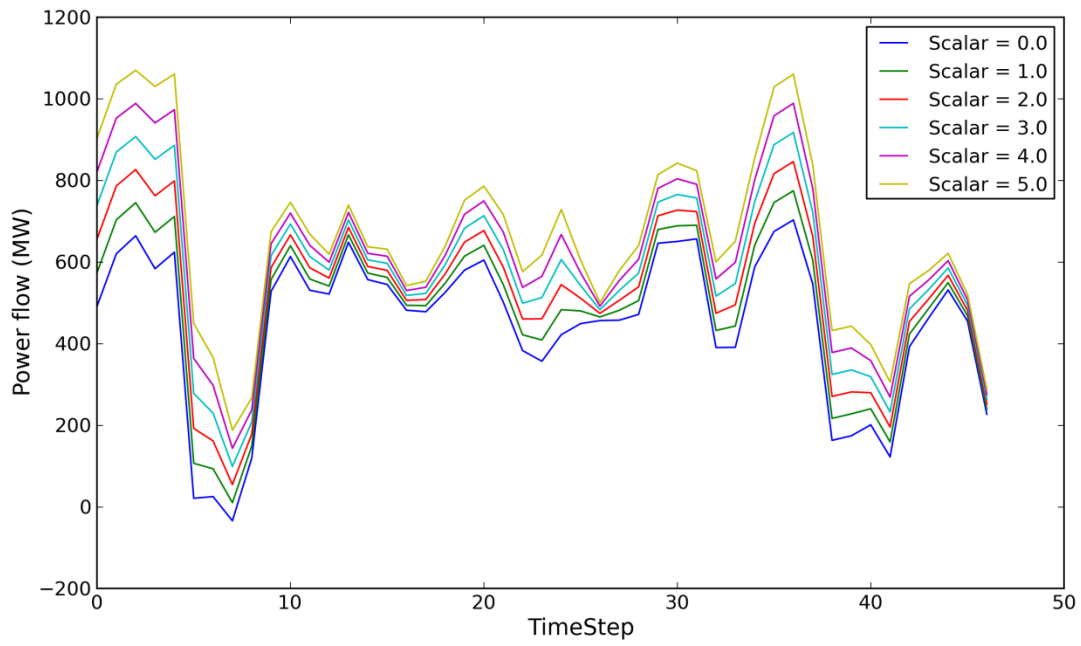


Figure 65: Power flows as a result of dispatched hydropower resources resulting from increased wind penetration and a transmission capacity of 1500 MW

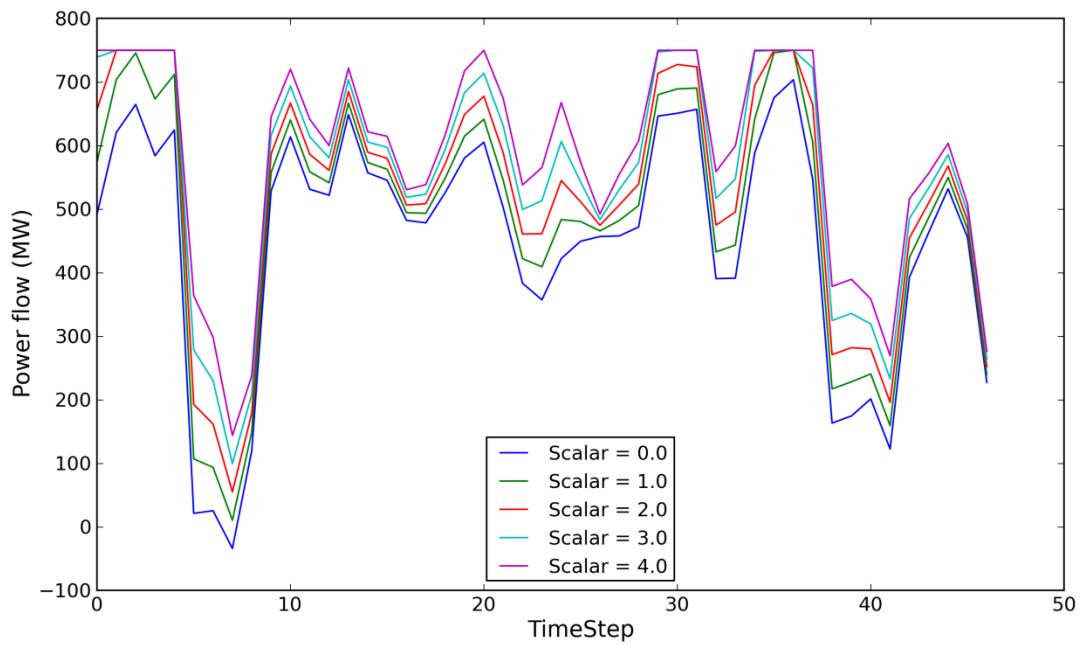


Figure 66: Power flows as a result of dispatch hydropower resources resulting from increased wind penetration and a transmission capacity of 750 MW

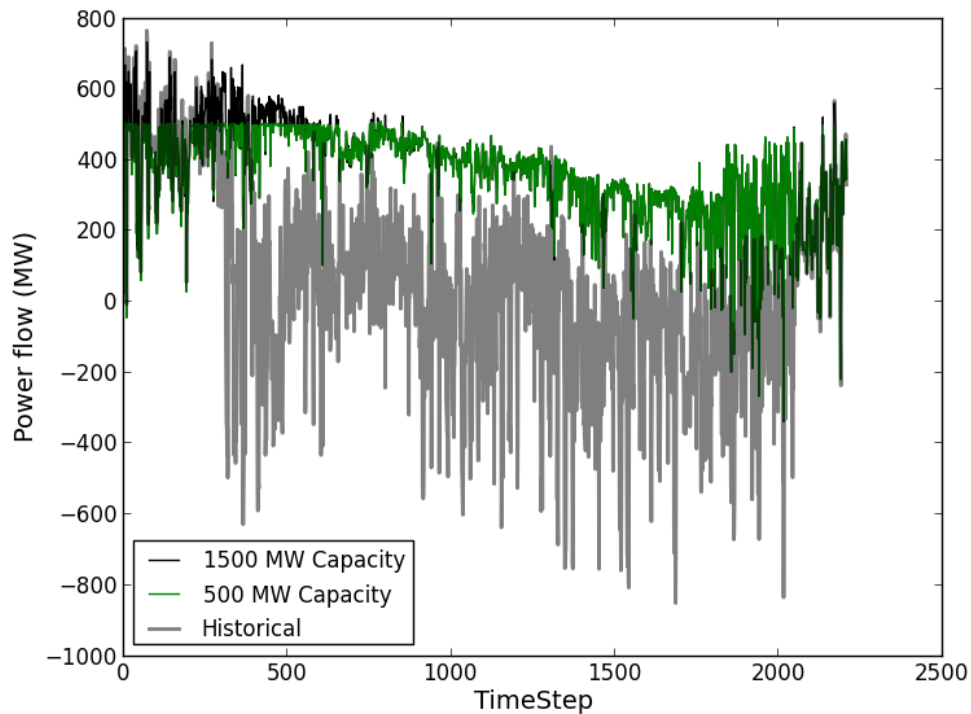


Figure 67: Power flows compared between two transmission scenarios for the entire modeled time period

When operating to mitigate power flow according to transmission limitations, longer-term reservoir levels are affected by transmission constraint operations as shown in Figure 68. Storage levels at Grand Coulee remained relatively unaffected by operational changes, but storage at Banks Lake is significantly impacted since high power flows across the transmission require more generation from Banks Lake (or less power consumption at its pumping facility). As a result, Banks Lake consistently has about 200,000 less acre-feet of storage after the first few weeks of the model simulation time period. The reliance on Banks Lake as the dispatchable resource is somewhat arbitrarily selected by the LP problem setup, which will often turn one unit on fully and leave another unused due to its solution procedure. If a quadratic or other nonlinear term is used in the power dispatch model, a more balanced re-dispatch between all reservoirs would likely ensue, which is an area for future research.

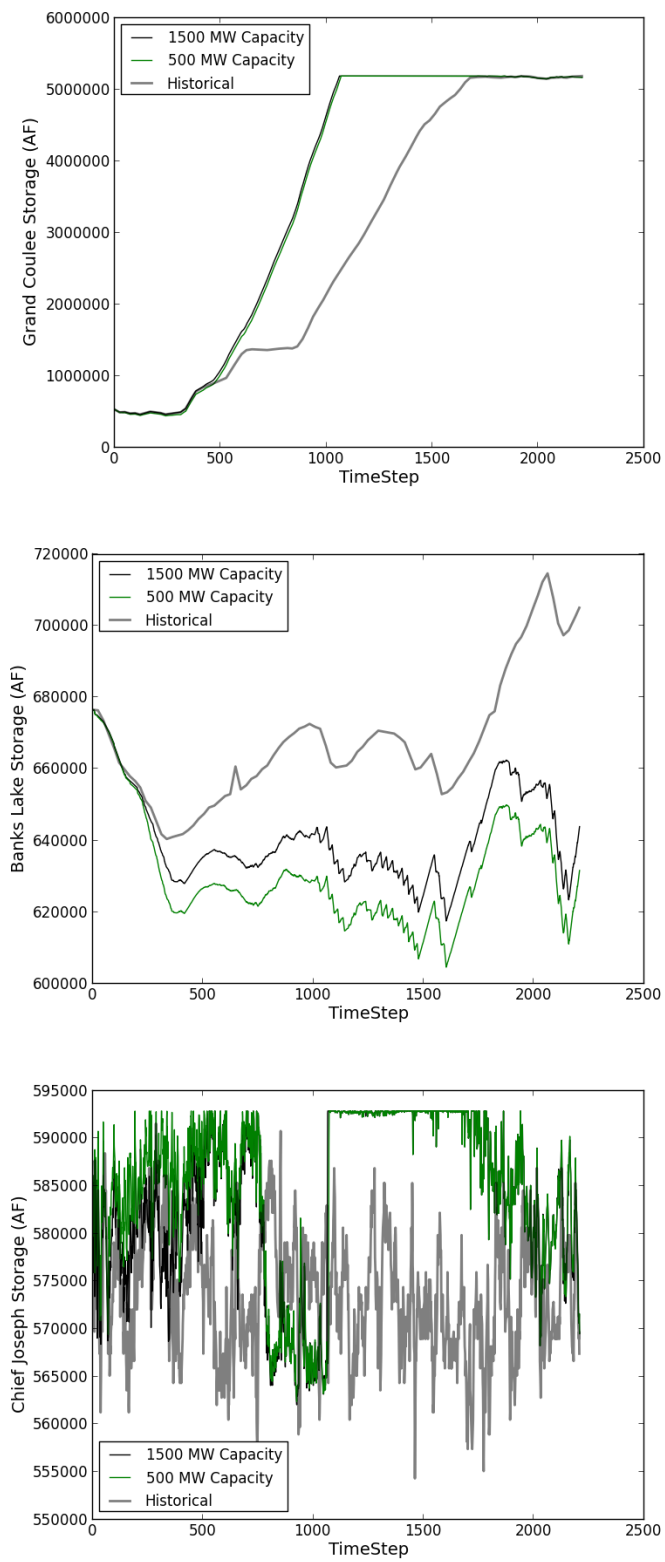


Figure 68: Storage levels at Grand Coulee (top), Banks Lake (middle), and Chief Joseph (bottom) as a result of restricted transmission capacity with no additional wind capacity

Results shown in Figure 68 display the effects of transmission capacity with no wind penetration capacity. However, with high wind penetration (modeled as a scalar multiplication of wind power production at each timestep), profiles of simulated storage levels within the reservoirs are more exaggerated. Grand Coulee again seems to remain more or less unaffected by limitations in the transmission capacity, however, the storage volume seems to be significantly impacted by wind penetration. As seen in Figure 69, both Banks Lake and Grand Coulee are emptied during re-dispatch in order to avoid transmission congestion when more wind is added to the system at the left bus.

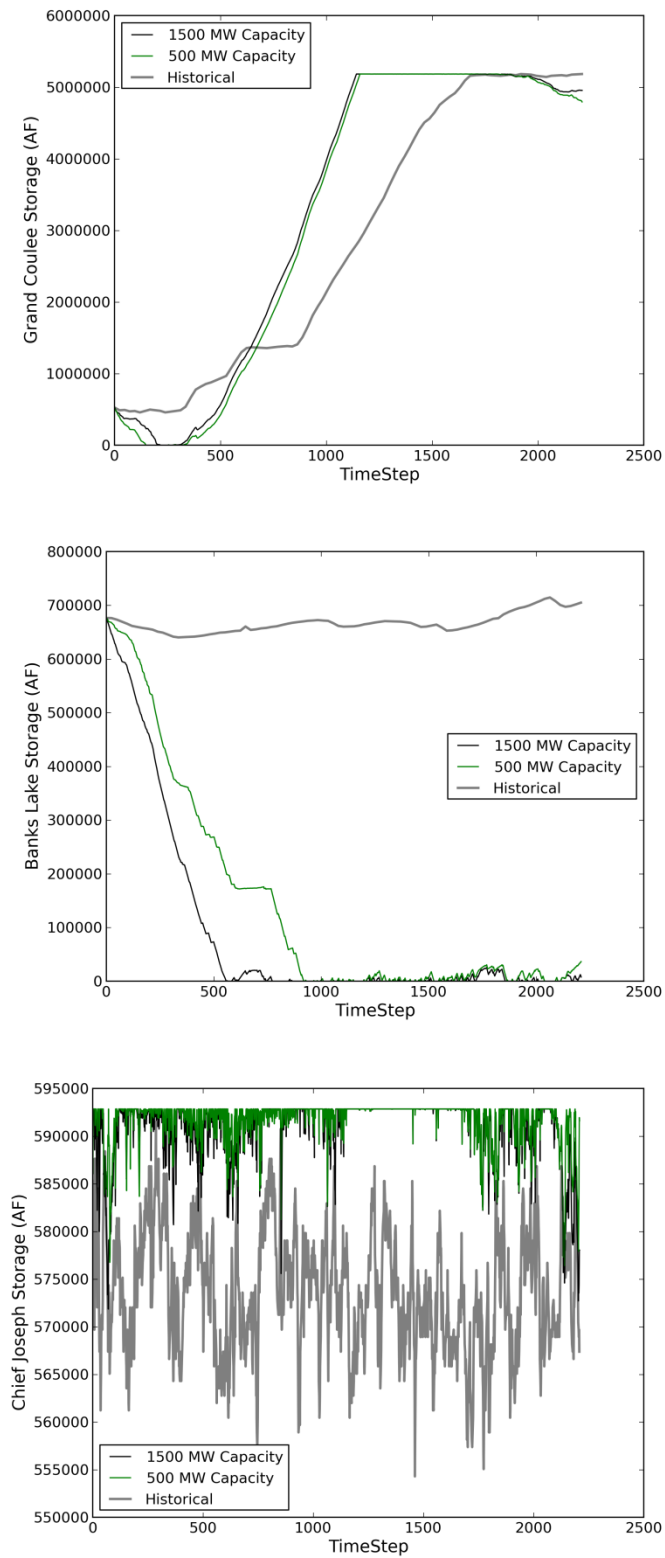


Figure 69: Storage levels at Grand Coulee (top), Banks Lake (middle), and Chief Joseph (bottom) as a result of restricted transmission capacity with extreme wind capacity penetration ($Scalar = 30x$)

At each timestep, power resources are re-dispatched to satisfy power constraints, and present therefore a target for the hydropower system to achieve. When much wind enters the system, power flows across the line inherently increase because Chief Joseph must pass water through its turbines to avoid high TDG levels. Figure 70 displays power flows across the line without any consideration of how well the hydropower system can actually match the required targets. Only utilizing minimum and maximum power generating or pumping capacities within the power dispatch model can lead to a “clean” result like the one shown in the figure. However, when hydropower resources are simulated and realism in head, turbine efficiency, and interconnections between the reservoirs is accounted for, power flows across the constrained transmission line would actually look like what is shown in Figure 71.

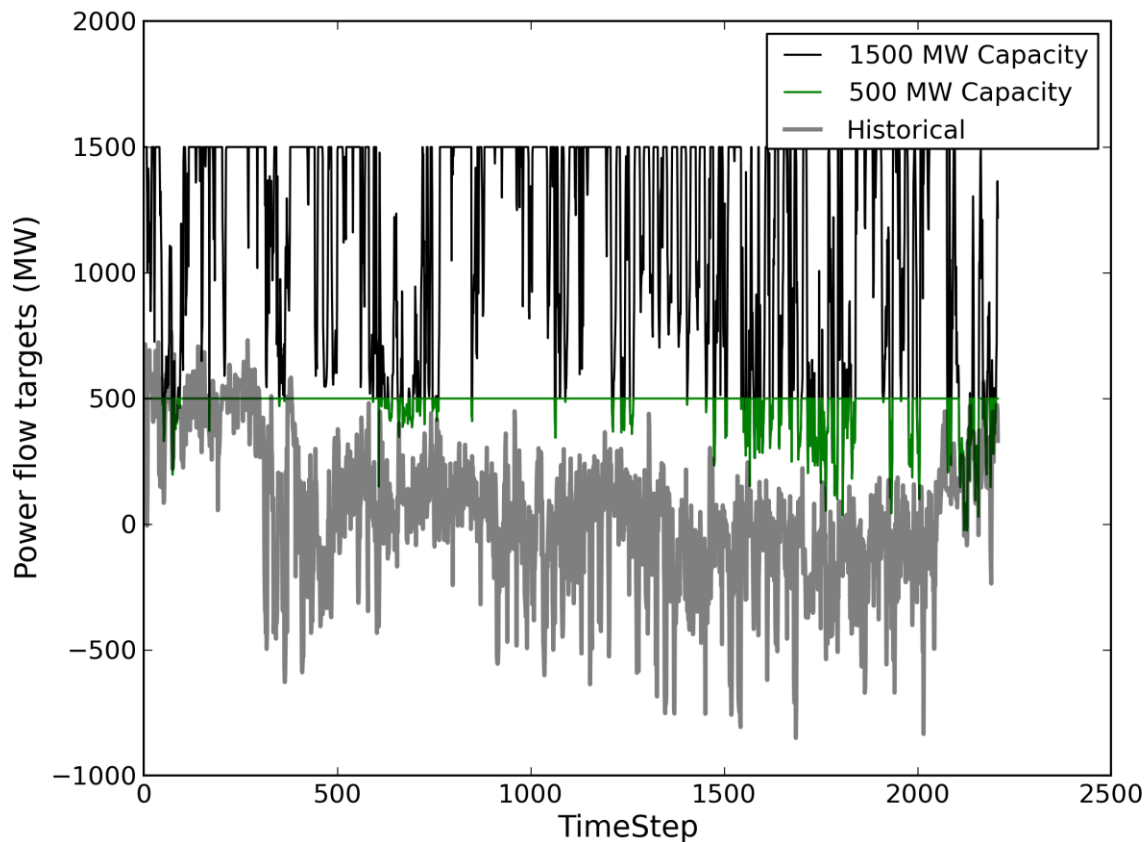


Figure 70: Power flow targets for high wind penetration scenario

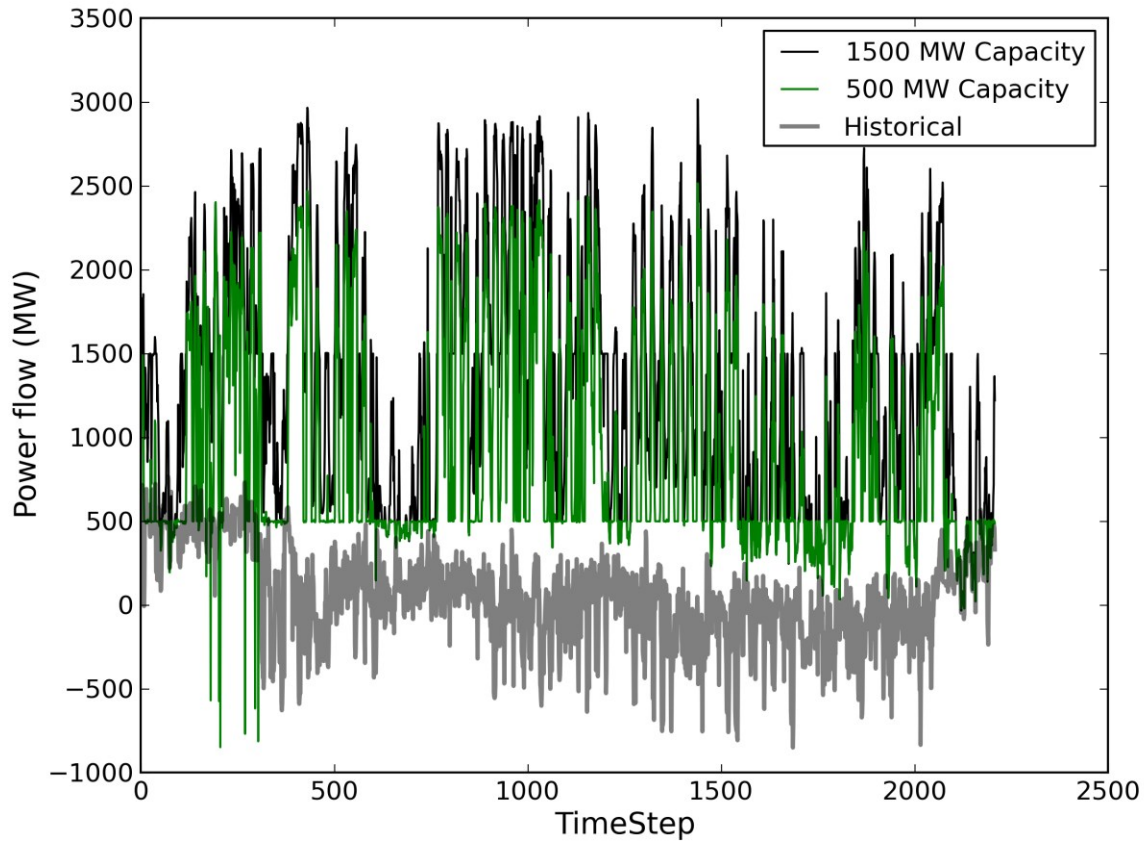


Figure 71: Simulated power flows for high wind penetration scenario

According to simulated power flows across the transmission line shown in Figure 71, power from elsewhere in the bulk electricity system would need to be imported to mitigate the transmission congestion and overloading problem. The power dispatching model by itself only observes a necessity for imported power between 0 and 2000 MW at various periods as shown in Figure 72, but when attached to a water network model, expected power importations range from slightly negative to 5000 MW which is about equivalent to the capacity of the penetrating wind resource as shown in Figure 73, which might indicate that the value of hydropower resources to mitigate increasing wind power penetration is much less than the generating capacity of the wind (in this case 5%). These power flows can be compared with the baseline model without any wind power penetration as shown in Figure 74, which range from -500 to 300 MW, a fraction of the

power flows required for the high wind scenario. Although wind penetration was increased linearly, average required power import increased in more of an exponential fashion until the plotted lines begin to increase linearly as shown in Figure 75. The “knees” of the curves of average power imports essentially represent the threshold on the flexibility of the hydropower system to be able to mitigate power flows and power capacity challenges associated with wind power penetration. For the various transmission capacity scenarios (500 MW, 750 MW, 1000 MW, and 1500 MW), the amount of wind power penetration that the hydropower system was able to mitigate was about 300 MW, 400 MW, 500 MW, and 600 MW, respectively.

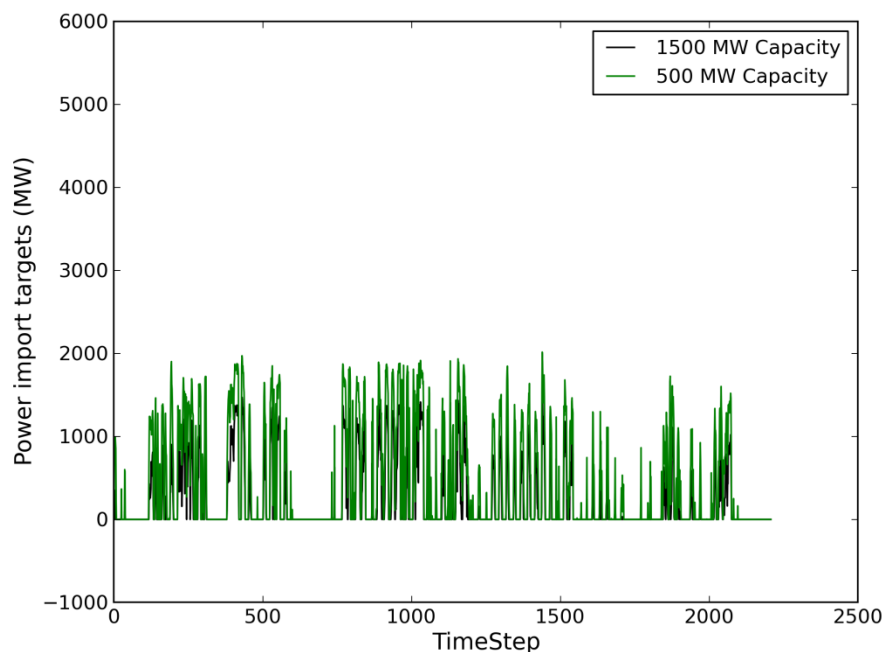


Figure 72: Simulated power imports into the right bus to mitigate high wind power penetration scenario without inclusion of water or non-power constraints, and are therefore called “targets”

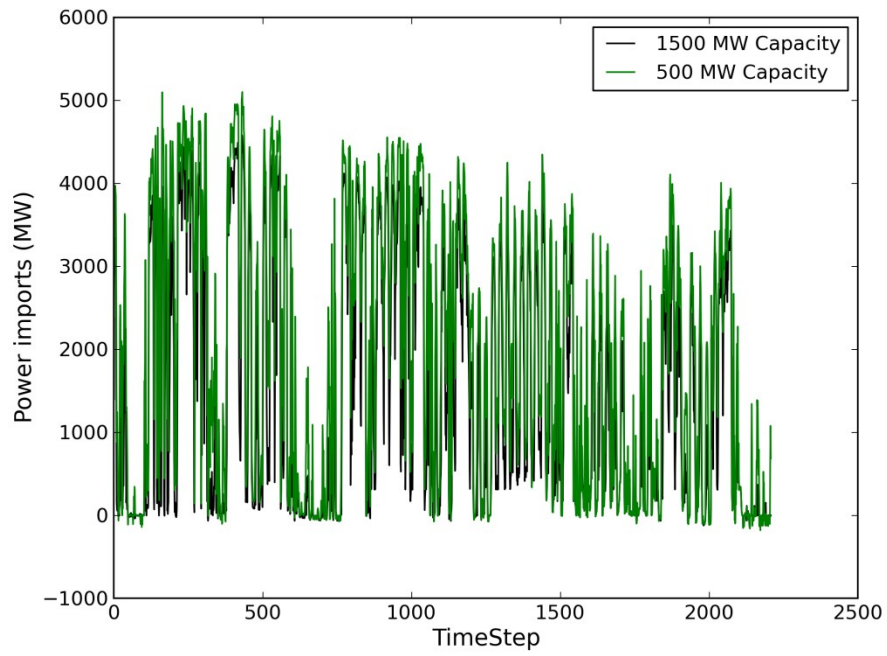


Figure 73: Simulated power imports into the right bus to mitigate high wind power penetration scenario with inclusion of water constraints

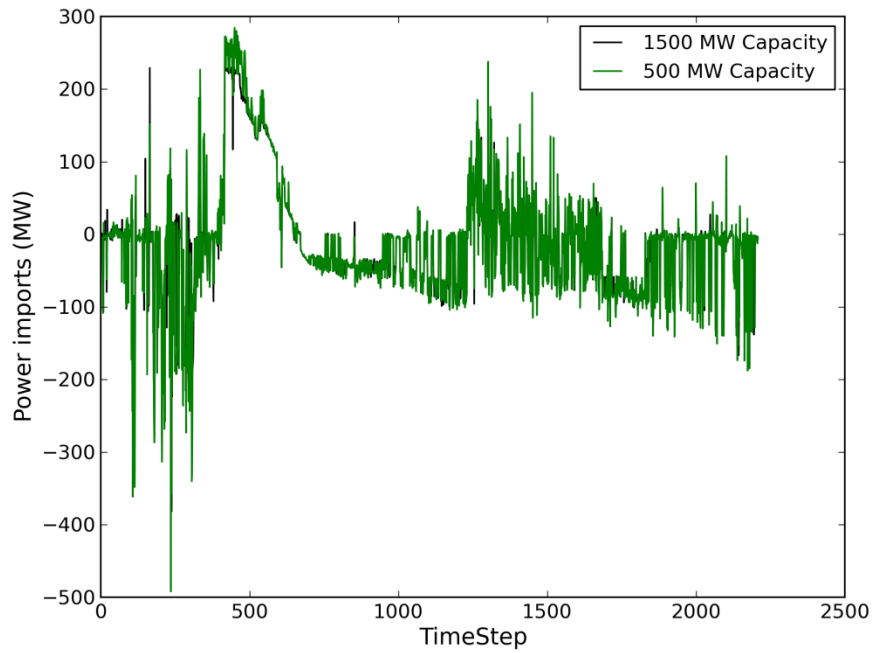


Figure 74: Simulated power imports into the right bus to mitigate power flows across the transmission line with no wind power penetration

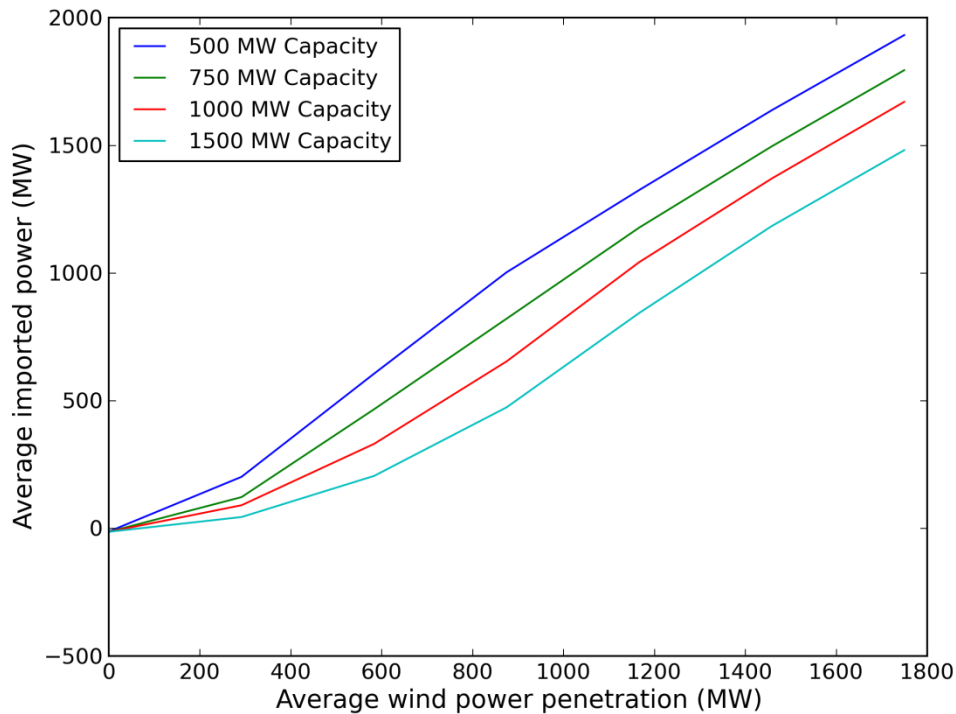


Figure 75: Average power import at right bus compared to average wind power penetration level in MW

Total dissolved gases were simulated for each of the scenarios. Impacts on simulated TDG levels within the river for various wind penetration levels are shown as a timeseries within Figure 76 and for various transmission capacity levels in Figure 77. Impacts on TDG seem to be fairly minimal at Grand Coulee, which is precisely the case, most likely due to the fact that the linear programming power dispatch problem selects Banks Lake consistently to mitigate power flows, and Grand Coulee has a much larger power capacity and energy storage, and is therefore more immune to susceptibility. Additionally, Grand Coulee is more hydraulically linked with Chief Joseph, and therefore, in order to increase production at Grand Coulee, production or spills at Chief Joseph would also increase, both of which are undesirable because of the power flow and TDG problems respectively. As described above, Banks Lake is emptied in order to integrate large amounts of wind, and even then power needs to be imported, which is also highly undesirable especially during the irrigation season when water is needed in Banks Lake to satisfy

irrigation demands. Therefore, the resulting set of operating policies may be deemed infeasible, but they still can provide tradeoffs for operators to be able to decide between operating policies.

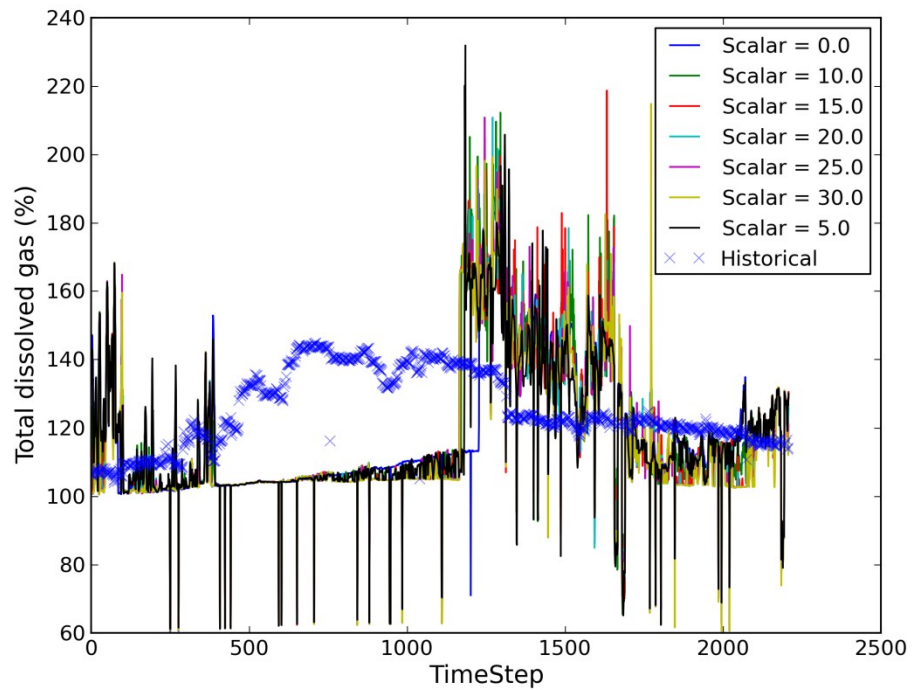


Figure 76: Simulated total dissolved gases for various wind penetration scenarios

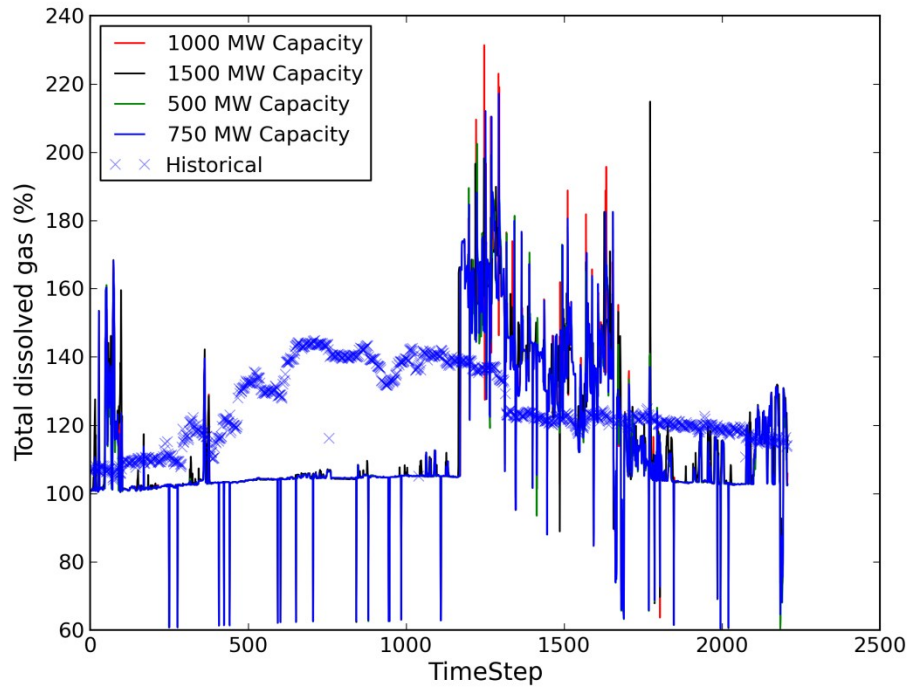


Figure 77: Simulated total dissolved gases for various transmission capacity scenarios

No attempt was made to calibrate simulation of spillway discharge through the dam evident in Figure 77. As shown by the simulation, though, holding reservoir releases until absolutely necessary increases the likelihood of having overly large spills, and TDG thresholds (typically between 110% and 120%) are significantly exceeded, and therefore likely causing gas bubble trauma on large populations of fish. So, the policies described here and simulated within the IWPM would likely be deemed highly undesirable, which shows the necessity for a dynamic optimization portion of the IWPM (still yet to be developed). A fully dynamic optimization of the IWPM could make look-ahead decisions to improve not only peaks in power flows across the transmission line, but also peaks in TDG levels by placing a larger penalty on sizable deviations from the threshold (using a squared term or a min-max type of optimization approach would both be suitable for such conditions) and tradeoffs between the two objectives could be analyzed by changing the weights on the penalty terms.

Simplistic modeling of the power system and obtaining steady-state DC estimates of the power system state from wind penetration data in Texas (rather than near the mid-Columbia) and hydropower targets contribute to the conclusions within this study, and therefore may differ from a more realistic scenario. However the integrated water and power model (IWPM) presented within this study may serve as a framework for further research opportunities in inter-related water and power fields of study. Future work on the IWPM could significantly benefit its utilization and practicality for use and therefore recommendations on future work is discussed in detail in Chapter VII.

VII Future Work on IWPM

A major portion of the first two levels of the IWPM has currently been placed into the IWPM using a transmission-constrained DC power dispatch model, although in a very simplified form. The Lagrangian relaxation technique has not been fully implemented in the form of the long-term goal described in Chapter III, but has been implemented for both satisfying routing requirements and constraining the water system to hydropower targets that are solved within the power dispatch model (Bertsekas 1995). A free-of-charge generalized power system model still needs to be connected to the IWPM for further research in integrated systems modeling. Once connected, the Lagrangian relaxation method in its full form should be applied to IWPM. Also, the dynamic optimization routine that makes forward-looking operational decisions has not yet been developed. The only forward-looking portion of the generalized model currently is the use of inflow forecasts to change the hydrologic state of the system and update target reservoir storage levels accordingly. Therefore, the application of a dynamic optimization routine to a realistic integrated water and power problem should still be explored. A reinforcement learning (RL) algorithm could be utilized as the dynamic, simulation-based optimization routine that update reservoir storage targets (or release targets) in order to fully realize tradeoffs between the water and power system operational objectives while still obtaining feasible answers. The technique would need to be extended to incorporate and mitigate uncertainty and operate in parallel, which would be relatively easily performed due to the structure of the RL algorithm.

Customization of model simulations can be accomplished by any programming language or framework that implements or connects to the .NET framework 3.5 or newer. This includes common research scripting languages like Matlab and Python as well as compiled languages such as Java. Therefore, a third-party power systems operations model could relatively easily be

integrated with MODSIM, which is implemented in the .NET framework 3.5. A set of scripts or classes for each of these languages should be built and stored for other researchers to utilize. Additionally, pre- and post- processing tools should be built in order to allow for specification, evaluation, and detection of failures of the IWPM to provide reasonable results, which is a common problem for many optimization routines.

Constraints within the water network model, MODSIM, should be added to include constraints such as minimum and maximum up-and-down times, and ramp rates for the hydropower controller in units of flow, because these terms are often defined in terms of flow as opposed to power production. Also, system evaluation tools should be built that will automatically perform sensitivity analysis and determine if multiple optimal solutions exist in order to avoid local minima.

When connected to a power systems operations model, several tests for validation of the model should take place on some sample test bus systems. In order to evaluate the capability of the model to address or mitigate transmission congestion caused by uncertain renewable energy production with spatially-diverse reservoirs throughout the grid, the IWPM should be implemented on several IEEE reliability test bus systems (Albrecht et al. 1979; Allan et al. 1979; Billinton and Jonnavithula 1996; Billinton et al. 1989; Grigg et al. 1999).

Uncertainty should be incorporated into the IWPM due to the highly variable and intermittent nature of wind power production as well as reservoir inflows and demands on both systems. Stochastic modeling of uncertain parameters and forcing variables as well as forecasting should be performed for forward-looking, risk-based decision making.

An integrated modeling interface should be developed or used that has the capability of building both water network and power network objects that can then be used for simulation and

optimization of the IWPM. The interface should include water network nodes and links as well as power network buses and branches with parameters and topology that can be easily manipulated from the interface. Selection of methods and optimization parameters should also be available within the interface to allow users to easily determine and analyze tradeoffs between implied operations of optimal policies.

Other models could potentially be integrated that would offer more insight into tradeoffs and economics of multiple commodities and sectors. Other infrastructure models having to do with the water-energy nexus such as oil and gas production and consumption should be integrated with an IWPM due to the importance of oil and gas on industrialized economy. Food and crop production models, socioeconomic models, land-use models, computational statistics models, climate change, hydrologic models, and groundwater models should also be integrated with an IWPM. Integrating models from different sectors would not only be a challenging and exciting interdisciplinary course of study, but could also potentially have significant impacts on the management of water, power, and energy systems as well as provide insight into macro-scale economics between large economic epicenters. Hosting a suite of tools like these on a distributed, internet-based system would provide necessary cyberinfrastructure to explore novel forms of decision making in a distributed fashion.

1 Expected Results

Academia and industry are anticipating research-based results on several pertinent questions related to the role of hydropower in solutions to power system challenges that could potentially be answered with an IWPM. In realizing the full potential of hydropower to mitigate uncertainty of renewable energy production, research questions that still remain to be answered and could potentially be answered by an IWPM include the following:

- How and when to reliably and economically switch from pump mode to turbine mode while using pumped storage hydropower to “load follow” renewable energy production,
- How can tradeoffs with nonpower objectives be quantified and realized,
- How can systems of reservoirs be exploited for any additional flexibility without violating system priorities,
- How can electricity markets be designed and operated to reduce regulatory-type curtailments of variable RESs within hydro rich areas,
- Value of replaced expensive or air-polluting energy sources resulting from coordinated firming agreements between RESs and hydropower sources (rather than between RESs and diesel engines, for example), and
- Solutions considering multiple, geographically diverse hydroelectric plants that can help mitigate transmission problems caused by unscheduled power flow from RESs.

National security is significantly affected by water and power operations. Irrigation water to farmers, drought conditions, electric power production and sales, and reliable electric power supply to industrial loads significantly impact economic welfare of entire regions. Dam breaches, floods, water contamination, power system faults, and electric shocks can substantially impact public safety and health. Poor operations or system failures within either a water system or a power system can cause worsened and more dangerous operation of the other system. So, an IWPM may potentially address the following questions:

- How can hydropower mitigate power system challenges as well as generate revenue without causing floods or negative impacts to irrigation and municipal water supply, or to water and environmental policy compliance,

- What impact do hydropower system operations have on environmental sustainability within both water and power systems, and
- “What if” scenarios that explore the effect of particular failures or emergencies on both water and power systems in an integrated fashion (e.g., dam breaches, power generator or transmission line failures or “N-1” analysis, water supply emergency procedures, or flooding response plans).

A free-of-charge, generalized IWPM may sufficiently provide the necessary framework for researchers and industry to practically address challenges in a water or power system, without adversely affecting operations of the other system. When more fully developed, an IWPM will likely be very beneficial in analyzing tradeoffs between various regulatory and proposed operating policies within both water and power sectors, in which case the IWPM serves as a platform over which decisions and policies can be quantitatively evaluated with less simplifying assumptions than previous studies.

2 Potential Applications

An integrated water and power model (IWPM) could eventually be used for many different purposes. Such applications include renewable energy integration, multi-commodity market analysis, hydropower producer participation in ancillary services, climate change effects and potential reciprocal operational impacts on climate, emergency response plan development.

The Bonneville Power Administration (BPA) in summer 2011 faced a dilemma caused by large snowmelt volumes and environmental law that forced them to generate a large amount of hydropower, and consequently, they had to curtail large amounts of wind energy to avoid overproduction. In situations like these, an IWPM might prove to be useful in providing operating decisions based on forecasts of inflow, electric load, and wind power production.

Problematic situations occur when unscheduled wind energy causes congestion within the transmission system, and consequently system operators need to curtail power producers to maintain security of the transmission system. We want to avoid situations in which economic global welfare is constrained or decreased because of regulatory actions. An IWPM could potentially provide optimal operating trajectories that utilize the geographic diversity of energy storage devices, namely hydropower, to mitigate congestion problems caused by intermittent energy production. In this way, the limited flexibility of interconnected water systems can be exploited to alleviate congestion in the transmission system.

Most power system operations models incorporate simplistic water system modeling that render them incapable for reliably producing feasible results. Many unit commitment or economic dispatch models have simple constraints on water systems without considering interconnected nature of reservoirs, uncertainty in inflows, routing across long reaches, evaporation, changing elevation head, groundwater contributions, etc. (Padhy 2004; Yamin 2004). Lund (2009) represents the water system in energy terms for simplicity, meaning water in a reservoir is expressed as a number of megawatt-hours. Such water system representation cannot incorporate much realism because water flow, elevation, speed, temperature, and other water quality criteria make significant impacts on water system operations. An IWPM with generalized models that adequately represent both water and power systems operations will help to ensure feasible results at the end of simulations.

With increasing renewable energy penetration and smart grid initiatives, the timescales for power system operations keeps narrowing. Additionally, water system operators are finding a need for finer timescales to analyze environmental impacts, improve irrigation and transportation scheduling, and manage floods in real-time. New modeling paradigms need to be adopted so that

simulations that produce feasible solutions can be performed simultaneously and quickly for both water and electric power systems, requiring the use of integrated modeling frameworks. Such improved modeling frameworks can be used to better explore the capability of hydropower to participate in ancillary services in addition to power production and sale. Finer timescales of operation may not only apply to water and power systems, but also to other interconnected critical infrastructure as in oil or natural gas.

Water systems stimulate economy via construction, recreation, navigation, hydropower, irrigation, water rights, food production, the environment, and wildlife. Power systems also stimulate economy via electric power (which has many indirect beneficiaries), construction, natural resource (oil and gas) extraction and transportation, markets for ancillary services, and the environment. Operations at hydropower plants can play a significant role in both water and power system economies. Economic tradeoffs between water and power systems could be analyzed with an IWPM in ways not possible before. The methods used within the IWPM can play a core role in how capable the IWPM is in investigating tradeoffs within multiobjective analysis.

Power system loads, generation, and transmission capacity vary with the climate, technology, and markets as does water system inflows, demands, and evapotranspiration losses. As climates, social interactions and styles, and electricity and water markets evolve, water and power systems operations will change, which will affect interconnections and coordination between water and power systems. Studies examining climate change impacts on system operations and the converse (i.e., system operational impacts on climate change) may require the use of an IWPM because of the interrelated nature of climate with the water balance, loads, and RES power production.

Emergency response plans are vital for planned recovery in the event of a disaster or national security breach, especially when involving critical infrastructure, which includes both water and power systems. The interrelated nature of water and power systems may be important in developing an emergency response plan in certain cases where, for example, a certain power generator or transmission line is not functional and requires additional hydropower to keep power flowing in a reliable and secure fashion.

VIII References

- Acker, T. L., and Pete, C. (2011). *Western Wind and Solar Integration Study: Hydropower Analysis*. National Renewable Energy Laboratory, Golden, CO.
- Albrecht, P. F., Bhavaraju, M. P., Biggerstaff, B. E., Billinton, Roy, Jorgensen, G. E., Reppen, N. D., and Shortley, P. B. (1979). "IEEE reliability test system." *IEEE Transactions on Power Apparatus and Systems*, PAS-98(6), 2047–2054.
- Alemu, E. T., Palmer, R. N., Polebitski, A., and Meaker, B. (2011). "Decision Support System for Optimizing Reservoir Operations Using Ensemble Streamflow Predictions." *Journal of Water Resources Planning and Management*, 137(1), 72.
- Allan, R. N., Billinton, Roy, and Abdel-Gawad, N. M. K. (1986). "The IEEE reliability test system - extensions to and evaluation of the generating system." *IEEE Transactions on Power Systems*, PWRS-1(4), 1–7.
- Aoki, K., Itoh, M., Satoh, T., Nara, K., and Kanezashi, M. (1989). "Optimal Long-Term Unit Commitment in Large Scale Systems including Fuel Constrained Thermal and Pumped-Storage Hydro." *IEEE Transactions on Power Systems*, 4(3), 1065–1073.
- Aoki, K., Satoh, T., Itoh, M., Ichimori, T., and Masegi, K. (1987). "Unit commitment in a large-scale power system including fuel constrained thermal and pumped-storage hydro." *IEEE Transactions on Power Systems*, IEEE, PWRS-2(4), 1077–1084.
- Arnold, E., Tatjewski, P., and Wołochowicz, P. (1994). "Two Methods for Large-Scale Nonlinear Optimization and their Comparison on a Case Study of Hydropower Optimization." *Journal of Optimization Theory and Applications*, 81(2), 221–248.
- Bard, J. F. (1988). "Short-term scheduling of thermal electric generators using Lagrangian relaxation." *Operations Research*, 36(5), 756–766.
- Barros, M. T. L., Tsai, F. T. C., Yang, S.-li, Lopes, J. E. G., and Yeh, W. W.-G. (2003). "Optimization of Large-Scale Hydropower System Operations." *Journal of Water Resources Planning and Management*, 129(3), 178.
- Baslis, C. G., and Bakirtzis, A. G. (2011). "Mid-Term Stochastic Scheduling of a Price-Maker Hydro Producer With Pumped Storage." *IEEE Transactions on Power Systems*, (99), 1–10.
- Batut, J., and Renaud, A. (1992). "Daily generation scheduling optimization with transmission constraints: a new class of algorithms." *IEEE Transactions on Power Systems*, IEEE, 7(3), 982–989.
- Beaudin, M., Zareipour, H., Schellenberglobe, A., and Rosehart, W. (2010). "Energy Storage for Mitigating the Variability of Renewable Electricity Sources: An Updated Review." *Energy for Sustainable Development*, 14(4), 302–314.
- Belanger, C., and Gagnon, L. (2002). "Adding wind energy to hydropower." *Energy Policy*, 30(14), 1279–1284.
- Belede, L., Jain, A., and Gaddam, R. R. (2009). "Unit Commitment with Nature and Biologically Inspired Computing." in *2009 World Congress on Nature & Biologically Inspired Computing (NaBIC)*, 824–829.

- Belloni, A., Lima, A. L. D. S., Maceira, M. E. P., and Sagastizábal, C. A. (2003). "Bundle Relaxation and Primal Recovery in Unit Commitment Problems. The Brazilian Case." *Annals of Operations Research*, 120(1), 21-44.
- Bertsekas, D. P. (1995). *Nonlinear Programming*. Athena Scientific, Belmont, Massachusetts.
- Billinton, R., and Jonnavithula, S. (1996). "A test system for teaching overall power system reliability assessment." *IEEE Transactions on Power Systems*, 11(4), 1670–1676.
- Billinton, Roy, Kumar, S., Chowdhury, N., Chu, K., Debnath, K., Goel, K., Khan, E., Kos, P., Nourbakhsh, G., and Oteng-Adjei, J. (1989). "A reliability test system for educational purposes - basic data." *IEEE Transactions on Power Systems*, 4(3), 1238–1244.
- Bitar, E., Khargonekar, P. P., and Poolla, K. (2011a). "Systems and Control Opportunities in the Integration of Renewable Energy into the Smart Grid." *Preprints of the 18th IFAC World Congress*, Milano, Italy, 4927-4932.
- Bitar, E., Rajagopal, R., Khargonekar, P., and Poolla, K. (2011b). "The Role of Co-Located Storage for Wind Power Producers in Conventional Electricity Markets." *American Control Conference (ACC)*, San Francisco, CA, USA, 3886–3891.
- Bonneville Power Administration (2010). "Statement on Environmental Redispatch and Negative Pricing." <<http://www.bpa.gov/corporate/AgencyTopics/ColumbiaRiverHighWaterMgmnt/Environmental%20Redispatch%20statement.pdf>> (Nov. 4, 2011).
- Borghetti, A., Frangioni, A., Lacalandra, F., Lodi, A., Martello, S., Nucci, C., and Trebbi, A. (2001). "Lagrangian relaxation and tabu search approaches for the unit commitment problem." *IEEE Porto Power Tech Proceedings*, IEEE, Porto, Portugal, 7–pp.
- Brännlund, H., Sjelvgren, D., and Bubenko, J. A. (1988). "Short Term Generation Scheduling with Security Constraints." *IEEE Transactions on Power Systems*, 3(1), 310–316.
- Bridgeman, S., Hurdowar-Castro, D., Allen, R., Olason, T., and Welt, F. (n.d.). "Complex Energy System Management Using Optimization Techniques." <www.fffydd.org/documents/congresspapers/342.pdf> (Oct. 4, 2011).
- Bucher, M. (2011). "Hydro-Power Planning Optimization." Swiss Federal Institute of Technology (ETC) Zurich.
- CADSWES, Center for Advanced Decision Support for Water and Environmental Systems (2007). "RiverWare™: River Basin Modeling for Today and Tomorrow." <<http://cadswes.colorado.edu/PDF/RiverWare/RiverWare-Brochure.pdf>> (Sep. 21, 2011).
- CADSWES, Center for Advanced Decision Support for Water and Environmental Systems (2010). "RiverWare Technical Documentation Version 6.0: RPL Language Structure" <<http://cadswes.colorado.edu/PDF/RiverWare/documentation/RPLLanguageStructure.pdf>> (Sep. 21, 2011).
- CADSWES, Center for Advanced Decision Support for Water and Environmental Systems (2012). "RiverWare Technical Documentation Version 6.2: Optimization." <<http://cadswes.colorado.edu/PDF/RiverWare/documentation/Optimization.pdf>> (Oct. 13, 2012).

- Capitanescu, F., Martinez Ramos, J. L., Panciatici, P., Kirschen, D., Marano Marcolini, a., Platbrood, L., and Wehenkel, L. (2011). "State-of-the-Art, Challenges, and Future Trends in Security Constrained Optimal Power Flow." *Electric Power Systems Research*, 81(8), 1731-1741.
- Carpentier, P., Gohen, G., Culioli, J. C., and Renaud, A. (1996). "Stochastic optimization of unit commitment: a new decomposition framework." *IEEE Transactions on Power Systems*, 11(2), 1067-1073.
- Catalão, J. P. S., Mariano, S., Mendes, V. M. F., and Ferreira, L. A. F. M. (2010). "Nonlinear Optimization Method for Short-Term Hydro Scheduling considering Head-Dependency." *European Transactions on Electrical Power*, 20(2), 172–183.
- CDWR, California Department of Water Resources (2000). "WRESL Language Reference: Draft Documentation" *CALSIM Water Resources Simulation Model Documentation*, <<http://modeling.water.ca.gov/hydro/model/WreslLanguageReference.pdf>> (Sep. 21, 2011).
- CDWR, California Department of Water Resources (2002). "CALSIM Water Resources Simulation Model." Modeling Support Branch – Computer Models, <<http://modeling.water.ca.gov/hydro/model/index.html>> (Sep. 21, 2011).
- Chen, C. L., and Lee, T. Y. (2007). "Impact Analysis of Transmission Capacity Constraints on Wind Power Penetration and Production Cost in Generation Dispatch." *International Conference on Intelligent Systems Applications to Power Systems (ISAP)*, IEEE, Toki Messe, Niigata, 1–6.
- Chen, C.-L. (2005). "Optimal Generation and Reserve Dispatch in a Multi-Area Competitive Market using a Hybrid Direct Search Method." *Energy Conversion and Management*, 46(18-19), 2856-2872.
- Chen, C.-L. (2007). "Non-Convex Economic Dispatch: A Direct Search Approach." *Energy Conversion and Management*, 48(1), 219-225.
- Chen, C.-L. (2008). "Optimal Wind–Thermal Generating Unit Commitment." *IEEE Transactions on Energy Conversion*, 23(1), 273-280.
- Chen, C.-L., and Chen, N. (2001a). "Direct Search Method for Solving Economic Dispatch Problem Considering Transmission Capacity Constraints." *IEEE Transactions on Power Systems*, 16(4), 764-769.
- Chen, C.-L., and Chen, N. (2001b). "Multi-Area Economic Generation and Reserve Dispatch." *22nd IEEE Power Engineering Society International Conference on Power Industry Computer Applications (PICA): Innovative Computing for Power - Electric Energy Meets the Market*, IEEE, Sydney, NSW, Australia, 368–373.
- Chen, C.-L., Hsieh, S.-C., Lee, T.-Y., and Lu, C.-L. (2008). "Optimal Integration of Wind Farms to Isolated Wind-Diesel Energy System." *Energy Conversion and Management*, 49(6), 1506-1516.
- Chen, C.-L., Jan, R.-M., Lee, T.-Y., and Chen, C.-H. (2011). "A Novel Particle Swarm Optimization Algorithm Solution of Economic Dispatch with Valve Point Loading." *Journal of Marine Science and Technology*, 19(1), 43–51.

- Chen, C.-L., Lee, T.-Y., and Jan, R.-M. (2006). "Optimal Wind-Thermal Coordination Dispatch in Isolated Power Systems with Large Integration of Wind Capacity." *Energy Conversion and Management*, 47(18-19), 3456-3472.
- Cheng, C.-P., Liu, C.-W., and Liu, C.-C. (2000). "Unit commitment by Lagrangian relaxation and genetic algorithms." *IEEE Transactions on Power Systems*, 15(2), 707-714.
- Chowdhury, B. H. (2004). "Load-Flow Analysis in Power Systems." *Handbook of Electric Power Calculations*, 3rd ed., The McGraw-Hill Companies, Inc., United States of America, 11.1-11.16.
- Chuco, B. (2008). "Electrical Software Tools Overview." *SINATEC-IEEE*, <<http://eurostag.regimov.net/files/DOC2.pdf>> (Oct. 4, 2011).
- Cohen, A. I., and Sherkat, V. R. (1987). "Optimization-Based Methods for Operations Scheduling." *Proceedings of the IEEE*, 75(12), 1574–1591.
- Cohen, A. I., and Wan, S. H. (1987). "A Method for Solving the Fuel Constrained Unit Commitment Problem." *IEEE Transactions on Power Systems*, 2(3), 608-614.
- Conejo, A. J., Castillo, E., Mínguez, R., and García-Bertrand, R. (2006). *Decomposition Techniques in Mathematical Programming: Engineering and Science Applications*, Springer Berlin, Heidelberg, Germany.
- Connolly, D., Lund, H., Mathiesen, B. V., and Leahy, M. (2010). "A review of computer tools for analysing the integration of renewable energy into various energy systems." *Applied Energy*, 87(4), 1059-1082.
- Dai, T., and Labadie, J. W. (2001). "River basin network model for integrated water quantity/quality management." *Journal of Water Resources Planning and Management*, 127(5), 295-305.
- Deltares (2009). "Ribasim (River Basin Simulation Model)." <<http://www.deltares.nl/en/software/101928/ribasim>> (Sep. 21, 2011).
- DeMeo, E. A., Grant, W., Milligan, M. R., and Schuerger, M. J. (2005). "Wind Plant Integration: Costs, Status, and Issues." *IEEE Power and Energy Magazine*, 3(6), 38-46.
- Dentcheva, D., and Romisch, W. (1998). "Optimal power generation under uncertainty via stochastic programming." *Stochastic Programming Methods and Technical Applications, Lecture Notes in Economics and Mathematical Systems*, K. Marti and P. Kall, eds., Citeseer.
- DHI, Danish Hydraulic Institute (2011). "MIKE BASIN – integrated river basin planning." *MIKE by DHI Software*, <<http://mikebydhi.com/Products/WaterResources/MIKEBASIN.aspx>> (Sep. 21, 2011).
- Divi, R., and Ruiu, D. (1989). "Optimal Management of Multi-Purpose Reservoirs in a Hydro-Thermal Power System." *Computerized decision support systems for water managers*, J. W. Labadie, L. E. Brazil, I. Corbu, and L. E. Johnson, eds., ASCE, Reston, Va., 413-424.
- Duncan, R. A., Seymore, G. E., Streiffert, D. L., and Engberg, D. J. (1985). "Optimal Hydrothermal Coordination for Multiple Reservoir River Systems." *IEEE Transactions on Power Apparatus and Systems*, PAS-104(5), 1154-1159.

- EIA, U.S. Energy Information Administration. "Electricity Restructuring by State." *Status of Electricity Restructuring by State*,
<http://205.254.135.24/cneaf/electricity/page/restructuring/restructure_elect.html> (Sept. 27, 2011).
- Enernex Corporation. (2011). "Eastern Wind Integration and Transmission Study." *Integration Studies & Operational Impacts*, Knoxville, Tennessee,
<http://www.nrel.gov/wind/systemsintegration/pdfs/2010/ewits_final_report.pdf> (Nov. 1, 2011).
- EPA, Environmental Protection Agency (2011). "Addressing the Challenge through SCIENCE and INNOVATION." *Aging Water Infrastructure Research*,
<<http://www.epa.gov/nrmrl/pubs/600f11010/600f11010.pdf>> (Sep. 22, 2011).
- Ferreira, L. A. F. M., Andersson, T., Imparato, C., Miller, T., Pang, C., Svoboda, A., and Vojdani, a. (1989). "Short-Term Resource Scheduling in Multi-Area Hydrothermal Power Systems." *International Journal of Electrical Power & Energy Systems*, 11(3), 200-212.
- Finardi, E. C., Silva, E. L. D., and Sagastizábal, C. (2005). "Solving the unit commitment problem of hydropower plants via Lagrangian Relaxation and Sequential Quadratic Programming." *Computational & Applied Mathematics*, 24(3), 317-341.
- Fisher, M. L. (1973). "Optimal Solution of Scheduling Problems Using Lagrange Multipliers: Part I." *Operations Research*, 21(5), 1114-1127.
- Fisher, M. L. (1985). "An applications Oriented Guide to Lagrangian Relaxation." *Interfaces*, 15(2), 10-21.
- Franco, P. E. C., Carvalho, M. F., and Soares, S. (1994). "A Network Flow Model for Short-Term Hydro-Dominated Hydrothermal Scheduling Problems." *IEEE Transactions on Power Systems*, 9(2), 1016-1022.
- Fox, J. (2008). "Bootstrapping Regression Models." *Applied Regression Analysis and Generalized Linear Models*, SAGE Publications, Inc.
- Frank, M., and Wolfe, P. (1956). "An Algorithm for Quadratic Programming." *Naval Research Logistics Quarterly*, 3(1-2), 95-110.
- GE Energy, General Electric Energy. (2010). "Western Wind and Solar Integration Study." *Integration Studies & Operational Impacts*,
<http://www.nrel.gov/wind/systemsintegration/pdfs/2010/wwsis_final_report.pdf> (Oct. 6, 2011).
- Grigg, C., Wong, P., Albrecht, P., Allen, R., Bhavaraju, M., Billinton, Roy, Chen, Q., Fong, C., Haddad, S., Kuruganty, S., Li, W., Mukerji, R., Patton, D., Rau, N., Reppen, D., Schneider, A., Shahidehpour, M., and Singh, C. (1999). "The IEEE reliability test system - 1996." *IEEE Transactions on Power Systems*, 14(3), 1010-1020.
- Grygier, J., and Stedinger, J. (1985). "Algorithms for Optimizing Hydropower System Operation." *Water Resources Research*, 21(1), 1-10.
- Gröwe-Kuska, N. G. R., Kiwiel, K. C., Nowak, M. P., Römisch, W., and Wegner, I. (2002). "Power Management in a Hydro-Thermal System under Uncertainty by Lagrangian Relaxation." *IMA Volumes in Mathematics and Its Applications*, 128, 1-32.

- Guan, X., Luh, P. B., and Zhang, L. (1995). "Nonlinear Approximation method in Lagrangian Relaxation-Based Algorithms for Hydrothermal Scheduling." *IEEE Transactions on Power Systems*, 10(2), 772-778.
- Guan, X., Luh, P. B., Yan, H., and Amalfi, J. A. (1992). "An Optimization-Based Method for Unit Commitment." *International Journal of Electrical Power & Energy Systems*, 14(1), 9-17.
- Guan, X., Ni, E., Li, R., and Luh, P. B. (1997). "An Optimization-Based Algorithm for Scheduling Hydrothermal Power Systems with Cascaded Reservoirs and Discrete Hydro Constraints." *IEEE Transactions on Power Systems*, 12(4), 1775-1780.
- Guan, X., Svoboda, A., and Li, C. (1999). "Scheduling Hydro Power Systems with Restricted Operating Zones and Discharge Ramping Constraints." *IEEE Transactions on Power Systems*, 14(1), 126-131.
- Habibollahzadeh, H., and Bubenko, J. A. (1986). "Application of Decomposition Techniques to Short-Term Operation Planning of Hydrothermal Power System." *IEEE Transactions on Power Systems*, PWRS-1(1), 41-47.
- Habibollahzadeh, H., Frances, D., and Sui, U. (1990). "A New Generation Scheduling Program at Ontario Hydro." *Power Systems, IEEE Transactions on*, IEEE, 5(1), 65-73.
- Handschin, E., and Slomski, H. (1990). "Unit Commitment in Thermal Power Systems with Long-Term Energy Constraints." *IEEE Transactions on Power Systems*, IEEE, 5(4), 1470-1477.
- Happ, H. H. (1977). "Optimal Power Dispatch - A Comprehensive Survey." *IEEE Transactions on Power Apparatus and Systems*, PAS-96(3), 841-854.
- Happ, H. H., Johnson, R. C., and Wright, W. J. (1971). "Large Scale Hydro-Thermal Unit Commitment-Method and Results." *IEEE Transactions on Power Apparatus and Systems*, PAS-90(3), 1373-1384.
- Hessami, M.-A., and Bowly, D. R. (2011). "Economic Feasibility and Optimisation of an Energy Storage System for Portland Wind Farm (Victoria, Australia)." *Applied Energy*, 88(8), 2755-2763.
- Heussen, K., Koch, S., Ulbig, A., and Andersson, G. (2010). "Energy Storage in Power System Operation: The Power Nodes Modeling Framework." *IEEE PES Conference on Innovative Smart Grid Technologies Europe (ISGT Europe)*, IEEE, Gothenburg, Sweden, 1-8.
- Hindsberger, M., and Ravn, H. F. (2001). "Multiresolution Modeling of Hydro-Thermal Systems." *Power Industry Computer Applications (PICA) 2001: 22nd IEEE Power Engineering Society International Conference on Innovative Computing for Power - Electric Energy Meets the Market*, 5-10.
- Hirst, E., and Kirby, B. (1996). *Electric-Power Ancillary Services*. Oak Ridge National Laboratory, Oak Ridge, Tennessee.
- Hodge, B.-M., Lew, D., and Milligan, M. (2011). *The Impact of High Wind Power Penetrations on Hydroelectric Unit Operations in the WWSIS*. Tech. Report No. NREL/TP-5500-52251. National Renewable Energy Laboratory, Golden, CO.

- Holttinen, H., Meibom, P., Orths, A., Hulle, F. van, Lange, B., O'Malley, M., Pierik, J., Ummels, B., Tande, J. O., Estanqueiro, A., Matos, M., Gomez, E., Soder, L., Strbac, G., Shakoor, A., Ricardo, J., Smith, J. C., Milligan, M., and Ela, E. (2009). *Design and operation of power systems with large amounts of wind power*. VTT Technical Research Centre of Finland. FI-02044 VTT, Finland.
- Hongling, L., Chuanwen, J., and Yan, Z. (2008). "A Review on Risk-Constrained Hydropower Scheduling in Deregulated Power Market." *Renewable and Sustainable Energy Reviews*, 12(5), 1465-1475.
- Huneault, M. (2001). "Electricity deregulation: Doubts brought on by the California debacle." *IEEE Canadian Review*, 37, 22.
- Jacobs, J. M., and Schultz, G. L. (2002). "Opportunities for Stochastic and Probabilistic Modeling in the Deregulated Electricity Industry." *Decision Making Under Uncertainty: Energy and Power*, C. Greengard and A. Ruszczynski, eds., Springer-Verlag, New York, New York, USA, 95-114.
- Jonas, P. (2011). "Predictive Power Dispatch for 100% Renewable Electricity Scenarios using Power Nodes Modeling Framework." M.S. Thesis. Swiss Federal Institute of Technology, Zurich, Switzerland.
- Kamath, C. (2010). "Understanding wind ramp events through analysis of historical data." *Transmission and Distribution Conference and Exposition 2010 IEEE PES*, IEEE, New Orleans, LA, USA, 1-6.
- Kazarlis, S. A., Bakirtzis, A. G., and Petridis, V. (1996). "A Genetic Algorithm Solution to the Unit Commitment Problem." *IEEE Transactions on Power Systems*, 11(1), 83-92.
- Kirschen, D., and Strbac, G. (2004). *Fundamentals of Power System Economics*. John Wiley & Sons, Ltd. The Atrium, Southern Gate, Chichester, West Sussex PO19 8SQ, England.
- Labadie, J. W. (2004). "Optimal Operation of Multireservoir Systems: State-of-the-Art Review." *Journal of Water Resources Planning and Management*, 130(2), 93.
- Labadie, J.W. (2010). "MODSIM 8.1: River Basin Management Decision Support System: User Manual and Documentation." Department of Civil and Environmental Engineering, Colorado State University, Fort Collins, CO.
- Labadie, J.W. (2011). "Water Rights Planning, Water Resources Management, & River Operations Decision Support System." *MODSIM-DSS*, <<http://modsim.engr.colostate.edu/version8.shtml>> (Sep. 21, 2011).
- Laird, D. (2011). "Conventional Hydropower: Integrated Technology Development." Brochure from Sandia National Laboratories, Albuquerque, New Mexico.
- Lauer, G. S., Sandell, N. R., Bertsekas, D. P., and Posbergh, T. A. (1982). "Solution of Large-Scale Optimal Unit Commitment Problems." *IEEE Transactions on Power Apparatus and Systems*, PAS-101(1), 79-86.
- Le, K., Day, J., Cooper, B., and Gibbons, E. (1983). "A Global Optimization Method for Scheduling Thermal Generation, Hydro Generation, and Economy Purchases." *Power Apparatus and Systems, IEEE Transactions on*, PAS-102(7), 1986-1993.

- Lee, J.-H., and Labadie, J. W. (2007). "Stochastic optimization of multireservoir systems via reinforcement learning." *Water Resources Research*, 43(11), 1–16.
- Li, C., Hsu, E., Svoboda, A. J., Tseng, C., and Johnson, R. B. (1997). "Hydro Unit Commitment in Hydro-Thermal Optimization." *IEEE Transactions on Power Systems*, 12(2), 764-769.
- Li, C., Jap, P. J., and Streiffert, D. L. (1993). "Implementation of Network Flow Programming to the Hydrothermal Coordination in an Energy Management System." *IEEE Transactions on Power Systems*, 8(3), 1045–1053.
- Li, C., Johnson, R. B., Svoboda, A. J., Tseng, C. L., and Hsu, E. (1998). "A Robust Unit Commitment Algorithm for Hydro-Thermal Optimization." *Proceedings of the 20th International Conference on Power Industry Computer Applications*, 186-191.
- Li, Y., and McCalley, J. D. (2008). "A General Benders Decomposition Structure for Power System Decision Problems." *IEEE International Conference on Electro/Information Technology*, IEEE, Ames, IA, 72–77.
- Lin, W.-M., Gow, H.-J., and Tsai, M.-T. (2011). "Combining of Direct Search and Signal-To-Noise Ratio for Economic Dispatch Optimization." *Energy Conversion and Management*, 52(1), 487-493.
- Loose, V. W. (2011). *Quantifying the value of hydropower in the electric grid: Role of hydropower in existing markets*. Sandia National Laboratory, Albuquerque, New Mexico.
- Lu, C.-L., Chen, C.-L., Hwang, D.-S., and Cheng, Y.-T. (2008). "Effects of wind energy supplied by independent power producers on the generation dispatch of electric power utilities." *International Journal of Electrical Power & Energy Systems*, 30(9), 553-561.
- Luh, P. B., Zhang, D., and Tomastik, R. N. (1998). "An Algorithm for Solving the Dual Problem of Hydrothermal Scheduling." *IEEE Transactions on Power Systems*, 13(2), 593-600.
- Lund, H. (2011). "EnergyPLAN: Advanced Energy System Analysis Computer Model." Aalborg University, Aalborg, Denmark.
- Ma, H., and Shahidehpour, S. M. (1999). "Unit Commitment with Transmission Security and Voltage Constraints." *IEEE Transactions on Power Systems*, IEEE, 14(2), 757–764.
- Madani, K., and Lund, J. R. (2009). "Modeling California's high-elevation hydropower systems in energy units." *Water Resources Research*, 45(9), 1-12.
- Makarov, Y., Etingov, P., Ma, J., Huang, Z., and Subbarao, K. (2011). "Incorporating Uncertainty of Wind Power Generation Forecast into Power System Operation Dispatch, and Unit Commitment Procedures." *IEEE Transactions on Sustainable Energy*, 2(4), 433-442.
- Mallick, S., Rajan, D. V., Thakur, S. S., Acharjee, P., and Ghoshal, S. P. (2011). "Development of a New Algorithm for Power Flow Analysis." *International Journal of Electrical Power & Energy Systems*, 33(8), 1479-1488.
- Mariano, S. J. P. S., Calado, M. R. A., and Ferreira, L. A. F. M. (2009). "Dispatch of Head Dependent Hydro Units: Modeling for Optimal Generation in Electricity Market." *2009 IEEE Bucharest PowerTech*, 1-6.

- Marmolejo, J. A., Litvinchev, I., Aceves, R., and Ramirez, J. M. (2011). "Multiperiod Optimal Planning of Thermal Generation using Cross Decomposition." *Journal of Computer and Systems Sciences International*, 50(5), 793-804.
- Matevosyan, J. (2008). "On the Coordination of Wind and Hydro Power." *Proc. 7th Int. Workshop on Large-Scale Integration of Wind Power Into Power Systems as Well as on Transmission Networks for Offshore Wind Farms*, 1-8.
- McGrath, K. E., Dawley, E. M., and Geist, D. R. (2006). *Total dissolved gas effects on fishes of the Lower Columbia River*. Pacific Northwest National Laboratory.
- McLaughlin, D., and Velasco, H. L. (1990). "Real-time control of a system of large hydropower reservoirs." *Water resources research*, 26(4), 623-635.
- Merlin, A., and Sandrin, P. (1983). "A New Method for Unit Commitment at Electricite De France." *IEEE Transactions on Power Apparatus and Systems*, PAS-102(5), 1218-1225.
- Meyer, A, and Dozier, A. (2012). "Symbolic math toolbox version 1.0." *ASquared Computational Modeling*. (Computer Program), Lakewood, CO.
- Microsoft. (2012). "Microsoft Solver Foundation 3.1." *MSDN Library: Development Tools and Languages*, <[http://msdn.microsoft.com/en-us/library/ff524509\(v=vs.93\).aspx](http://msdn.microsoft.com/en-us/library/ff524509(v=vs.93).aspx)> (Oct. 22, 2012).
- Milano, F. (2005). "An Open Source Power System Analysis Toolbox." *IEEE Transactions on Power Systems*, 20(3), 1199–1206.
- Moeini, R., Afshar, A., and Afshar, M. H. (2011). "Fuzzy Rule-Based Model for Hydropower Reservoirs Operation." *International Journal of Electrical Power & Energy Systems*, 33(2), 171-178.
- Moussa, A. M., Gammal, M. E., Ghazala, A. A., and Attia, A. I. (2011). "An Improved Particle Swarm Optimization Technique for Solving the Unit Commitment Problem." *The Online Journal on Power and Energy Engineering (OJPEE)*, 2(3), 217-222.
- Muckstadt, J. A., and Koenig, S. A. (1977). "An Application of Lagrangian Relaxation to Scheduling in Power-Generation Systems." *Operations Research*, JSTOR, 25(3), 387–403.
- Wan, Y.H. on behalf of National Renewable Energy Laboratory (2011). "Wind power data." E-mail message to the author (June 28, 2011).
- Nieva, R., Inda, A., and Guillén, I. (1987). "Lagrangian Reduction of Search-Range for Large-Scale Unit Commitment." *IEEE Transactions on Power Systems*, IEEE, PWRS-2(2), 465–473.
- Nowak, M. P. (2000). "Stochastic Lagrangian Relaxation Applied to Power Scheduling in a Hydro-Thermal System under Uncertainty." *Annals of Operations Research*, 100, 251-272.
- Nürnberg, R., and Römis, W. (2002). "A Two-Stage Planning Model for Power Scheduling in a Hydro-Thermal System under Uncertainty." *Optimization and Engineering*, 3, 355-378.
- Ongsakul, W., and Petcharaks, N. (2004). "Unit Commitment by Enhanced Adaptive Lagrangian Relaxation." *IEEE Transactions on Power Systems*, IEEE, 19(1), 620–628.

- Orero, S. O., and Irving, M. R. (1998). "A Genetic Algorithm Modelling Framework and Solution Technique for Short Term Optimal Hydrothermal Scheduling." *IEEE Transactions on Power Systems*, 13(2), 501–518.
- Owens, D. K. (2008). "Electricity: 30 Years of Industry Change." *30 Years of Energy Information and Analysis*, <http://www.eia.gov/conf_pdfs/Monday/owens.pdf> (Sep. 22, 2011).
- Padhy, N. P. (2001). "Unit Commitment using Hybrid Models: A Comparative Study for Dynamic Programming, Expert System, Fuzzy System and Genetic Algorithms." *International Journal of Electrical Power & Energy Systems*, 23(8), 827-836.
- Padhy, N. P. (2003). "Unit Commitment Problem under Deregulated Environment - A Review." *2003 IEEE Power Engineering Society General Meeting (IEEE Cat. No.03CH37491)*, Ieee, 1088-1094.
- Padhy, N. P. (2004). "Unit Commitment—A Bibliographical Survey." *IEEE Transactions on Power Systems*, 19(2), 1196-1205.
- Pandya, K. S., and Joshi, S. K. (2008). "A Survey of Optimal Power Flow Methods." *Journal of Theoretical and Applied Information Technology*, 4(5), 450-458.
- Patel, S. B. (2009). "Super Super Decoupled Loadflow." in *IEEE Toronto International Conference: Science and Technology for Humanity (TIC-STH)*, IEEE, Toronto, Ontario, Canada, 652–659.
- Paudyal, G. N., Shrestha, D. L., and Bogardi, J. J. (1990). "Optimal Hydropower System Configuration Based on Operational Analysis." *Journal of Water Resources Planning and Management*, 116(2), 233.
- Pereira, M. V. F., and Pinto, L. M. V. G. (1982). "A Decomposition Approach to the Economic Dispatch of Hydrothermal Systems." *IEEE Transactions on Power Apparatus and Systems*, (10), 3851-3860.
- Petrovic, R., and Kralj, B. (1993). "Economic and environmental power dispatch." *European Journal of Operational Research*, 64, 2-11.
- Rakic, M. V., and Markovic, Z. M. (1994). "Short Term Operation and Power Exchange Planning of Hydro-Thermal Power Systems." *IEEE Transactions on Power Systems*, 9(1), 359–365.
- Rakic, M. V., and Markovic, Z. M. (2007). "Hydraulically Coupled Power-Plants Commitment within Short-Term Operation Planning in Mixed Hydro-Thermal Power Systems." *European Transactions on Electrical Power*, 7(5), 323-330.
- Rebennack, S., Flach, B., Pereira, M. V. F., and Pardalos, P. M. (2011). "Stochastic Hydro-Thermal Scheduling under CO2 Emissions Constraints." *IEEE Transactions on Power Systems*, in press.
- Redondo, N. J., and Conejo, A. (1999). "Short-Term Hydro-Thermal Coordination by Lagrangian Relaxation: Solution of the Dual Problem." *IEEE Transactions on Power Systems*, 14(1), 89–95.

- Rubiales, A. J., Lotito, P. A., and Mayorano, F. J. (2008). "Numerical solutions to the hydrothermal coordination problem considering an oligopolistic market structure." *Proc. Int. Conf. Eng. Optim., EngOPT 2008*, 1-8.
- Rudolf, A., and Bayrleithner, R. (1999). "A Genetic Algorithm for Solving the Unit Commitment Problem of a Hydro-Thermal Power System." *IEEE Transactions on Power Systems*, 14(4), 1460–1468.
- Ruzic, S., and Rajakovic, N. (1991). "A New Approach for Solving Extended Unit Commitment Problem." *IEEE Transactions on Power Systems*, 6(1), 269–277.
- Ruzic, Slobodan, Rajakovic, Nikola, and Vuckovic, A. (1996). "A Flexible Approach to Short-Term Hydro-Thermal Coordination Part I: Problem Formulation and General Solution Procedure." *IEEE Transactions on Power Systems*, 11(3), 1564–1571.
- Saad, M., Bigras, P., Turgeon, A., and Duquette, R. (1996). "Fuzzy Learning Decomposition for the Scheduling of Hydroelectric Power Systems." *Water Resources Research*, 32(1), 179.
- Sen, S., and Kothari, D. P. (1998). "Optimal Thermal Generating Unit Commitment: A Review." *International Journal of Electrical Power & Energy Systems*, 20(7), 443-451.
- Salas, J. D. (1993). "Analysis and modeling of hydrologic time series." *Handbook of Hydrology*, D. R. Maidment, ed., McGraw-Hill, Inc., 19.1–19.72.
- Sharp, P., et al. (1998). *Maintaining Reliability in a Competitive U.S. Electricity Industry*. Secretary of Energy Advisory Board, U.S. Department of Energy, p. 14.
- Shaw, J. J. (1995). "A Direct Method for Security-Constrained Unit Commitment." *IEEE Transactions on Power Systems*, 10(3), 1329–1342.
- Shaw, J. J., Gendron, R. F., and Bertsekas, D. P. (1985). "Optimal Scheduling of Large Hydro-Thermal Power Systems." *IEEE Transactions on Power Apparatus and Systems*, PAS-104(2), 286-294.
- Sheble, G. B., and Fahd, G. N. (1994). "Unit Commitment Literature Synopsis." *IEEE Transactions on Power Systems*, 9(1), 128–135.
- Sherkat, V., Campo, R., and Moslehi, K. (1985). "Stochastic long-term hydrothermal optimization for a multireservoir system." *IEEE Transactions on Power Apparatus and Systems*, PAS-104(8), 2040-2050.
- Singh, A., and Chauhan, D. (2011). "Electricity Sector Restructuring Experience of Different Countries." *International Journal of Scientific & Engineering Research*, 2(4), 1-8.
- Soares, S., Lyra, C., and Tavares, H. (1980). "Optimal Generation Scheduling of Hydrothermal Power Systems." *IEEE Transactions on Power Apparatus and Systems*, PAS-99(3), 1107-1118.
- Song, S., Han, X., and Yu, D. (2011). "Impacts of Pumped Storage Power Station on Large-Scale Wind Power Integration into Grid." in *4th International Conference on Electric Utility Deregulation and Restructuring and Power Technologies (DRPT)*, IEEE, Weihai, Shandong, 1081–1085.

- Sriyanyong, P., and Song, Y. H. (2005). "Unit Commitment using Particle Swarm Optimization Combined with Lagrange Relaxation." *IEEE Power Engineering Society General Meeting*, San Francisco, CA, USA, 2752–2759.
- Takriti, S., and Birge, J. R. (2000). "Using Integer Programming to Refine Lagrangian-Based Unit Commitment Solutions." *IEEE Transactions on Power Systems*, 15(1), 151–156.
- Tejada-Guibert, J. A., Stedinger, J. R., and Staschus, K. (1990). "Optimization of Value of CVP's Hydropower Production." *Journal of Water Resources Planning and Management*, 116(1), 52.
- Tilmant, A., Vanclooster, M., Duckstein, L., and Persoons, E. (2002). "Comparison of Fuzzy and Nonfuzzy Optimal Reservoir Operating Policies." *Journal of Water Resources Planning and Management*, 128(6), 390.
- Tong, S. K., and Shahidehpour, S. M. (1989). "Combination of Lagrangian-Relaxation and Linear-Programming Approaches for Fuel-Constrained Unit Commitment Problems." *IEEE Proceedings Generation, Transmission and Distribution*, IET, 162–174.
- Tong, S. K., and Shahidehpour, S. M. (1990). "An Innovative Approach to Generation Scheduling in Large-Scale Hydro Thermal Power Systems with Fuel Constrained Units." *IEEE Transactions on Power Systems*, 5(2), 665–673.
- Trezos, T. (1991). "Integer programming application for planning of hydropower production." *Journal of Water Resources Planning and Management*, 117(3), 340–351.
- Tsai, M.-T., Gow, H.-J., and Lin, W.-M. (2011). "A Novel Stochastic Search Method for the Solution of Economic Dispatch Problems with Non-Convex Fuel Cost Functions." *International Journal of Electrical Power & Energy Systems*, 33(4), 1070–1076.
- Turgeon, A. (1980). "Optimal operation of multireservoir power systems with stochastic inflows." *Water Resources Research*, American Geophysical Union, 16(2), 275–283.
- U.S. Department of Energy (USDOE). (2011). *Energy Storage: Program Planning Document*. USDOE, Office of Electricity Delivery & Energy Reliability, Washington, DC.
- USACE, U.S. Army Corps of Engineers (2007). "HEC-ResSim Reservoir System Simulation: User's Manual." *HEC-ResSim 3.0 Documentation*, <http://www.hec.usace.army.mil/software/hec-ressim/documentation/HEC-ResSim_30_UsersManual.pdf> (Sep. 26, 2011).
- USACE, U.S. Army Corps of Engineers (2011). "HEC-ResSim." The Hydrologic Engineering Center (HEC), <<http://www.hec.usace.army.mil/software/hec-ressim/index.html>> (Sep. 21, 2011).
- USDHS, U.S. Department of Homeland Security. (2008). "National power grid simulation capability: Needs and issues." *Report of the Science and Technology Directorate*, <<http://www.anl.gov/eesa/pdfs/brochures/PowerGridBrochure.pdf>> (Oct. 6, 2011).
- USDOE, U.S. Department of Energy (2005). "How Hydropower Works." *Hydropower: Hydropower Basics*, <http://www1.eere.energy.gov/windandhydro/hydro_how.html> (Sep. 21, 2011).

- USDOE, U.S. Department of Energy (2008). "History of Hydropower." *Hydropower: Hydropower Basics*, < http://www1.eere.energy.gov/windandhydro/hydro_history.html> (Sep. 21, 2011).
- Vardanyan, Y., and Amelin, M. (2011). "The State-of-the-Art of the Short Term Hydro Power Planning with Large Amount of Wind Power in the System." in *8th International Conference on the European Energy Market (EEM)*, Zagreb, Croatia, 448-454.
- Virmani, S., Adrian, E. C., Imhof, K., and Mukherjee, S. (1989). "Implementation of a Lagrangian Relaxation Based Unit Commitment Problem." *IEEE Transactions on Power Systems*, 4(4), 1373–1380.
- Wang, C., and Shahidehpour, S. M. (1993). "Power Generation Scheduling for Multi-Area Hydro-Thermal Systems with Tie Line Constraints Cascaded Reservoirs and Uncertain Data." *IEEE Transactions on Power Systems*, 8(3), 1333-1340.
- Wang, C., and Shahidehpour, S. M. (1994). "Ramp-Rate Limits in Unit Commitment and Economic Dispatch Incorporating Rotor Fatigue Effect." *IEEE Transactions on Power Systems*, 9(3), 1539-1545.
- Wang, H., Murillo-Sánchez, C. E., Zimmerman, R. D., and Thomas, R. J. (2007). "On Computational Issues of Market-Based Optimal Power Flow." *IEEE Transactions on Power Systems*, 22(3), 1185–1193.
- Wang, S. J., and Shahidehpour, S. M. (1995). "Short-Term Generation Scheduling with Transmission and Environmental Constraints using an Augmented Lagrangian Relaxation." *IEEE Transactions on Power Systems*, 10(3), 1294-1301.
- Warsono, W., Ozveren, C. S., King, D. J., and Bradley, D. (2008). "A Review of the Use of Genetic Algorithms in Economic Load Dispatch." in *43rd International Universities Power Engineering Conference (UPEC)*, IEEE, Padova, Italy, 1-5.
- Wei, H., and Sasaki, H. (1998). "A Decoupled Solution of Hydro-Thermal Optimal Power Flow Problem by Means of Interior Point Method and Network Programming." *IEEE Transactions on Power Systems*, 13(2), 286-293.
- Weitkamp, D. E., and Katz, M. (1980). "A Review of Dissolved Gas Supersaturation Literature." *Transactions of the American Fisheries Society*, 109, 659–702.
- Wong, K. P., and Wong, Y. W. (1994). "Short-Term Hydrothermal Scheduling Part I. Simulated Annealing Approach." in *IEE Proceedings - Generation, Transmission and Distribution*, 497-501.
- Wood, A.J. and Wollenberg, B.F. (1984). *Power generation, operation, and control*. Wiley.
- Wurbs, R. A. (2011). "Water Rights Analysis Package (WRAP) Modeling System." Texas A&M University, <<https://ceprofs.civil.tamu.edu/rwurbs/wrap.htm>> (Sep. 21, 2011).
- Xia, X., and Elaiw, A. M. (2010). "Optimal Dynamic Economic Dispatch of Generation: A Review." *Electric Power Systems Research*, 80(8), 975-986.
- Xie, L., Carvalho, P. M. S., Ferreira, L. A. F. M., Liu, J., Krogh, B. H., Popli, N., and Ilić, M. D. (2011). "Wind Integration in Power Systems, Operational Challenges and Possible Solutions." *Proceedings of the IEEE*, 99(1), 214-232.

- Yamin, H. (2004). "Review on Methods of Generation Scheduling in Electric Power Systems." *Electric Power Systems Research*, 69(2-3), 227-248.
- Yan, H., and Luh, P. B. (1997). "A Fuzzy Optimization-Based Method for Integrated Power System Scheduling and Inter-Utility Power Transaction with Uncertainties." *IEEE Transactions on Power Systems*, 12(2), 756-763.
- Yan, H., Luh, P., and Guan, X. (1993). "Scheduling of Hydrothermal Power Systems." *IEEE Transactions on Power Systems*, 8(3), 1358-1365.
- Yi, J., Labadie, J. W., and Stitt, S. (2003). "Dynamic Optimal Unit Commitment and Loading in Hydropower Systems." *Journal of Water Resources Planning and Management*, 129(5), 388.
- Yoo, J. H. (2009). "Maximization of Hydropower Generation through the Application of a Linear Programming Model." *Journal of Hydrology*, 376, 182-187.
- Zahraie, B., and Karamouz, M. (2004). "Hydropower Reservoirs Operation: A Time Decomposition Approach." *Scientia Iranica*, 11(1&2), 92-103.
- Zhuang, F., and Galiana, F. D. (1988). "Towards a More Rigorous and Practical Unit Commitment by Lagrangian Relaxation." *IEEE Transactions on Power Systems*, 3(2), 763-773.
- Zoumas, C. E., Bakirtzis, a G., Theocharis, J. B., and Petridis, V. (2004). "A Genetic Algorithm Solution Approach to the Hydrothermal Coordination Problem." *IEEE Transactions on Power Systems*, 19(3), 1356-1364.